Estimate of Instant Release Fractions Using ORIGEN-S and FEMAXI

NWMO TR-2011-19 December 2011

F. Iglesias
Candesco Corporation

M. Kaye
University of Ontario Institute of Technology

B. Lewis
Royal Military College of Canada

nwmo
NUCLEAR WASTE MANAGEMENT ORGANIZATION
SOCIÉTÉ DE GESTION DES DÉCHETS NUCLÉAIRES

Nuclear Waste Management Organization
22 St. Clair Avenue East, 6th Floor
Toronto, Ontario
M4T 2S3
Canada

Tel: 416-934-9814
Web: www.nwmo.ca

Estimate of Instant Release Fractions Using ORIGEN-S and FEMAXI

NWMO TR-2011-19

December 2011

F. Iglesias
Candesco Corporation

M. Kaye
University of Ontario Institute of Technology

B. Lewis
Royal Military College of Canada

ABSTRACT

Title: **Estimate of Instant release Fractions Using ORIGEN-S and FEMAXI**
Report No.: **NWMO TR-2011-19**
Author(s): F. Iglesias, M. Kaye, and B. Lewis
Company: Candesco Corporation, University of Ontario Institute of Technology, and Royal Military College of Canada
Date: December 2011

Abstract
The purpose of this work was to determine conservative yet realistic estimates of the fractions of used fuel radionuclide inventories that are available for instant release upon simultaneous breach of the fuel sheath and saturation of a used fuel container. The estimates were obtained by using ORIGEN-S to calculate the radioactive inventory of ten spent CANDU fuel bundles at discharge while FEMAXI V6.1 was used to calculate the Instant Release Fractions (IRFs) at the grain boundary and fuel-to-sheath-gap. The IRFs were successfully calculated and compared with a set of experimental results (Stroes-Gascoyne, 1996). Additional estimates were performed for four fuel bundle conditions, representing average and pessimistic conditions.

Chemical speciation calculations were carried out using the pessimistic case (a bundle power of 900 kW and a bundle burnup of 320 MWh/kgU) since it yielded higher inventories for the radionuclides of interest. The results of these calculations show the chemical speciation of the radionuclides in the gap and grain boundaries and their amounts for the most important compounds; specifically, volatile species, soluble fission products in the UO_2 fuel, the solid solution U(Pd-Rh-Ru)3, noble metals inclusions (Mo, Rh, Pd, Ru, Tc) in BCC and HCP crystallographic form, and other solid and liquid compounds.

TABLE OF CONTENTS

LIST OF TABLES

Page

LIST OF FIGURES

Page

1. INTRODUCTION

The reference concept for long-term isolation and containment of used CANDU fuel is emplacement of used fuel in robust containers in a deep geologic repository. The reference containers consist of a steel inner vessel within a copper outer vessel. Such containers are extremely durable in the reducing environment that exists far underground and are therefore expected to survive intact for thousands of years. However, safety assessments generally consider the consequences of container failure scenarios.

In some container failure scenarios, water is assumed to enter some containers shortly after they are placed in the underground facility. Since the fuel sheath is not credited as a retention barrier, this water can immediately contact the fuel matrix (UO_2). While the uranium fuel matrix has a very slow dissolution rate, some of the radioactive products present in the fuel-to-sheath gap and the grain boundaries of the fuel are assumed to be readily available for release into the water – this is referred to as the "instant release fraction" (IRF).

The IRF for a specific radionuclide is defined as that fraction of the total inventory of the specific radionuclide that is located in the grain boundaries and the fuel-to-sheath gap (hereinafter referred to as gap) at the time of contact with water. This amount of the radionuclide is assumed to rapidly escape from the fuel when water contacts the fuel.

IRFs for used CANDU fuel have been measured at Atomic Energy of Canada Limited (AECL) Whiteshell Laboratories (Stroes-Gascoyne, 1996). However, there is limited amount of data since the experiments are costly.

For this project, work was divided into two tasks:

Task 1: Evaluation of Experimental Instant Release Fractions

Stroes-Gascoyne (1996) experimentally determined IRFs for selected fission products by measuring the gap and grain boundary inventories in several used CANDU fuel bundles. In this task, a fuel performance code was used to theoretically estimate radionuclide IRFs for the fuels reported by Stroes-Gascoyne, (1996). The estimated values were compared to experimental measurements and the accuracy of the calculated results was assessed.

Task 2: Calculation of Average and Pessimistic Instant Release Fractions

Using the methodology developed in Task 1, the IRFs for an average fuel bundle and a pessimistic fuel bundle (Table 1-1) with the following power histories were estimated:

Table 1-1: Average and Pessimistic Power Histories

Fuel	Bundle Power (kW)	Burnup (MWh/kgU)
Average	455	220, 320
Pessimistic	900	220, 320

2. ANALYSIS SCOPE

2.1 Evaluation of Experimental Instant Release Fractions

CANDU fuel bundles irradiated in the Bruce and Pickering Nuclear Power Generating Stations were used for IRF experimental determination, as reported by Stroes-Gascoyne (1996). From these bundles, certain fuel elements were removed, fuel samples were taken and ground to a powder form. The size of the powder particles was designed such that the grain-boundary inventories would be available for direct dissolution in HCl acid. The powders were individually leached with 0.1 mol/L HCl and the leached amount of ^{137}Cs, ^{129}I, ^{99}Tc and ^{90}Sr was measured in the solvent.

From the reported fuel samples, a subset of samples from fuel bundles irradiated at the Bruce Station was selected. The reason for this choice was based on the availability of the power histories for these Bruce bundles. The irradiation history of the Bruce bundles was simulated to calculate the fission product production and the inventory distribution between grains, grain-boundaries and gap. The bundle identifications and the location of the fuel elements within these bundles from which samples were taken are detailed in Table 2-1.

Using a fuel bundle fission product transport model, the IRFs for the isotopes ^{137}Cs, ^{129}I, ^{99}Tc and ^{90}Sr were calculated and compared with the reported values (Stroes-Gascoyne, 1996). In order to confirm that inventories stored in the grain-boundaries and gap were fully released during the dissolution process used by Stroes-Gascoyne, chemical speciation calculations for the elements Bi, Cs, I, Pb, Se, Tc, Ba, Mo, Pd, Rb, Rh, Ru, Sr, and Te were also performed. Notable discrepancies between the estimated and measured values are discussed and possible causes of the discrepancies are proposed.

Table 2-1: Fuel Sample Source Information - Bundle and Element Location

Bundle Identification	Fuel Element Location
F21271C	Outer ring
F21271C	Intermediate ring
G00815W	Outer ring
G00815W	Intermediate ring
F12059C	Outer ring
F12059C	Intermediate ring
J49093C	Outer ring
J49093C	Inner ring
G13374S	Outer ring
G13374S	Intermediate ring

2.2 Calculation of Average and Pessimistic Instant Release Fractions

In Task 2, instant release fractions were calculated for 30 year old Bruce fuel bundles with average power (450 kW) and pessimistic power (900 kW) ratings and for burnups of 220 MWh/kgU and 320 MWh/kgU, for a total of 4 bundle power/burnup histories (see Table 2-2). The bundles were assumed to remain constant at the indicated powers until the specified bundle burnup was obtained.

The geometry of the Bruce bundles is assumed to be the same as the dimensions used in Task 1. The bundle calculations were carried out for four different groups of bundle elements (outer, intermediate, inner and centre) because each group is irradiated at a different power as a result of the bundle radial power distribution. The bundle power radial distribution used for this task, based on a burnup of 350 MWh/kgU (closest reported burnup), was:

- Outer elements = 1.115*AELP,
- Intermediate elements = 0.9160*AELP,
- Inner elements = 0.8217*AELP, and
- Center element = 0.8124*AELP.

Where AELP (Average Element Linear Power) = bundle power/(0.4953 m x 37 elements). The reference bundle powers corresponded to 24 and 49 kW/m AELP.

Table 2-2: Average and Pessimistic Power Histories

Fuel	Liner Power (kW/bundle)	Burnup (MWh/kgU)
Average 1	455	220
Average 2	455	320
Pessimistic 1	900	220
Pessimistic 2	900	320

The fractional inventory in the grain boundaries and gaps were calculated for the radionuclides of interest. As well, the likely chemical speciation of the following elements was evaluated at irradiation conditions: (Xe+Kr), Mo, Ru, Cs, Pd, Ba, Tc, Rh, Sr, Te, Rb, I, Ag, Cd, Sn, Se, Br, Sb, H, Pb, Bi, U and O_2.

3. ANALYSIS METHODOLOGY

The methodology used to estimate the IRFs included the following activities:

- Simulate the generation, diffusion and accumulation of fission products in the grain-boundaries and fuel gap for the selected fuel samples, and
- Use an existing thermodynamic model to estimate the chemical speciation of the chemical elements of interest in the gap and grain boundaries; thereby confirming that the measurements of the IRFs by Stroes-Gascoyne (1996) were not significantly affected by the chemical form of the compounds present at the grain-boundaries and in the fuel gap.

3.1 Simulation of the Generation, Diffusion and Accumulation of Fission Products

The activation and fission products generated in the fuel grains, while the fuel is in the reactor, diffuse to the grain-boundaries as a function of the particular elemental diffusion coefficient and the concentration gradient in the fuel grains. As the diffusion coefficients are a function of the local temperature, it can be stated that the diffusion of isotopes is a temperature and concentration driven process.

The diffusive release of fission products from the uranium dioxide grains is complicated by the charge of the migrating complex, the specific characteristics of the migrating isotope and other mechanisms, e.g., trapping at point defects in a polycrystalline material. Also, the releases are

strongly dependent of the fuel stoichiometry, burnup and density. However, the release of fission products can still be characterized using appropriate solutions to Fick's Law if an 'effective' diffusion coefficient is used, which smooths out the complicating mechanisms over all the diffusing atoms (Lawrence, 1978). These diffusion coefficients are a function of the chemical composition and physical properties of the UO_2 and of the conditions under which it is measured. It appears to be most sensitive to deviations in the fuel stoichiometry (Lawrence, 1978).

It is important to note that, at irradiation temperatures, the effective diffusion coefficients for volatile species are not very different from those of the noble gases. This was demonstrated in several experiments (Lewis et al., 1996). Specifically, this reference shows that, for the reducing condition in the HEVA-6 test, the releases as a function of time for ^{131}I, ^{137}Cs and ^{140}Ba are indistinguishable. Also, the same reference demonstrates that, for the conditions of the VERCORS-3 test, the release profiles of ^{135}Xe, ^{131}I, and ^{137}Cs are also indistinguishable. In view of the findings of these tests (Lewis et al., 1996), in this report, the effective diffusion coefficients for volatile species have been assumed to be the same as those of the noble gases (Lewis et al., 2008; Lewis et al., 1998).

These and other similar experimental data have been used to formulate the conceptual model that is used by most fission product release codes such as FASTGRASS, SOURCE, TRANSURANUS, PROFESS and others. These models represent the fission product release as a two step process: a) diffusion of fission products to the gap and b) release of the different species, depending on the volatility of the formed compounds, from the fuel element after sheath failure.

For the first step, it is further assumed that the noble gas diffusion coefficients can be used to represent the diffusion behaviour of other fission products. As noted above, this assumption is consistent with most of the experimental evidence available (Lewis et al., 2008; Lawrence, 1978; Lewis et al., 1998).

It is of interest to note that ^{123}Te releases follow the other fission product release profiles only after the sheath has been completely oxidized, showing that Te reacts with the Zircaloy cladding and is only released after the cladding has been oxidized. Other experiments have shown that, under oxidizing conditions, Ba is not volatile because its oxide has a very low volatility. However, under reducing conditions, Ba is released in a similar manner to the noble gases (Prussin, 1988; Lewis et al., 2008). This shows that fission product chemical speciation can dramatically affect their releases.

Currently, there is no available code that couples thermodynamic interaction models with fission product diffusion. France and the US are in the process of developing this type of code. However, these codes are for accident conditions and their applicability to the undefected fuel under consideration in this report would need to be demonstrated.

As previously mentioned, the diffusional releases of fission products are estimated by the behaviour of noble gases (mainly Xe and Kr). The principal processes affecting noble gas releases are:

- The fission gas produced in UO_2 grains is transported to grain boundaries through two mechanisms:
    - Gas atom diffusion within grains

    - Sweeping of gas atoms to grain boundaries by grain growth
- The gas that reaches the grain boundaries forms grain-boundary bubbles. When the amount of fission gas atoms (of Xe and Kr) in the grain-boundary bubbles reaches a certain saturation value, the bubbles interconnect and tunnels are formed, permitting a pathway for the possible release of volatile fission products to the fuel-to-sheath gap.
- After the tunnels are formed, additional gas which has diffused from within grains to the grain boundaries enters the tunnels and is immediately released into the gap.
- A fraction of the gas accumulated at the grain boundaries also re-dissolves back into the grains by fission-fragment bombardment.
- Diffusion of gas atoms inside the fuel grains is affected by the presence of very small bubbles (intragranular) and/or UO_2 defects inside the grains that may trap the migrating atoms. Simulation of the diffusion release includes fission gas trapping by the intragranular bubbles/defects and re-dissolution of the gas from the traps into the matrix.

3.2 Calculation of Chemical Speciation

After reaching the grain-boundary bubbles, tunnels and gap, activation and fission products (with the exception of noble gases) can interact amongst themselves forming various chemical compounds. The chemical speciation in these zones can be estimated using the thermodynamic properties of the reactants, their concentration, the local environmental conditions and Gibb's energy minimization methods.

The volatility of the chemical compounds formed in the grain-boundaries and gap can affect the measured IRFs reported by Stroes-Gascoyne (1996) and Stroes-Gascoyne et al. (1987). This is particularly important in the case of formation of insoluble chemical compounds located within the grain-boundaries or in the fuel-to-sheath gap. These compounds may remain undissolved and not transfer into solution when the powdered fuel is leached with HCl (Stroes-Gascoyne 1996); thereby, causing the measured IRF to be underestimated.

In particular, depending on their chemical form, the fission products can segregate as:

- Soluble fission products in the fuel oxide,
- Noble metals inclusions (Mo, Rh, Pd, Ru, Tc),
- Zirconate, uranate and molybdate phases,
- Second metal solid solution U(Pd-Rh-Ru)3, and
- Volatile species within an inert gas phase (Lewis et al., 2011; Kaye et al., 2007; Thompson et al., 2007).

Moreover, an equilibrium thermodynamic analysis can provide a means to better assess the leachability of these fission products in an acid solution (i.e., as used in the IRF-experimentation technique) or their aqueous behaviour in groundwater in various waste management scenarios (which can be assessed through a Pourbaix analysis) (Piro et al., 2010).

To perform the activities described above, the inventory of fission products and their distribution inside the fuel elements was calculated with the codes identified in Section 3.3 below; and the amount of the selected chemical elements in the grain-boundaries and gap was estimated. The temperature used for the chemical speciation analysis at the grain-boundary was the average between the calculated pellet center temperature and pellet surface temperature and the temperature used for the analysis at the gap was the average between the calculated pellet surface temperature and cladding inner temperature. This information, together with an

existing fuel thermodynamic database and a Gibb's energy minimization code (Lewis et al., 2011; Kaye et al., 2007; Thompson et al., 2007; Piro et al., 2010), was used to calculate the chemical form of I, Cs, Tc and Sr in the grain boundaries and gap. This analysis is required to assess the leachability of the formed chemical compounds in HCl solution used in the experiments of Stroes-Gascoyne (1996). However, as a first approximation, the dissolution of these element bearing compounds in 0.1 mol/L HCl was assumed to be complete. This assumption was confirmed by the chemical speciation analysis.

3.3 Computer Codes

The codes selected for this work were ORIGEN-S and FEMAXI v6.1. These codes are used internationally to perform inventory calculations and fission product release distributions. The use of these tools ensures that the performed analysis is aligned with best international practices.

For calculations of the isotopic production and decay, the latest released version of ORIGEN-S code by the international Radiation Safety Information Computational Center (RSICC) of the Oak Ridge National Laboratory was used. This ORIGEN-S version was released as a component of the code suite of the SCALE 6 package (Gauld et al., 2009).

The fuel performance and fission product distribution in the fuel was simulated using the latest version of the FEMAXI code released by RSICC. This code is capable of producing an accurate prediction of the fission gas release fraction and atomic distribution (Suzuki and Hiroaki, 2005).

The following assumptions and inputs were used in the FEMAXI code calculations:

- The Turnbull diffusion coefficient for Xe was selected. This expression of the diffusion coefficient is used for the simulation of CANDU fuel in ELESTRES (COG, 2001).
- All fission products diffusion coefficients were represented by the Xe diffusion coefficient, for reasons discussed in Section 3.1,
- Power-burnup histories for each fuel element were provided by NWMO,
- Fuel element and components geometries were obtained from NWMO, and
- Grain boundary coverage at bundle interconnection was consistent with the value used in ELESTRES (COG, 2001).

The parameters and values specified in Table 3-1 were used to model a CANDU fuel element in FEMAXI v6.1.

Table 3-1: CANDU Fuel Element Dimensions

Parameter	Value	Reference
Sheath inside diameter (cm)	1.224	OPG 37-el bundle
Sheath outside diameter (cm)	1.266	OPG 37-el bundle
Fuel pellet length (cm)	1.215	OPG 37-el bundle
U-235 enrichment	0.0072	OPG 37-el bundle
Pellet dish diameter (cm)	1.171	OPG 37-el bundle
Dish depth (cm)	0.0241	OPG 37-el bundle
Upper/lower plenum volume (cm^3)	1.381	OPG 37-el bundle
Initial gas pressure (MPa)	0.1013	COG ELESTRES theory manual
Helium in initial gas composition (%)	80.0	COG ELESTRES theory manual
Argon in initial gas composition (%)	20.0	COG ELESTRES theory manual

The calculation of fission product chemical speciation was performed using the available fuel thermodynamic database and Gibb's minimization techniques as reported by Lewis et al. (2011); Kaye et al. (2007); Thompson et al. (2007) and Piro et al. (2010). It is important to note that this database and technique were used in the development of the Canadian Industry Standard Toolset (IST) code SOURCE 2.

3.4 Evaluation of Experimental Instant Release

For Task 1, the calculation of the IRFs was performed by dividing the simulation into four separate activities. These activities were:

- Calculation of fission products inventories during irradiation and decay,
- Simulation of the fuel-element irradiation history, fission product releases and stored inventories in the grain-boundaries and gap,
- Comparison of the grain-boundary and gap inventories with corresponding experimental results, and
- Calculation of chemical speciation of the selected elements and their solubilities in 0.1 mol/L HCl.

3.4.1 Calculation of Fission Product Inventories

Ten ORIGEN-S runs were performed to estimate the inventories of the fission products of interest produced during fuel bundle irradiations. These irradiations were simulated on a fuel-element basis using the CANDU-37 fuel element type option in ORIGEN-S.

A constant linear power, equal to the reported average power (Stroes-Gascoyne, 1996), was assumed and the burnup was set to the reported measured or estimated reported exit burnup (Stroes-Gascoyne, 1996). These stylized power-burnup histories are acceptable for long-lived fission products because the inventories are mostly dependent on burnup. Table 3-2 presents the irradiation parameters for each of these runs.

The bundle discharge dates were only known for F21271C (May, 1979) and F12059C (September, 1979) (Hocking et al. 1994). To determine the probable discharge date of the other bundles, the discharge dates of sister bundles (corresponding to the same ID pattern) were searched in the Bruce Station records. It was determined that bundle G00815W was probably discharged in June of 1979, bundle G13374S in October of 1984 and bundle J49093C in April of 1984. A decay time of 7 years was then assumed for all cases. The impact of this assumption is considered minor because this work is focused on long-lived fission products.

The inventory of the elements Bi, Cs, I, Pb, Se, Tc, Ba, Mo, Pd, Rb, Rh, Ru, Sr, and Te were calculated as well as the isotopes ^{137}Cs, ^{129}I, ^{99}Tc and ^{90}Sr to facilitate the comparison with the experimental results.

Hand calculations for the production of ^{137}Cs for fuel element F12059C (outer) and G13374S (intermediate) were done and compared with the corresponding ORIGEN-S code calculation to ensure that the irradiation history was properly simulated with ORIGEN-S for CANDU fuel. This comparison showed that the analytical results and the ORIGEN-S output displayed the same trend over the whole irradiation period, having only small differences not exceeding 3%. These differences are due to the fact that the analytical model takes into account only the dominant

mechanisms for direct production of ^{137}Cs from ^{235}U fission and the ^{137}Cs decay into ^{137}Ba, while some of the subtle details of ^{137}Cs transmutation (e.g., neutron capture, accurate cross sections and other constants values, etc.) were left outside the scope of the analytical model.

Table 3-2: Identification and Parameters for Each of the 10 Inventory Runs

Case	Bundle ID	Element	Burnup (MWh/kgU) (Stroes-Gascoyne, 1996)	Average Linear Power (kW/m) (Stroes-Gascoyne, 1996)	Decay (years)
1	F21271C	Outer	328*	47	7
2	F21271C	Intermediate	261	39	7
3	G00815W	Outer	163	41	7
4	G00815W	Intermediate	131	33	7
5	F12059C	Outer	264	46	7
6	F12059C	Intermediate	225	38	7
7	J49093C	Outer	308*	50	7
8	J49093C	Inner	225*	37	7
9	G13374S	Outer	300*	50	7
10	G13374S	Intermediate	244*	42	7

** Estimated burnup*

3.4.2 Simulation of Fission Product Distributions

Ten FEMAXI v6.1 runs were performed to simulate the fuel element irradiation and to estimate the fission product releases and stored inventories in the grain-boundaries and gap. These irradiations were simulated following the irradiation histories for each element of interest provided by NWMO. The power-burnup histories as received contained more data points than can be input into FEMAXI v6.1. The power-burnup histories were therefore reduced by taking every ‘x’th power-burnup point, plus the last data point of the history. The value of ‘x’ used to reduce the data set depends on the size of the original power-burnup history. For large power-burnup histories, ‘x’ is greater than for shorter power-burnup histories. The target number of power-burnup data points in each reduced history was between 20 and 30, depending on the complexity of the history as-received from AECL.

Table B-1 to Table B-5 (in Appendix B) list the reduced power-burnup history for each element as used in FEMAXI v6.1 input files. Figure B-1 to Figure B-10 (in Appendix B) compare the original power-burnup history provided in COG (2001) with the reduced power-burnup history used in FEMAXI v6.1 for each element.

3.4.3 Fission Product Chemical Speciation

The dissolution behaviour and/or volatility of the chemical compounds formed in the grain-boundaries and gap can affect the measured values of IRF (Stroes-Gascoyne, 1996). This is particularly important in the case of formation of insoluble chemical compounds that are located in the grain-boundaries and gap which can remain undissolved and not transferred into solution.

The amounts of the chemical elements Bi, Cs, I, Pb, Se, Tc, Ba, Mo, Pd, Rb, Rh, Ru, Sr, and Te in the grain-boundaries and gap were calculated and used with the existing fuel thermodynamic database and a Gibb's energy minimization computation (Piro et al., 2010) to confirm that the chemical form of the I, Cs, Te and Sr compounds found at both these locations would have no significant impact on the simulated results.
For this activity, the temperature and pressure were required. As the gap and interconnected grain-boundaries pressures are bounded by the coolant pressure, these pressures were assumed equal to the coolant pressure for all cases. The grain-boundary temperatures vary with the pellet radius. However, as the purpose of the fission product speciation is to confirm the assumption of complete dissolution of the compounds formed by the radionuclides of interest, an average grain-boundary temperature is considered sufficient.

The version of the thermodynamic database used is detailed in the Annex of Lewis et al. (2011).

The calculated IRFs reported in this report were calculated under the assumption that the dissolution of the compounds bearing the chemical element of interest was complete. This assumption was confirmed to be valid by the chemical speciation calculations for the chemical elements I, Cs, Te and Sr.

3.5 Calculations of Average and Pessimistic Instant Release Fractions

In the Task 2 work, the IRF calculations were performed by implementing three activities:

- Calculation of fission products inventories during irradiation and 30 years of decay for the average and pessimistic fuel bundle irradiation assumptions,
- Simulation of the fuel bundle irradiation history, fission product releases and stored inventories in the grain-boundaries and gap, and
- Calculation of chemical speciation of the selected chemical elements stored at grain boundaries and gap.

3.5.1 Calculation of Fission Product Inventories

Four ORIGEN-S runs were performed to estimate the inventories of the fission products produced during fuel bundle irradiations. These irradiations were simulated on a bundle basis using the CANDU 37-fuel element type option in ORIGEN-S. A constant linear power, equal to the powers indicated in Table 2-2, was assumed until the indicated bundle burnup was achieved. Again, these stylized power-burnup histories are acceptable for long-lived fission products because the inventories are mostly dependent on burnup. A decay time of 30 years was assumed for the four cases.

The inventories of the elements Xe, Mo, Cs, Ru, Ba, Sr, Tc, Pd, Te, Rh, Kr, Rb, I, Ag, Se, Sn, Cd, Br, Sb, In, Ge, As, H, Zn, C, Ra, Pb, Bi, Rn, Tl and Po was calculated.

3.5.2 Simulation of Fission Product Distributions

Sixteen FEMAXI v6.1 runs were performed to simulate the fuel bundle irradiations (four bundles) and to estimate the fission product releases and stored inventories in the grain-boundaries and gap of the groups of fuel elements in the 37-element bundle design (four element groups). These irradiations were simulated following the irradiation histories and

bundle radial power distributions indicated in Section 2.2. Table B-6 (in Appendix B) lists the power-burnup histories for each element group used for the average and pessimistic cases.

3.5.3 Fission Product Chemical Speciation

The number of chemical elements considered was limited to 23 which is the current limit for the database used (Piro et al., 2010). The amount of the chemical elements (Xe+Kr), Mo, Ru, Cs, Pd, Ba, Tc, Rh, Sr, Te, Rb, I, Ag, Cd, Sn, Se, Br, Sb, H, Pb, Bi, U and O_2 in the grain-boundaries and gap were estimated, and used with the existing fuel thermodynamic database (Lewis et al., 2011) and a Gibb's energy minimization computation (Piro et al. 2010) to determine the most likely compounds that could be found in the grain boundaries and gaps of fuel element groups for the "Pessimistic 2" case of Table 2-2.

4. RESULTS

The results obtained following the methodology described in Section 3 are presented in this section.

4.1 Evaluation of Experimental Instant Release Fractions

4.1.1 Fission Product Inventories

ORIGEN-S (Gauld et al., 2009) was run to simulate inventories for the fuel element cases listed in Table 3-2 (including 7 years of decay). The output comprises total inventories of selected fission products which are generated during the irradiation and decay of the analyzed fuel elements. These fission products include the following chemical elements: Ba, Bi, Cs, H, I, Kr, Mo, Pb, Pd, Rb, Rh, Rn, Ru, Se, Sr, Tc, Te, U, Xe, and the following specific isotopes: ^{137}Cs, ^{129}I, ^{99}Tc, and ^{90}Sr.

For each of the ten fuel elements analyzed, four tables of the ORIGEN-S output files were prepared as follows:

- Chemical element inventories during irradiation (g),
- Nuclear isotope inventories during irradiation (g),
- Chemical element inventories during decay (g), and
- Nuclear isotope inventories during decay (g).

The inventory calculations for each of the fuel elements under consideration are compiled in Appendix A.

4.1.2 Fuel Element Temperatures

For each fuel element at the maximum observed power, the temperature at the pellet centerline, pellet surface and sheath inner surface were obtained from the FEMAXI v6.1 output files. Based on the values calculated for the fuel centerline, pellet surface and sheath inner surface, approximations of the grain-boundary temperature and gap temperature were determined as follows:

$$T_{GrainAvg}\left(P_{\max}\right) = \frac{T_{CenterLine}\left(P_{\max}\right) + T_{PelletSurface}\left(P_{\max}\right)}{2}$$

$$T_{GapAvg}\left(P_{\max}\right) = \frac{T_{PelletSurface}\left(P_{\max}\right) + T_{SheathInnerSurface}\left(P_{\max}\right)}{2}$$

The calculated values for the average grain-boundary temperature and average gap temperature for the ten fuel elements under consideration are shown in Table 4-1.

Table 4-1: Calculated Fuel Grain and Fuel-to-Sheath Gap Temperatures

Bundle	Element	$T_{grain\ avg}$ (°C)	$T_{gap\ avg}$ (°C)	Element	$T_{grain\ avg}$ (°C)	$T_{gap\ avg}$ (°C)
F12059C	Intermediate	824	331	Outer	992	344
F21271C	Intermediate	793	329	Outer	990	355
G00815W	Intermediate	773	327	Outer	916	336
G13374S	Intermediate	889	335	Outer	1120	364
J49093C	Inner	819	331	Outer	1150	368

4.1.3 Fission Gas Release

The fuel element is divided into ten equal axial segments and the pellet in ten radial concentric annuli. The grain-boundary and gap fractional inventories were calculated using FEMAXI v6.1 outputs for grain-boundary, free and released concentrations [atoms/cm^3]. The code outputs these values for each pellet annular ring and per axial segment. The fractional inventories were calculated as:

$$FR = \frac{\sum_1^{10}\sum_1^{10} c_{ij}V_{ij}}{\sum_1^{10}\sum_1^{10} p_{ij}V_{ij}}$$

Where:

- FR = total fractional inventory (grain-boundary or gap),
- c_{ij} = grain-boundary or gap concentration in annulus i and segment j corrected by decay (atoms/cm^3),
- p_{ij} = amount of atoms produced in annulus i and segment j corrected by decay (atoms/cm^3),
- $V_{ij} = l \times A_{ij}$ = volume of annulus i and segment j (cm^3),
- l = segment length (cm), and
- A_{ij} = annulus cross-sectional area for annulus i and segment j (cm^2).

The percentage of fission gas in the grain, grain boundary and released to the gap are shown in Table 4-2.

Table 4-2: Summary of Xe Fission Gas Inventory in Fuel Grain, Grain Boundary and Gap

Bundle	Element	% FG in: Grain	Grain Boundary	Gap Release	Element	% FG in: Grain	Grain Boundary	Gap Release
F12059C	Intermediate	97.68	2.32	0.00	Outer	94.49	2.59	2.92
F21271C	Intermediate	97.64	2.36	0.00	Outer	93.12	2.61	4.27
G00815W	Intermediate	97.69	2.31	0.00	Outer	95.83	4.10	0.07
G13374S	Intermediate	97.44	2.47	0.09	Outer	90.56	2.42	7.02
J49093C	Inner	97.67	2.33	0.00	Outer	88.96	2.41	8.63

4.1.4 Comparison between Experimental Results and Calculated Results for Xe Release

To confirm that the FEMAXI v6.1 implementation properly modelled the irradiation and fission product distribution of a CANDU fuel element, a comparison was performed between the FEMAXI v6.1 Xe gap release prediction and the measured Xe gap release results, as reported by Stroes-Gascoyne et al. (1987).

Table 4-3 compares the FEMAXI v6.1 release fractions for Xe to the experimental data presented by Stroes-Gascoyne (1996).

The difference between the estimated and measured values is large for the case of fuel element F21271C outer and G13374S outer. To assess the probable origin of this difference, a modified case was run where the fuel-element irradiation power, obtained from COG (2001) was reduced by 5% (The typical uncertainty in the individual fuel bundle power is around 5%). The calculated fission gas release for F21271C outer with a 5% lower power history is shown in Figure 4-1. It is clear from the figure that the typical uncertainty in irradiation power is sufficient to explain the observed difference in the gap release.

Table 4-3: Comparison between FEMAXI v6.1 and Experimental Results (Stroes-Gascoyne et al., 1987) for Xe Gap Releases (%)

Bundle	Element	Calculated	Experimental	Element	Calculated	Experimental
F12059C	Intermediate	0.00	0.09	Outer	2.92	3.44
F21271C	Intermediate	0.00	0.13	Outer	4.27	2.75
G00815W	Intermediate	0.00	~0.06	Outer	0.07	0.17
G13374S	Intermediate	0.09	0.07	Outer	7.02	4.18
J49093C	Inner	0.00	0.07	Outer	8.63	7.03

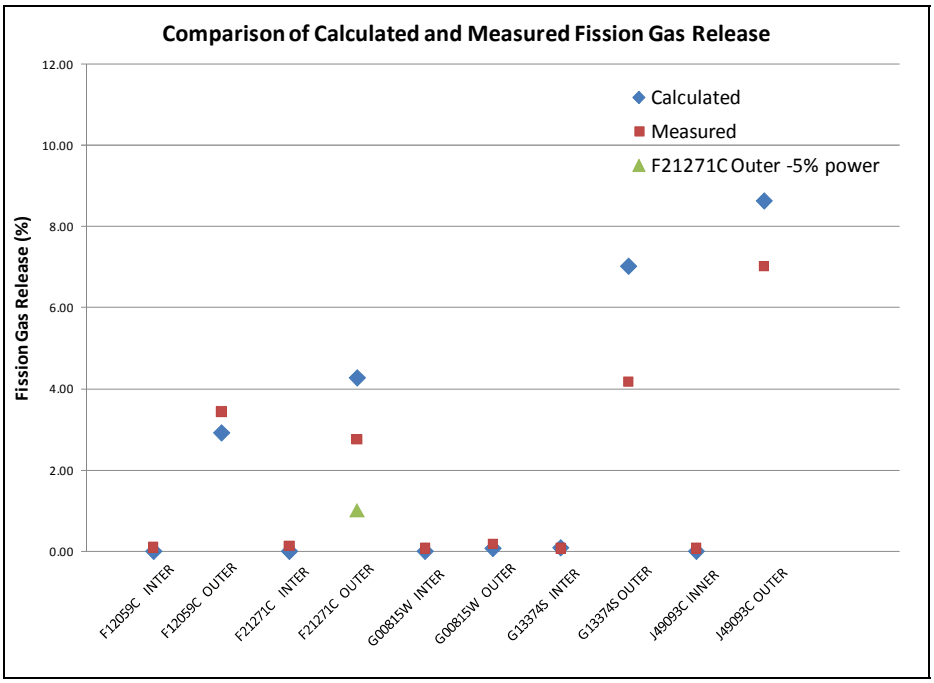

Figure 4-1: Comparison Between Calculated and Experimental Fission Gas Release

In summary, the FEMAXI v6.1 gap release estimates were very good considering the uncertainty in the irradiation power. It is interesting to note that the differences between the FEMAXI v6.1 estimates and experimental data are, in some cases, significantly smaller than the corresponding differences between the ELESIM estimates and experimental data (Stroes-Gascoyne, 1996).

4.1.5 Comparison between Experimental Results and Calculated Releases for Fission Products

The results obtained from the calculations outlined in the previous section were compared with the experimental results for grain-boundary, gap and total release percent for the isotopes ^{137}Cs, ^{129}I, ^{99}Tc and ^{90}Sr. As the specific diffusion coefficients for these isotopes are not reported in the literature, the release calculations were performed assuming that their diffusion coefficients are equal to the Xe diffusion coefficient (see Section 3.1).

As a first approximation, the dissolution of these elements in 0.1 mol/L HCl was assumed to be complete. A confirmation of this assumption by assessing the characteristics of the most stable chemical compounds associated with these isotopes was also performed (see Section 4.1.8).

Table 4-4, Table 4-5 and Table 4-6 present the results for grain-boundary fractional inventories, gap fractional inventories and the instant release fraction (grain-boundary plus gap fractional releases), respectively.

Please note that ^{99}Tc was not included as no values were reported by Stroes-Gascoyne (1996) because the correction for matrix contribution rendered negative IRFs for this isotope.

Also, in Table 4-6, some of the values for ^{137}Cs and ^{90}Sr are flagged as the average of the measured values. In some cases, measured values for the same fuel differ by a factor greater than three.

Table 4-4: Comparison Between FEMAXI v6.1 Estimated Grain-Boundary Fractional Inventories and Reported Values

Sample	Grain-Boundary Fractional Inventories (%)			
	Calculated	^{137}Cs	^{129}I	^{90}Sr
F12059C Inter	2.32	2.7	2.11	NR
F12059C Outer	2.59	-0.61	1.32	NR
F21271C Inter	2.36	2.69	2.17	NR
F21271C Outer	2.61	3.01	1.01	NR
G00815W Inter	2.31	2.91	2.25	NR
G00815W Outer	4.10	4.53	4.2	NR
G13374S Inter	2.47	4.47	1.84	NR
G13374S Outer	2.42	2.31	2.65	NR
J49093C Inner	2.33	2.39	3.25	NR
J49093C Outer	2.41	4	5.5	NR

NR = Not Reported

The grain-boundary fractional inventories predicted by FEMAXI v6.1 agree well with the experimental results as can be seen in Table 4-4, except for G13374S intermediate and J49093C outer. For G13374S intermediate and F21271C outer, the measured values of ^{137}Cs and ^{129}I vary by a factor of about three. Stroes-Gascoyne (1996) provides possible causes for some discrepancies/differences in the reported results.

As for the grain-boundary fractional inventory, it is expected that gap releases of Xe, Cs and I are very close because these fission products are volatile at fuel irradiation temperatures. This can also be observed in the measurements presented in Table 4-5 with the exception of the fuel sample obtained from element J49093C outer, where there is a significant 6-fold difference between ^{137}Cs and ^{129}I gap releases. The cause of this difference is not specifically addressed by Stroes-Gascoyne (1996) and no modelling explanation could be found to explain the apparent FEMAXI v6.1 overestimation of the gap fractional inventory for this sample. However, as the measured grain-boundary inventory is determined as the difference between the measured gap plus grain inventory minus the measured gap inventory (Stroes-Gascoyne, 1996), this could also partially explain the apparent FEMAXI v6.1 underprediction for this sample in Table 4-4. Similarly, no reason could be found for the FEMAXI v6.1 overestimation of the gap inventories for sample G13374S outer for ^{137}Cs and ^{129}I. However, it is important to note that for this sample, the measured gap release for Xe are significantly larger that the corresponding values for ^{137}Cs or ^{129}I despite the similarity between these releases for the other samples. This may indicate experimental discrepancies during measurements.

Table 4-5: Comparison Between FEMAXI v6.1 Estimated Gap Fractional Inventories and Reported Values

Sample	Average Linear Power (kW/m) (Stroes-Gascoyne, 1996)	Gap Fractional Inventories (%)				
		Calculated	^{137}Cs	^{129}I	^{90}Sr	Xe
F12059C Inter	38	0.00	0.01	0.01	NR	0.09
F12059C Outer	46	2.92	2.81	1.29	NR	3.44
F21271C Inter	39	0.00	0.05	0.01	NR	0.13
F21271C Outer	47	4.27	1.35	2.5	NR	2.75
G00815W Inter	33	0.00	0.01	0.02	NR	0.07
G00815W Outer	41	0.07	0.02	0.02	NR	0.17
G13374S Inter	42	0.09	0.01	BDL	NR	0.07
G13374S Outer	50	7.02	1.6	0.14	NR	4.18
J49093C Inner	37	0.00	0.01	BDL	NR	0.07
J49093C Outer	50	8.63	5.57	0.94	NR	7.03

NR = Not reported
BDL= Below detection limit

Table 4-6 shows that FEMAX-6.1-predicted IRFs and measured IRFs are in good agreement with the exception of sample G13374S outer, as discussed above.

Table 4-6: Comparison Between FEMAXI v6.1 Calculated Instant Release Fractions and Reported Values for Fission Products

Sample	Instant Release Fractions (%)			
	Calculated	^{137}Cs	^{129}I	^{90}Sr
F12059C Inter	2.32	2.71	2.12	1.65
F12059C Outer	5.51	2.2	2.61	2.74
F21271C Inter	2.36	2.74	2.18	3.34
F21271C Outer	6.88	4.36	3.51	2.87
G00815W Inter	2.31	2.92	2.27	3.46
G00815W Outer	4.17	4.45*	4.21	2.86*
G13374S Inter	2.56	4.48*	1.84	2.92*
G13374S Outer	9.44	3.18*	2.79	2.35*
J49093C Inner	2.33	4.01*	5.5	2.37
J49093C Outer	11.04	7.96*	4.19	3.9

**Average of reported values (Stroes-Gascoyne, 1996)*

4.1.6 Sensitivity of Results to Diffusion Coefficient Selection

To test the sensitivity of the results to the estimated diffusion coefficient used in the FEMAXI v6.1 calculations, a sensitivity study was carried out. The reference case used in the sensitivity study and the variations between cases are described below. The results of each case considered in the sensitivity analysis are presented in Table 4-7.

The Turnbull diffusion coefficient used in FEMAXI v6.1 (Suzuki and Hiroaki, 2005) is defined as:

$$D = 7.6\times10^{-10}\exp\left(\frac{-7\times10^{4}}{RT}\right)+\frac{S^{2}\,j\upsilon V}{2\times10^{-40}F}\ \text{m}^2/\text{s}$$

Where:

- R: gas constant = 1.987 (cal/mol/K),
- T: temperature (K),
- S: atom jump distance = $\Omega^{1/3}$,
- Ω: atom volume = 4.09×10^{-29} (m^3),
- $j\upsilon$: $10^{13}\exp(-5.52\times10^{4}/RT)$,

$$V=\frac{\left(\partial_s S^2+ZV_0\right)}{2Z}\left[\left(1+\frac{4K'Z}{j\upsilon\left(\partial_s S^2+ZV_0\right)^2}\right)^{\frac{1}{2}}-1\right]$$

- ∂_s: sink intensity = 10^{15} (m^{-2}),
- Z: number of lost points = 2,
- K': loss ratio per atom = 10^{4},
- V_0: $\exp(-5.52\times10^{4}/RT)$, and
- F: fission rate = 10^{19} fissions/m^3.s.

The first term in the expression for the diffusion coefficient is due to high-temperature intrinsic effects, the second term is for intermediate temperature effects from vacancy-enhanced diffusion and the last low-temperature term accounts for athermal effects. A review of experimental investigations into the diffusion coefficient of noble gases in uranium dioxide was conducted by Lawrence (1978). A large spread in the results of experimental data was observed. From the review of experimental results, uncertainty in the diffusion coefficients is observed to be approximately within a factor of 4 (i.e., 2 times greater or smaller). In the conclusion of the work performed by Lawrence, a diffusion coefficient for low burnup sintered uranium dioxide fuel is given as:

$$D = 7.6\times10^{-6}\exp\left(\frac{-7000}{RT}\right)\ \text{cm}^2/\text{s}$$

Six cases were therefore considered for the sensitivity analysis. The reference case selected for the sensitivity analysis is the outer element from a 900 kW bundle with a burnup of 220 MWh/kgU, using the reference Turnbull diffusion coefficient. Consistent with the reported uncertainty in the noble gas diffusion coefficient, five other cases were defined as described in Table 4-7.

Table 4-7: Sensitivity of Calculated Xe Fractional Fission Gas Inventory in Fuel Grain, Grain Boundary and Gap (%) to Diffusion Coefficient for Outer Element from 900 kW Bundle with 220 MWh/kgU Burnup

Diffusion Coefficient	Grain	Boundary	Release
Turnbull	77.3	8.5	14.1
1/2 x Turnbull	80.4	6.9	12.8
2 x Turnbull	74.0	10.0	16.1
1/5 x Turnbull	84.7	5.3	10.0
5 x Turnbull	69.2	12.6	18.2
Lawrence's diffusion coefficient (Lawrence, 1978)	77.6	8.3	14.1

As expected, the calculated Xe release is larger than for the reference case when the diffusion coefficient is multiplied by a factor >1 and the Xe release is smaller than for the reference case when it is multiplied by a factor <1. Use of Lawrence's diffusion coefficient (Lawrence, 1978) yields results that are very similar to those with the Turnbull diffusion coefficient. Lawrence's diffusion coefficient is the same as the first term on the right hand side of the Turnbull equation. This implies that the second term on the right hand side of the Turnbull equation plays a very small role in the diffusion coefficient, when applied to CANDU fuel (i.e., relevant to intermediate temperature effects).

In the most extreme cases (1/5 x Turnbull and 5 x Turnbull), the variation of fission gas released to the gap is approximately ±30% difference, relative to the reference case.

4.1.7 Parameters of the Uncertainty Distribution Extracted from Results of Task 1

Task 1 of this work involved an ORIGEN-S/FEMAXI v6.1 model calculation of the IRFs of I, Cs and Sr for the ten analyzed CANDU fuel elements. These calculated IRFs are compared in Table 4-6 with the experimental results of Stroes-Gascoyne (1996).

Applying standard techniques for estimating parameters of statistical distributions Korn & Korn, (2000), results from Table 4-3 were used as a statistical sample to estimate the average and the standard deviation of the calculation uncertainty. The underlying assumption for such an estimate is that the magnitude of the computational errors is similar for all the evaluated cases, regardless of the actual release value. In particular the error was assumed to be normally distributed with a given standard deviation around their centre (average) value. Using the values from Table 4-3, the average uncertainty in the Xe release is $\langle x \rangle = 0.5\%$ while the standard deviation is $\sigma = 1.1$.

The graphical representation of the calculated uncertainties distributed around their average is given in Figure 4-2. The "one standard deviation" band $[\langle x \rangle - \sigma, \langle x \rangle + \sigma] \approx [-0.6, 1.6]$ around the average uncertainty is also shown in the figure. It can be seen that most of the sample uncertainties are closely grouped around the average value.

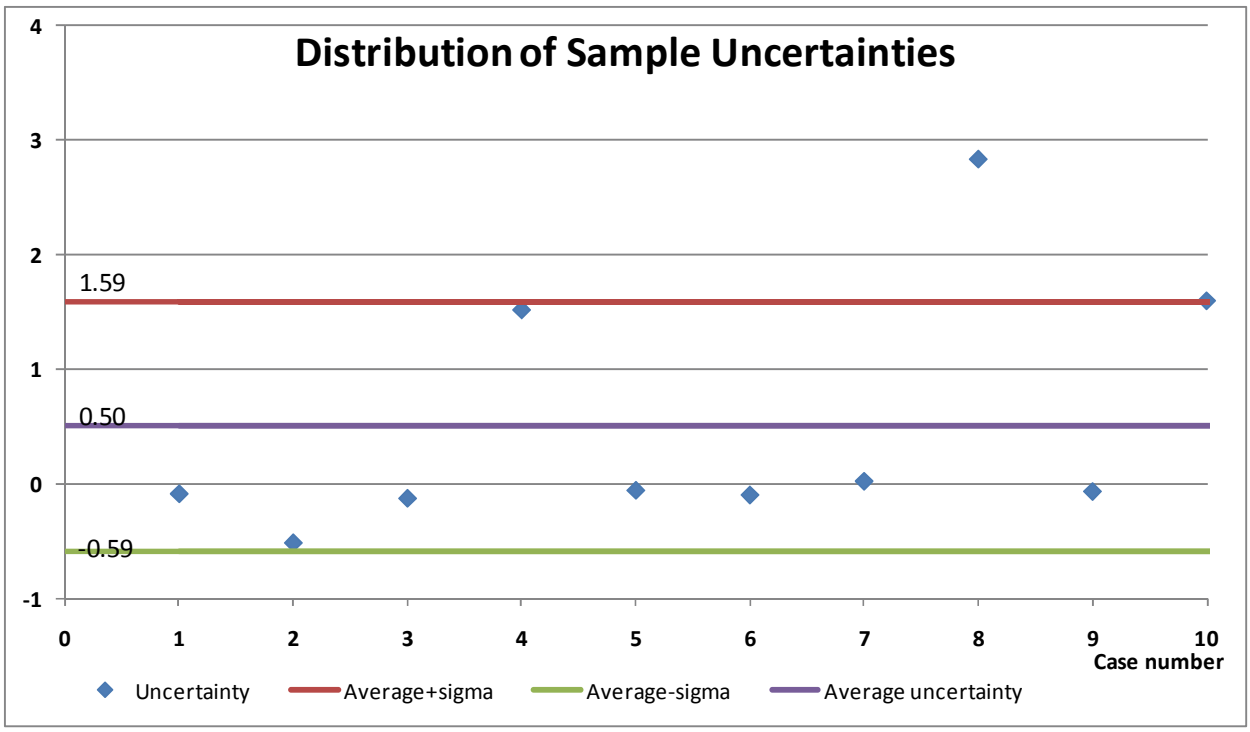

Figure 4-2: Graphical Representation of the Distribution of the ORIGEN-S/FEMAXI v6.1 Calculation Uncertainties

4.1.8 Fission Product Chemical Speciation

For the cases listed in Table 2-1, the mass inventories at the grain-boundary and/or gap releases and the estimated temperatures at irradiation were calculated and used as inputs to the Gibb's minimization algorithm, along with the included in the database that contains all relevant thermodynamic properties for the chemical elements listed in Section 2.1.

The following cases were considered for this assessment:

Case 2B = F12059C Outer – Grain Boundary
Case 2R = F12059C Outer – Gap
Case 4R = F21271C Outer – Gap
Case 6B = G00815W Outer – Grain Boundary
Case 8R = G13374S Outer – Gap
Case 9B = GJ49093C Outer – Grain Boundary

The results of this calculation give the amounts and species of the most important compounds: (i) volatile species within an inert gas phase, (ii) soluble fission products in the fuel oxide (iii) solid solution U(Pd-Rh-Ru)3, (iv) noble metals inclusions (Mo, Rh, Pd, Ru, Tc) in BCC and HCP crystallographic form, and (v) other solids and liquids compounds (Lewis et al. 2011; Kaye et al., 2007; Thompson et al., 2007; Piro et al., 2010).

The assessment of the solubility of the chemical species of interest was determined by assessing chemical reactions of the type:

$$0.1 \text{ mol HCl} + 55.5 \text{ mol } H_2O + \text{species} \rightarrow \text{Products}$$

Ten reactions were considered, based on the estimated compounds found not associated with the gaseous phase, uranium solid solutions or metallic inclusions. These reactions were:

Reaction 1: 0.1 mol HCl + 55.5 mol H_2O + CsI
Reaction 2: 0.1 mol HCl + 55.5 mol H_2O + Cs_2Te
Reaction 3: 0.1 mol HCl + 55.5 mol H_2O + BaI_2
Reaction 4: 0.1 mol HCl + 55.5 mol H_2O + RbI
Reaction 5: 0.1 mol HCl + 55.5 mol H_2O + $Tc_{11}Mo_9$
Reaction 6: 0.1 mol HCl + 55.5 mol H_2O + BaSe
Reaction 7: 0.1 mol HCl + 55.5 mol H_2O + BaO
Reaction 8: 0.1 mol HCl + 55.5 mol H_2O + Ba_2Pb
Reaction 9: 0.1 mol HCl + 55.5 mol H_2O + Rb
Reaction 10: 0.1 mol HCl + 55.5 mol H_2O + Cs

The results of these reactions at 298.15 K and atmospheric pressure are summarized in Table 4-8, where column 1 identifies the chemical reaction number, column 2 identifies the species, columns 3 to 8 indicate if the species was present in the particular case and the last column shows the results of the solubility assessment.

From the species considered, only three were estimated to be non-soluble. These species involved significant quantities of the chemical elements Te, Tc, and Pb.

It is of particular interest to point out that the estimated insolubility of Tc was consistent with the results reported by Stroes-Gascoyne (1996), where inconclusive results of the presence of Tc in the solute were indicated.

Table 4-8: Solubility Assessment of Species of Interest

Reaction	Species	Case 2B	Case 2R	Case 4R	Case 6B	Case 8R	Case 9B	Soluble?
1a	$CsI_{(sol)}$	No	Yes	Yes	No	Yes	No	Yes
1b	$CsI_{(liq)}$	Yes	No	No	Yes	No	Yes	Yes
2	$Cs_2Te_{(s)}$	Yes	Yes	Yes	No	Yes	Yes	No
3	$BaI_{2\ (liq)}$	No	No	No	No	No	Yes	Yes
4	$RbI_{(liq)}$	No	No	No	No	No	Yes	Yes
5	$Tc_{11}Mo_{9\ (s)}$	No	Yes	Yes	No	Yes	Yes	No
6	$BaSe_{(s)}$	Yes	Yes	Yes	Yes	Yes	Yes	Yes
7	$BaO_{(s)}$	No	Yes	Yes	No	Yes	No	Yes
8	$Ba_2Pb_{(s)}$	No	Yes	Yes	No	Yes	No	No
9	$Rb_{(liq)}$	No	Yes	Yes	No	Yes	No	Yes
10	$Cs_{(liq)}$	No	Yes	Yes	Yes	Yes	No	Yes

4.2 Calculation of Average and Pessimistic Instant Release Fractions

4.2.1 Fission Product Inventories

As stated in Section 2.2, inventory calculations were carried out for fuel bundles irradiated in the Bruce nuclear plant. The geometry of these bundles follows the standard 37-element bundle design. The bundle calculations were broken down into four groups of elements (outer,

intermediate, inner and centre) because each of these groups is irradiated at different powers as a result of the bundle radial power distribution. The bundle radial power distribution used for this Task is indicated in Section 2.2.

ORIGEN-S (Gauld et al., 2009) was run to simulate inventories for the four fuel bundle cases listed in Table 2-2 (including 30 years of decay). The output comprises total inventories of selected fission products which are generated during the irradiation and decay of the analyzed fuel elements. These fission products include the following chemical elements (Xe+Kr), Mo, Ru, Cs, Pd, Ba, Tc, Rh, Sr, Te, Rb, I, Ag, Cd, Sn, Se, Br, Sb, H, Pb, Bi, U, and O_2.

As described in Section 4.1.1, for each of the four fuel bundles that were analyzed four tables of ORIGEN-S output files were prepared. The results of the inventory calculations for the four fuel bundles are compiled in Appendix A.

As the 37 elements in the bundles are grouped into four types (18 outer elements, 12 intermediate elements, 6 inner elements and 1 centre element), 16 runs were performed to properly simulate fuel element conditions. For each fuel element in the average and pessimistic irradiated bundles, temperatures were obtained from FEMAXI v6.1 analysis at the last burnup step. This step was selected because for the type of irradiation history used for these bundles, the temperatures at the pellet centerline, pellet surface and sheath inner surface corresponding to this step were the most representative of the irradiation. These calculations were performed using the same equations used in Section 4.1.2.

The calculated values for the average grain-boundary temperature and average gap temperature (in ^{o}C) for the ten fuel elements under consideration are shown in Table 4-9.

Table 4-9: Calculated Fuel Grain and Fuel-to-Sheath Gap Temperatures (^{o}C)

Case		Outer		Intermediate		Inner		Centre	
Power	Burnup	Grain	Gap	Grain	Gap	Grain	Gap	Grain	Gap
450 kW	220 MWh/kgU	633.1	317.0	563.2	310.9	531.7	307.9	529.0	307.7
450 kW	320 MWh/kgU	652.5	317.8	578.3	311.2	544.9	308.1	541.7	307.8
900 kW	220 MWh/kgU	1283.3	411.4	1018.0	369.5	873.6	342.7	875.8	345.8
900 kW	320 MWh/kgU	1412.4	455.0	1170.9	417.6	1022.7	389.6	1004.1	385.3

4.2.2 Fission Gas Release

As mentioned in the previous section, the 37 elements in the bundles are grouped into four types (18 outer elements, 12 intermediate elements, 6 inner elements and 1 centre element). Thus, 16 runs were performed to properly simulate fuel element conditions. Each fuel element was also divided into ten equal axial segments and ten pellet radial concentric annuli. The grain-boundary and gap fractional inventories were calculated using FEMAXI v6.1 outputs for grain-boundary, and released concentrations (atoms/cm^3). The code outputs these values for each pellet annular ring and per axial segment. The fractional inventories were calculated by using the formula described in Section 4.1.3.

For each element, weighted fractional releases were calculated, as part of the total inventory. The percentage of fission gas in the grain, grain boundary and gap are shown in Table 4-10. Table 4-11 presents the IRF for the bundle and each type of element.

Table 4-10: Summary of Se Fission Gas Inventory in Fuel Grain, Grain Boundary and Gap Calculated Fission Gas Inventories (%)

Case		Outer			Intermediate			Inner			Centre		
Power (kW)	Burnup MWh/kgU	Grain	Grain Boundary	Gap Release	Grain	Grain Boundary	Gap Release	Grain	Grain Boundary	Gap Release	Grain	Grain Boundary	Gap Release
450	220	97.7	2.3	0.0	97.7	2.3	0.0	97.7	2.3	0.0	97.7	2.3	0.0
450	320	97.7	2.3	0.0	97.7	2.3	0.0	97.7	2.3	0.0	97.7	2.3	0.0
900	220	77.3	8.5	14.1	86.5	7.0	6.5	93.5	5.1	1.4	93.6	5.1	1.3
900	320	68.3	8.1	23.6	76.2	7.8	16.0	84.4	6.5	9.0	85.7	6.4	8.0

Table 4-11: FEMAXI v6.1 Estimated Instant Release Fractions for the Average and Pessimistic Power Histories

Case		Instant Release Fractions (%)				
Power (kW)	Burnup (MWh/kgU)	Outer	Intermediate	Inner	Centre	Total
450	220	2.3	2.3	2.3	2.3	2.3
450	320	2.3	2.3	2.3	2.3	2.3
900	220	22.7	13.5	6.5	6.4	16.6
900	320	31.7	23.8	15.6	14.3	26.1

4.2.3 Fission Product Chemical Speciation

From the cases listed in Table 2-2, case 900 kW - 320 MWh/kgU was selected for chemical speciation calculations. As the calculated inventories of radionuclides of interest at grain boundaries and gap are larger, it was considered of more significance for this work. For this case, the mass inventories at the grain-boundary and gap releases and the estimated temperatures at irradiation were calculated and used as inputs to the Gibb's minimization algorithm along with the database that contains all relevant thermodynamic properties for the chemical elements listed in Section 2.2. The species were calculated at the gap temperatures and pressures. Appendix C details the temperatures and pressures that the speciation calculations took into consideration.

The results of this calculation show the amounts and species of the most important compounds: (i) volatile species within an inert gas phase, (ii) soluble fission products in the fuel oxide, (iii) solid solution U(Pd-Rh-Ru)3, (iv) noble metals inclusions (Mo, Rh, Pd, Ru, Tc) in BCC and HCP crystallographic form, and (v) other solid and liquid compounds (Lewis et al., 2011; Kaye et al., 2007; Thompson et al., 2007; Piro et al., 2010).

The mass of O_2 was calculated from the mass of U present in each case. The molar mass of U is 238.029 g/mol while the molar mass of O_2 is 32 g/mol. Table 4-12 shows the input parameters for both the noble gas and O_2. The reported values were obtained using the calculated inventories and the fractional releases. Appendix C shows the amounts of the other fission products under consideration.

Table 4-12: Selected Amounts of Main Species in Grain Boundaries and Gap in Fuel Element

Grain Boundaries

Element Type	Xe (g)	Kr (g)	U (g)	U (mol)	O_2 (mol)	O_2 (g)
Outer	1.96	0.101	9150	38.441	38.441	1230.100
Inter	1.03	0.0533	6100	25.627	25.627	820.040
Inner	0.385	0.0199	3050	12.814	12.814	410.030
Centre	0.0625	0.00323	508	2.134	2.134	68.294

Gap

Element Type	Xe (g)	Kr (g)	U (g)	U (mol)	O_2 (mol)	O_2 (g)
Outer	5.69	0.294	9150	38.441	38.441	1230.100
Inter	2.11	0.109	6100	25.627	25.627	820.040
Inner	0.535	0.0276	3050	12.814	12.814	410.030
Centre	0.0780	0.00403	508	2.134	2.134	68.294

From the results in Appendix C, it can be seen that in the grain boundaries, the most abundant species were those fission products which are stable as oxides but are incompatible with the UO_2 matrix and thus separate into precipitates, often referred to as grey phases. These are mainly the oxides of Cs, Sr, and Ba.

Appendix C also presents the estimated amount of the various chemical species in the gap. The species were calculated at the gap temperatures and pressures.

It summary, the formation of chemical species is not related to the location of the fuel element within the 37-element fuel bundle (outer, intermediate, inner or centre) but is a function of the irradiation time and power. As can be seen from the results in Appendix C:

- the gas phase is dominated by xenon and krypton with some cesium iodide,
- the fluorite phase consists of metal oxides dissolved in the UO_2 matrix,
- the U(Pd-Rh-Ru)3 phase comprises the metals binding with uranium,
- the HCP and BCC phases include the species stable as metals rather than oxides mainly (Mo, Ru, Tc), and
- the remainder of the chemical species expected to form in the bundle are predominantly $Tc_{11}Mo_9(s)$, $Cs_2Te(s)$, and BaSe(s).

5. CONCLUSIONS

5.1 Evaluation of Experimental Instant Release Fractions

From the results presented in this report it can be concluded that:

- On average, the FEMAXI v6.1 estimates of IRFs are considered fairly good with a slight tendency to overestimate IRFs (Stroes-Gascoyne, 1996),
- The average uncertainty in the calculated IRF for Xe was estimated to be 0.5%, and
- The assumption of complete dissolution in 0.1 mol/L HCl of the compounds for Cs, I and Sr, was confirmed, while compounds of Te, Tc and Pb were likely to be poorly soluble or insoluble.

5.2 Calculation of Average and Pessimistic Instant Release Fractions

The IRFs were calculated for four fuel bundle conditions, representing average and pessimistic conditions (Table 1).

The calculated release for the average power bundle cases showed insignificant variation in the percent of IRF with burnup and radial location in the bundle. This was because the fuel element linear powers were low and the thermally activated release processes are not dominant contributors in comparison to the release mechanisms which are independent of temperature.

Calculated release for the pessimistic power cases show a marked dependency on the burnup, the radial location of the grain boundary inventories in the bundle and the gap inventories.

At grain boundaries conditions, the chemical speciation calculations showed:

- The principal components in the gas phase were Xe, Kr, CsI, Rb and Cd,
- The fluorite phase showed, in addition to UO_2, the presence of Cs_2O, (species dissolved in the UO_2 matrix),
- The metal precipitates were mainly composed of Mo, Tc and Ru, and
- Cs_2Te is the most abundant (non-fluorite) solid followed by BaSe, and CsI and Ag as liquids.

At gap conditions, the chemical speciation showed:

- The principal components in the gas phase were Xe, Kr, Cs, and Rb,
- The fluorite phase showed, in addition of UO_2, the presence of and Cs_2O, BaO and SrO,
- The metal precipitates were mainly composed of Mo, Te and Ru, and
- BaO is the most abundant non-fluorite solid followed by Cs_2Te and $Tc_{11}Mo_9$.

REFERENCES

CANDU Owners Group (COG). 2001. ELESTRES-IST 1.0: Theory Manual. COG Report COG-00-191. Toronto, Ontario.

Gauld, I. C., O. W. Hermann and R. M. Westfall. 2009. ORIGEN-S: SCALE system module to calculate fuel depletion, actinide transmutation, fission product buildup and decay, and associated radiation source terms. Oak Ridge National Laboratory ORNL/TM-2005/39. USA.

Hocking, W. H., A. M. Duclos and L. H. Johnson. 1994. Study of fission-product segregation in used CANDU fuel by X-ray photoelectron spectroscopy (XPS) II. Journal of Nuclear Materials 209, 1.

Kaye, M. H., B. J. Lewis and W. T. Thompson. 2007. Thermodynamic treatment of noble metal fission products in nuclear fuel. Journal of Nuclear Materials 366, 8.

Korn, G. A. and T. M. Korn. 2000. Mathematical handbook for scientists and engineers. Dover Publications, Inc.

Lawrence, G. T. 1978. A review of the diffusion coefficient of fission-product rare gases in uranium dioxide. Journal of Nuclear Materials 71,195.

Lewis, B. J., B. Andre, G. Ducros and D. Maro. 1996. A model for nonvolatile fission product release during reactor accident conditions. Nuclear Technology 116, 34.

Lewis, B. J., B.J. Corse, W.T. Thompson, M.H. Kaye, F.C. Iglesias, P. Elder, R. Dickson and Z. Liu. 1998. Low volatile fission-product release and fuel volatilization during severe reactor accident conditions Journal of Nuclear Materials 252, 235.

Lewis, B. J., R. Dickson, F.C. Iglesias and G. Ducros. 2008. Overview of experimental programs on core melt progression and fission product release behaviour. Journal of Nuclear Materials 380, 126.

Lewis, B. J., W. T. Thompson and F. C. Iglesias. 2011. Fission product chemistry in oxide fuels. In R. Konings (Ed.), Comprehensive Nuclear Materials. Elsevier Press, in press.

Liu. 1998. Low volatile fission-product release and fuel volatilization during severe reactor accident conditions Journal of Nuclear Materials 252, 235.

Piro, M. H., G.M.F. Bruni, B.J. Lewis, W.T. Thompson, F.C. Iglesias, M.A. Guoping, R. Nashiem and J.G. Roberts. 2010. Computation of actinide Pourbaix diagrams at 298 K and 550 K (U,Np,Pu,Am,Cm – H_2O). CANDU Fuel Conference, Niagara Falls, October 18, 2010. Niagara Falls, Ontario.

Prussin, S.G., D.R. Olander, W.K. Lau, L. Hansson. 1988, Release of fission products (Xe, I, Te, Cs, Mo and Tc) from policrystatine UO_2. Journal of Nuclear Materials 154, 25.

Stroes-Gascoyne, S. 1996. Measurement of instant-release source terms for Cs-137, Sr-90, Tc-99, I-129 and C-14 in used CANDU fuels. Journal of Nuclear Materials 238, 264. Elsevier B.V.

Stroes-Gascoyne, S., L. H. Johnson and D. M. Sellinger. 1987. The relationship between gap inventories of stable xenon, 137Cs, and 129I in used CANDU fuel. Nuclear Technology 77, 320.

Suzuki, M., and S. Hiroaki. 2005. Light Water Reactor Fuel Analysis Code FEMAXI-6 (Ver. 1) Detailed Structure and User's Manual. JAEA Document JAEA-Data/Code 2005-003.

Thompson, W.T., B.J. Lewis, E.C. Corcoran, M.H. Kaye, S.J. White, F. Akbari, Z. He, R. Verrall, J.D. Higgs, D.M. Thompson, T.M. Besmann, S.C. Vogel. 2007. Thermodynamic treatment of uranium dioxide based nuclear fuel. International Journal of Materials Research 98(10), 1004.

APPENDIX A: ORIGEN-S OUTPUT TABLES

CONTENTS

Page

A.1 EVALUATION OF EXPERIMENTAL INSTANT RELEASE FRACTIONS

Table A-1: CANDU F21271C outer (burnup=328 MWh/kgU, linear power=47 kW/m). Decay. Masses of chemical elements (g).

Time (y)	1.00E-03	3.00E-03	1.00E-02	3.00E-02	1.00E-01	3.00E-01	1.00E+00	3.00E+00	7.00E+00
U	5.03E+02	5.03E+02	5.03E+02	5.03E+02	5.03E+02	5.03E+02	5.03E+02	5.03E+02	5.03E+02
Xe	1.22E+00	1.22E+00	1.22E+00	1.22E+00	1.22E+00	1.22E+00	1.22E+00	1.22E+00	1.22E+00
Mo	6.32E-01	6.32E-01	6.33E-01	6.35E-01	6.46E-01	6.71E-01	6.95E-01	6.96E-01	6.96E-01
Cs	5.56E-01	5.57E-01	5.59E-01	5.61E-01	5.62E-01	5.60E-01	5.53E-01	5.35E-01	5.08E-01
Ru	6.01E-01	6.00E-01	5.98E-01	5.93E-01	5.80E-01	5.58E-01	5.30E-01	5.02E-01	4.94E-01
Pd	2.99E-01	2.99E-01	3.00E-01	3.01E-01	3.05E-01	3.13E-01	3.36E-01	3.63E-01	3.72E-01
Ba	2.88E-01	2.87E-01	2.86E-01	2.82E-01	2.77E-01	2.77E-01	2.85E-01	3.02E-01	3.29E-01
Tc	1.77E-01	1.77E-01	1.78E-01	1.79E-01	1.79E-01	1.79E-01	1.79E-01	1.79E-01	1.79E-01
Sr	1.74E-01	1.74E-01	1.73E-01	1.72E-01	1.68E-01	1.62E-01	1.57E-01	1.52E-01	1.44E-01
Rh	1.03E-01	1.03E-01	1.04E-01	1.08E-01	1.18E-01	1.31E-01	1.36E-01	1.36E-01	1.36E-01
Te	1.09E-01	1.08E-01	1.07E-01	1.06E-01	1.05E-01	1.04E-01	1.04E-01	1.05E-01	1.06E-01
Kr	6.63E-02	6.63E-02	6.63E-02	6.63E-02	6.63E-02	6.62E-02	6.60E-02	6.55E-02	6.47E-02
Rb	5.97E-02	5.97E-02	5.97E-02	5.97E-02	5.97E-02	5.98E-02	6.00E-02	6.05E-02	6.13E-02
I	5.88E-02	5.81E-02	5.69E-02	5.54E-02	5.41E-02	5.47E-02	5.53E-02	5.54E-02	5.54E-02
Se	1.08E-02	1.08E-02	1.08E-02	1.08E-02	1.08E-02	1.08E-02	1.08E-02	1.08E-02	1.08E-02
H	1.17E-05	1.17E-05	1.17E-05	1.17E-05	1.17E-05	1.15E-05	1.11E-05	9.91E-06	7.91E-06
Pb	9.51E-13	9.59E-13	9.88E-13	1.08E-12	1.43E-12	2.84E-12	1.29E-11	8.65E-11	3.99E-10
Bi	1.11E-15	1.14E-15	1.15E-15	1.25E-15	1.53E-15	2.19E-15	4.23E-15	1.01E-14	1.87E-14
Rn	1.19E-17	1.20E-17	1.23E-17	1.31E-17	1.62E-17	2.60E-17	6.05E-17	1.68E-16	3.72E-16
Total	5.13E+02	5.13E+02	5.13E+02	5.13E+02	5.13E+02	5.13E+02	5.13E+02	5.13E+02	5.13E+02

Table A-2: CANDU F21271C outer (burnup=328 MWh/kgU, linear power=47 kW/m). Decay. Masses of isotopes (g)

Time (y)	1.00E-03	3.00E-03	1.00E-02	3.00E-02	1.00E-01	3.00E-01	1.00E+00	3.00E+00	7.00E+00
Cs137	2.73E-01	2.73E-01	2.73E-01	2.73E-01	2.72E-01	2.71E-01	2.67E-01	2.55E-01	2.32E-01
Tc99	1.77E-01	1.77E-01	1.78E-01	1.79E-01	1.79E-01	1.79E-01	1.79E-01	1.79E-01	1.79E-01
Sr90	9.79E-02	9.79E-02	9.79E-02	9.78E-02	9.76E-02	9.72E-02	9.55E-02	9.09E-02	8.24E-02
I129	4.18E-02	4.19E-02	4.19E-02	4.21E-02	4.26E-02	4.31E-02	4.33E-02	4.33E-02	4.33E-02
C14	5.60E-09	5.60E-09	5.60E-09	5.60E-09	5.60E-09	5.60E-09	5.60E-09	5.60E-09	5.59E-09

Table A-3: CANDU F21271C intermediate (burnup=261 MWh/kgU, linear power=39 kW/m). Decay. Masses of chemical elements (g).

Time (y)	1.00E-03	3.00E-03	1.00E-02	3.00E-02	1.00E-01	3.00E-01	1.00E+00	3.00E+00	7.00E+00
U	5.05E+02	5.05E+02	5.05E+02	5.05E+02	5.05E+02	5.05E+02	5.05E+02	5.05E+02	5.05E+02
Xe	9.60E-01	9.61E-01	9.61E-01	9.61E-01	9.61E-01	9.62E-01	9.62E-01	9.62E-01	9.62E-01
Mo	5.04E-01	5.04E-01	5.04E-01	5.06E-01	5.16E-01	5.36E-01	5.57E-01	5.58E-01	5.58E-01
Cs	4.45E-01	4.45E-01	4.47E-01	4.49E-01	4.50E-01	4.48E-01	4.43E-01	4.30E-01	4.09E-01
Ru	4.61E-01	4.61E-01	4.59E-01	4.56E-01	4.45E-01	4.28E-01	4.07E-01	3.87E-01	3.81E-01
Pd	2.12E-01	2.12E-01	2.13E-01	2.14E-01	2.16E-01	2.23E-01	2.39E-01	2.59E-01	2.66E-01
Ba	2.31E-01	2.30E-01	2.29E-01	2.26E-01	2.21E-01	2.21E-01	2.27E-01	2.40E-01	2.61E-01
Tc	1.42E-01	1.42E-01	1.43E-01	1.44E-01	1.44E-01	1.44E-01	1.44E-01	1.44E-01	1.44E-01
Sr	1.49E-01	1.49E-01	1.48E-01	1.47E-01	1.43E-01	1.38E-01	1.33E-01	1.29E-01	1.22E-01
Rh	8.25E-02	8.27E-02	8.35E-02	8.65E-02	9.48E-02	1.05E-01	1.09E-01	1.09E-01	1.09E-01
Te	8.57E-02	8.53E-02	8.44E-02	8.33E-02	8.26E-02	8.20E-02	8.18E-02	8.24E-02	8.29E-02
Kr	5.57E-02	5.57E-02	5.57E-02	5.57E-02	5.57E-02	5.56E-02	5.55E-02	5.50E-02	5.43E-02
Rb	5.04E-02	5.04E-02	5.04E-02	5.04E-02	5.04E-02	5.05E-02	5.06E-02	5.10E-02	5.18E-02
I	4.60E-02	4.54E-02	4.44E-02	4.31E-02	4.21E-02	4.26E-02	4.30E-02	4.31E-02	4.31E-02
Se	8.86E-03	8.86E-03	8.86E-03	8.86E-03	8.86E-03	8.86E-03	8.86E-03	8.86E-03	8.86E-03
H	9.21E-06	9.21E-06	9.21E-06	9.20E-06	9.16E-06	9.06E-06	8.71E-06	7.78E-06	6.22E-06
Pb	6.75E-13	6.81E-13	7.02E-13	7.66E-13	1.02E-12	2.05E-12	9.29E-12	6.07E-11	2.73E-10
Bi	7.38E-16	7.59E-16	7.64E-16	8.27E-16	1.02E-15	1.48E-15	2.91E-15	6.85E-15	1.26E-14
Rn	9.03E-18	9.09E-18	9.30E-18	9.93E-18	1.22E-17	1.96E-17	4.51E-17	1.26E-16	2.94E-16
Total	5.13E+02	5.13E+02	5.13E+02	5.13E+02	5.13E+02	5.13E+02	5.13E+02	5.13E+02	5.13E+02

Table A-4: CANDU F21271C intermediate (burnup=261 MWh/kgU, linear power=39 kW/m). Decay. Masses of isotopes (g).

Time (y)	1.00E-03	3.00E-03	1.00E-02	3.00E-02	1.00E-01	3.00E-01	1.00E+00	3.00E+00	7.00E+00
Cs137	2.17E-01	2.17E-01	2.17E-01	2.17E-01	2.16E-01	2.15E-01	2.12E-01	2.02E-01	1.84E-01
Tc99	1.42E-01	1.42E-01	1.43E-01	1.44E-01	1.44E-01	1.44E-01	1.44E-01	1.44E-01	1.44E-01
Sr90	8.33E-02	8.33E-02	8.33E-02	8.32E-02	8.31E-02	8.27E-02	8.13E-02	7.73E-02	7.01E-02
I129	3.27E-02	3.27E-02	3.28E-02	3.29E-02	3.33E-02	3.38E-02	3.39E-02	3.39E-02	3.39E-02
C14	4.46E-09	4.46E-09	4.46E-09	4.46E-09	4.46E-09	4.46E-09	4.46E-09	4.46E-09	4.46E-09

Table A-5: CANDU F12059C outer (burnup=264 MWh/kgU, linear power=46 kW/m). Decay. Masses of chemical elements (g).

Time (y)	1.00E-03	3.00E-03	1.00E-02	3.00E-02	1.00E-01	3.00E-01	1.00E+00	3.00E+00	7.00E+00
U	5.05E+02	5.05E+02	5.05E+02	5.05E+02	5.05E+02	5.05E+02	5.05E+02	5.05E+02	5.05E+02
Xe	9.75E-01	9.76E-01	9.76E-01	9.76E-01	9.76E-01	9.77E-01	9.77E-01	9.77E-01	9.77E-01
Mo	5.02E-01	5.03E-01	5.03E-01	5.05E-01	5.16E-01	5.40E-01	5.63E-01	5.65E-01	5.65E-01
Cs	4.47E-01	4.48E-01	4.50E-01	4.53E-01	4.54E-01	4.52E-01	4.47E-01	4.33E-01	4.12E-01
Ru	4.74E-01	4.73E-01	4.72E-01	4.67E-01	4.55E-01	4.36E-01	4.14E-01	3.93E-01	3.86E-01
Pd	2.13E-01	2.14E-01	2.14E-01	2.15E-01	2.18E-01	2.24E-01	2.42E-01	2.63E-01	2.70E-01
Ba	2.35E-01	2.34E-01	2.33E-01	2.29E-01	2.24E-01	2.24E-01	2.29E-01	2.43E-01	2.64E-01
Tc	1.44E-01	1.44E-01	1.45E-01	1.46E-01	1.46E-01	1.46E-01	1.46E-01	1.46E-01	1.46E-01
Sr	1.53E-01	1.52E-01	1.52E-01	1.50E-01	1.46E-01	1.40E-01	1.35E-01	1.31E-01	1.23E-01
Rh	8.04E-02	8.06E-02	8.16E-02	8.51E-02	9.48E-02	1.07E-01	1.12E-01	1.12E-01	1.12E-01
Te	8.75E-02	8.70E-02	8.59E-02	8.46E-02	8.38E-02	8.31E-02	8.29E-02	8.34E-02	8.40E-02
Kr	5.63E-02	5.63E-02	5.63E-02	5.62E-02	5.62E-02	5.62E-02	5.60E-02	5.56E-02	5.49E-02
Rb	5.09E-02	5.09E-02	5.09E-02	5.09E-02	5.09E-02	5.09E-02	5.11E-02	5.15E-02	5.22E-02
I	4.72E-02	4.65E-02	4.53E-02	4.38E-02	4.26E-02	4.31E-02	4.36E-02	4.37E-02	4.37E-02
Se	8.96E-03	8.96E-03	8.96E-03	8.96E-03	8.96E-03	8.96E-03	8.96E-03	8.96E-03	8.96E-03
H	9.36E-06	9.36E-06	9.36E-06	9.35E-06	9.31E-06	9.21E-06	8.85E-06	7.91E-06	6.32E-06
Pb	4.69E-13	4.74E-13	4.90E-13	5.42E-13	7.52E-13	1.63E-12	8.11E-12	5.62E-11	2.61E-10
Bi	5.80E-16	5.97E-16	6.03E-16	6.61E-16	8.37E-16	1.26E-15	2.60E-15	6.42E-15	1.22E-14
Rn	7.10E-18	7.15E-18	7.34E-18	7.91E-18	1.00E-17	1.68E-17	4.08E-17	1.19E-16	2.86E-16
Total	5.13E+02	5.13E+02	5.13E+02	5.13E+02	5.13E+02	5.13E+02	5.13E+02	5.13E+02	5.13E+02

Table A-6: CANDU F12059C outer (burnup=264 MWh/kgU, linear power=46 kW/m). Decay. Masses of isotopes (g).

Time (y)	1.00E-03	3.00E-03	1.00E-02	3.00E-02	1.00E-01	3.00E-01	1.00E+00	3.00E+00	7.00E+00
Cs137	2.20E-01	2.20E-01	2.20E-01	2.20E-01	2.19E-01	2.18E-01	2.15E-01	2.05E-01	1.87E-01
Tc99	1.43E-01	1.44E-01	1.45E-01	1.46E-01	1.46E-01	1.46E-01	1.46E-01	1.46E-01	1.46E-01
Sr90	8.42E-02	8.42E-02	8.42E-02	8.41E-02	8.40E-02	8.36E-02	8.21E-02	7.82E-02	7.09E-02
I129	3.30E-02	3.30E-02	3.31E-02	3.32E-02	3.37E-02	3.42E-02	3.44E-02	3.44E-02	3.44E-02
C14	4.52E-09	4.52E-09	4.52E-09	4.52E-09	4.52E-09	4.52E-09	4.52E-09	4.52E-09	4.52E-09

Table A-7: CANDU F12059C intermediate (burnup=225 MWh/kgU, linear power=38 kW/m). Decay. Masses of chemical elements (g).

Time (y)	1.00E-03	3.00E-03	1.00E-02	3.00E-02	1.00E-01	3.00E-01	1.00E+00	3.00E+00	7.00E+00
U	5.06E+02	5.06E+02	5.06E+02	5.06E+02	5.06E+02	5.06E+02	5.06E+02	5.06E+02	5.06E+02
Xe	8.26E-01	8.26E-01	8.27E-01	8.27E-01	8.27E-01	8.27E-01	8.27E-01	8.27E-01	8.27E-01
Mo	4.31E-01	4.31E-01	4.31E-01	4.33E-01	4.42E-01	4.62E-01	4.82E-01	4.84E-01	4.84E-01
Cs	3.84E-01	3.84E-01	3.86E-01	3.88E-01	3.89E-01	3.87E-01	3.83E-01	3.72E-01	3.55E-01
Ru	3.92E-01	3.91E-01	3.90E-01	3.87E-01	3.77E-01	3.62E-01	3.44E-01	3.28E-01	3.22E-01
Ba	2.01E-01	2.00E-01	1.99E-01	1.96E-01	1.91E-01	1.91E-01	1.96E-01	2.07E-01	2.24E-01
Pd	1.68E-01	1.69E-01	1.69E-01	1.70E-01	1.72E-01	1.77E-01	1.91E-01	2.07E-01	2.13E-01
Tc	1.23E-01	1.24E-01	1.24E-01	1.25E-01	1.25E-01	1.25E-01	1.25E-01	1.25E-01	1.25E-01
Sr	1.35E-01	1.35E-01	1.35E-01	1.33E-01	1.30E-01	1.24E-01	1.20E-01	1.16E-01	1.09E-01
Rh	6.94E-02	6.96E-02	7.04E-02	7.32E-02	8.10E-02	9.09E-02	9.46E-02	9.46E-02	9.46E-02
Te	7.37E-02	7.33E-02	7.24E-02	7.13E-02	7.07E-02	7.01E-02	6.99E-02	7.04E-02	7.09E-02
Kr	4.96E-02	4.96E-02	4.96E-02	4.96E-02	4.96E-02	4.96E-02	4.94E-02	4.90E-02	4.84E-02
Rb	4.50E-02	4.50E-02	4.50E-02	4.50E-02	4.50E-02	4.51E-02	4.52E-02	4.56E-02	4.62E-02
I	3.94E-02	3.89E-02	3.79E-02	3.66E-02	3.56E-02	3.61E-02	3.65E-02	3.65E-02	3.65E-02
Se	7.77E-03	7.77E-03	7.77E-03	7.77E-03	7.77E-03	7.77E-03	7.77E-03	7.77E-03	7.77E-03
H	7.89E-06	7.89E-06	7.89E-06	7.88E-06	7.85E-06	7.76E-06	7.46E-06	6.67E-06	5.33E-06
Pb	4.29E-13	4.33E-13	4.48E-13	4.93E-13	6.76E-13	1.43E-12	6.81E-12	4.53E-11	2.04E-10
Bi	4.87E-16	5.02E-16	5.05E-16	5.51E-16	6.91E-16	1.04E-15	2.11E-15	5.06E-15	9.40E-15
Rn	6.47E-18	6.52E-18	6.68E-18	7.18E-18	8.98E-18	1.47E-17	3.49E-17	1.01E-16	2.52E-16
Total	5.13E+02	5.13E+02	5.13E+02	5.13E+02	5.13E+02	5.13E+02	5.13E+02	5.13E+02	5.13E+02

Table A-8: CANDU F12059C intermediate (burnup=225 MWh/kgU, linear power=38 kW/m). Decay. Masses of isotopes (g).

Time (y)	1.00E-03	3.00E-03	1.00E-02	3.00E-02	1.00E-01	3.00E-01	1.00E+00	3.00E+00	7.00E+00
Cs137	1.87E-01	1.87E-01	1.87E-01	1.87E-01	1.86E-01	1.86E-01	1.83E-01	1.74E-01	1.59E-01
Tc99	1.23E-01	1.24E-01	1.24E-01	1.25E-01	1.25E-01	1.25E-01	1.25E-01	1.25E-01	1.25E-01
Sr90	7.48E-02	7.48E-02	7.48E-02	7.48E-02	7.47E-02	7.43E-02	7.30E-02	6.95E-02	6.30E-02
I129	2.77E-02	2.78E-02	2.78E-02	2.80E-02	2.83E-02	2.87E-02	2.89E-02	2.89E-02	2.89E-02
C14	3.86E-09	3.86E-09	3.86E-09	3.86E-09	3.86E-09	3.86E-09	3.86E-09	3.85E-09	3.85E-09

Table A-9: CANDU G00815W outer (burnup=163 MWh/kgU, linear power=41 kW/m). Decay. Masses of chemical elements (g).

Time (y)	1.00E-03	3.00E-03	1.00E-02	3.00E-02	1.00E-01	3.00E-01	1.00E+00	3.00E+00	7.00E+00
U	5.08E+02	5.08E+02	5.08E+02	5.08E+02	5.08E+02	5.08E+02	5.08E+02	5.08E+02	5.08E+02
Xe	5.91E-01	5.92E-01	5.92E-01	5.92E-01	5.92E-01	5.93E-01	5.93E-01	5.93E-01	5.93E-01
Mo	2.99E-01	2.99E-01	3.00E-01	3.02E-01	3.10E-01	3.30E-01	3.50E-01	3.51E-01	3.51E-01
Cs	2.73E-01	2.74E-01	2.76E-01	2.78E-01	2.79E-01	2.79E-01	2.76E-01	2.68E-01	2.56E-01
Ru	2.76E-01	2.75E-01	2.74E-01	2.71E-01	2.62E-01	2.49E-01	2.37E-01	2.26E-01	2.22E-01
Ba	1.49E-01	1.49E-01	1.47E-01	1.44E-01	1.39E-01	1.38E-01	1.41E-01	1.48E-01	1.60E-01
Pd	9.96E-02	9.98E-02	1.00E-01	1.01E-01	1.02E-01	1.06E-01	1.15E-01	1.26E-01	1.29E-01
Tc	8.98E-02	9.01E-02	9.08E-02	9.15E-02	9.17E-02	9.17E-02	9.17E-02	9.17E-02	9.17E-02
Sr	1.11E-01	1.11E-01	1.10E-01	1.09E-01	1.04E-01	9.78E-02	9.32E-02	9.04E-02	8.53E-02
Rh	4.38E-02	4.40E-02	4.47E-02	4.74E-02	5.48E-02	6.42E-02	6.77E-02	6.78E-02	6.78E-02
Te	5.31E-02	5.27E-02	5.17E-02	5.06E-02	4.99E-02	4.94E-02	4.92E-02	4.95E-02	4.98E-02
Kr	3.82E-02	3.82E-02	3.82E-02	3.82E-02	3.82E-02	3.81E-02	3.80E-02	3.77E-02	3.72E-02
Rb	3.48E-02	3.48E-02	3.48E-02	3.48E-02	3.48E-02	3.48E-02	3.49E-02	3.52E-02	3.57E-02
I	2.85E-02	2.79E-02	2.69E-02	2.55E-02	2.44E-02	2.47E-02	2.51E-02	2.52E-02	2.52E-02
Se	5.78E-03	5.78E-03	5.78E-03	5.78E-03	5.78E-03	5.78E-03	5.78E-03	5.78E-03	5.78E-03
H	5.60E-06	5.60E-06	5.60E-06	5.59E-06	5.57E-06	5.51E-06	5.30E-06	4.73E-06	3.78E-06
Pb	1.20E-13	1.22E-13	1.28E-13	1.46E-13	2.23E-13	5.67E-13	3.22E-12	2.28E-11	1.03E-10
Bi	1.69E-16	1.75E-16	1.77E-16	1.99E-16	2.67E-16	4.45E-16	1.00E-15	2.53E-15	4.82E-15
Rn	2.63E-18	2.65E-18	2.74E-18	3.02E-18	4.02E-18	7.28E-18	1.93E-17	6.34E-17	1.88E-16
Total	5.13E+02	5.13E+02	5.13E+02	5.13E+02	5.13E+02	5.13E+02	5.13E+02	5.13E+02	5.13E+02

Table A-10: CANDU G00815W outer (burnup=163 MWh/kgU, linear power=41 kW/m). Decay. Masses of isotopes (g).

Time (y)	1.00E-03	3.00E-03	1.00E-02	3.00E-02	1.00E-01	3.00E-01	1.00E+00	3.00E+00	7.00E+00
Cs137	1.34E-01	1.34E-01	1.34E-01	1.34E-01	1.34E-01	1.33E-01	1.31E-01	1.25E-01	1.14E-01
Tc99	8.96E-02	9.00E-02	9.08E-02	9.15E-02	9.17E-02	9.17E-02	9.17E-02	9.17E-02	9.17E-02
Sr90	5.85E-02	5.85E-02	5.85E-02	5.85E-02	5.84E-02	5.81E-02	5.71E-02	5.43E-02	4.92E-02
I129	1.89E-02	1.90E-02	1.90E-02	1.92E-02	1.95E-02	1.99E-02	2.01E-02	2.01E-02	2.01E-02
C14	2.78E-09	2.78E-09	2.78E-09	2.78E-09	2.78E-09	2.78E-09	2.78E-09	2.78E-09	2.78E-09

Table A-11: CANDU G00815W intermediate (burnup=131 MWh/kgU, linear power=33 kW/m). Decay. Masses of chemical elements (g).

Time (y)	1.00E-03	3.00E-03	1.00E-02	3.00E-02	1.00E-01	3.00E-01	1.00E+00	3.00E+00	7.00E+00
U	5.08E+02	5.08E+02	5.08E+02	5.08E+02	5.08E+02	5.08E+02	5.08E+02	5.08E+02	5.08E+02
Xe	4.73E-01	4.73E-01	4.73E-01	4.73E-01	4.73E-01	4.73E-01	4.73E-01	4.73E-01	4.73E-01
Mo	2.41E-01	2.41E-01	2.42E-01	2.43E-01	2.50E-01	2.66E-01	2.83E-01	2.84E-01	2.84E-01
Cs	2.21E-01	2.22E-01	2.23E-01	2.25E-01	2.26E-01	2.26E-01	2.23E-01	2.18E-01	2.08E-01
Ru	2.15E-01	2.14E-01	2.13E-01	2.11E-01	2.04E-01	1.95E-01	1.85E-01	1.77E-01	1.75E-01
Ba	1.21E-01	1.20E-01	1.19E-01	1.16E-01	1.12E-01	1.12E-01	1.14E-01	1.19E-01	1.29E-01
Pd	7.21E-02	7.22E-02	7.25E-02	7.29E-02	7.39E-02	7.64E-02	8.30E-02	9.09E-02	9.35E-02
Sr	9.34E-02	9.32E-02	9.27E-02	9.14E-02	8.78E-02	8.22E-02	7.83E-02	7.59E-02	7.17E-02
Tc	7.27E-02	7.30E-02	7.36E-02	7.41E-02	7.43E-02	7.43E-02	7.43E-02	7.43E-02	7.43E-02
Rh	3.48E-02	3.50E-02	3.56E-02	3.76E-02	4.34E-02	5.06E-02	5.34E-02	5.34E-02	5.34E-02
Te	4.21E-02	4.18E-02	4.10E-02	4.01E-02	3.96E-02	3.92E-02	3.90E-02	3.92E-02	3.95E-02
Kr	3.19E-02	3.19E-02	3.19E-02	3.19E-02	3.19E-02	3.18E-02	3.17E-02	3.15E-02	3.11E-02
Rb	2.91E-02	2.91E-02	2.91E-02	2.91E-02	2.91E-02	2.92E-02	2.93E-02	2.95E-02	2.99E-02
I	2.24E-02	2.19E-02	2.10E-02	1.99E-02	1.90E-02	1.93E-02	1.96E-02	1.96E-02	1.96E-02
Se	4.74E-03	4.74E-03	4.74E-03	4.74E-03	4.74E-03	4.74E-03	4.74E-03	4.74E-03	4.74E-03
H	4.46E-06	4.46E-06	4.45E-06	4.45E-06	4.43E-06	4.38E-06	4.21E-06	3.77E-06	3.01E-06
Pb	9.60E-14	9.73E-14	1.02E-13	1.16E-13	1.77E-13	4.46E-13	2.47E-12	1.68E-11	7.34E-11
Bi	1.29E-16	1.34E-16	1.35E-16	1.51E-16	2.01E-16	3.35E-16	7.48E-16	1.82E-15	3.42E-15
Rn	2.20E-18	2.22E-18	2.30E-18	2.52E-18	3.34E-18	5.98E-18	1.59E-17	5.40E-17	1.72E-16
Total	5.13E+02	5.13E+02	5.13E+02	5.13E+02	5.13E+02	5.13E+02	5.13E+02	5.13E+02	5.13E+02

Table A-12: CANDU G00815W intermediate (burnup=131 MWh/kgU, linear power=33 kW/m). Decay. Masses of isotopes (g).

Time (y)	1.00E-03	3.00E-03	1.00E-02	3.00E-02	1.00E-01	3.00E-01	1.00E+00	3.00E+00	7.00E+00
Cs137	1.08E-01	1.08E-01	1.08E-01	1.08E-01	1.08E-01	1.07E-01	1.05E-01	1.01E-01	9.18E-02
Tc99	7.26E-02	7.29E-02	7.35E-02	7.41E-02	7.43E-02	7.43E-02	7.43E-02	7.43E-02	7.43E-02
Sr90	4.92E-02	4.92E-02	4.92E-02	4.92E-02	4.91E-02	4.88E-02	4.80E-02	4.57E-02	4.14E-02
I129	1.49E-02	1.49E-02	1.49E-02	1.51E-02	1.53E-02	1.57E-02	1.58E-02	1.58E-02	1.58E-02
C14	2.24E-09	2.24E-09	2.24E-09	2.24E-09	2.24E-09	2.24E-09	2.24E-09	2.24E-09	2.24E-09

Table A-13: CANDU J49093C outer (burnup=308 MWh/kgU, linear power=50 kW/m). Decay. Masses of chemical elements (g).

Time (y)	1.00E-03	3.00E-03	1.00E-02	3.00E-02	1.00E-01	3.00E-01	1.00E+00	3.00E+00	7.00E+00
U	5.03E+02	5.03E+02	5.03E+02	5.03E+02	5.03E+02	5.03E+02	5.03E+02	5.03E+02	5.03E+02
Xe	1.14E+00	1.14E+00	1.14E+00	1.14E+00	1.14E+00	1.14E+00	1.14E+00	1.14E+00	1.14E+00
Mo	5.88E-01	5.88E-01	5.89E-01	5.91E-01	6.03E-01	6.29E-01	6.54E-01	6.56E-01	6.56E-01
Cs	5.21E-01	5.22E-01	5.24E-01	5.27E-01	5.28E-01	5.26E-01	5.19E-01	5.03E-01	4.78E-01
Ru	5.64E-01	5.63E-01	5.62E-01	5.57E-01	5.43E-01	5.21E-01	4.94E-01	4.68E-01	4.60E-01
Pd	2.70E-01	2.70E-01	2.71E-01	2.72E-01	2.75E-01	2.83E-01	3.05E-01	3.30E-01	3.39E-01
Ba	2.72E-01	2.72E-01	2.70E-01	2.66E-01	2.60E-01	2.60E-01	2.67E-01	2.83E-01	3.08E-01
Tc	1.66E-01	1.66E-01	1.67E-01	1.68E-01	1.68E-01	1.68E-01	1.68E-01	1.68E-01	1.68E-01
Sr	1.69E-01	1.69E-01	1.68E-01	1.66E-01	1.62E-01	1.55E-01	1.50E-01	1.46E-01	1.38E-01
Rh	9.44E-02	9.47E-02	9.58E-02	9.97E-02	1.11E-01	1.24E-01	1.30E-01	1.30E-01	1.30E-01
Te	1.03E-01	1.02E-01	1.01E-01	9.95E-02	9.86E-02	9.78E-02	9.76E-02	9.82E-02	9.89E-02
Kr	6.33E-02	6.33E-02	6.33E-02	6.33E-02	6.33E-02	6.32E-02	6.30E-02	6.25E-02	6.17E-02
Rb	5.70E-02	5.70E-02	5.70E-02	5.70E-02	5.70E-02	5.71E-02	5.73E-02	5.78E-02	5.86E-02
I	5.55E-02	5.47E-02	5.35E-02	5.18E-02	5.05E-02	5.11E-02	5.17E-02	5.18E-02	5.18E-02
Se	1.03E-02	1.03E-02	1.03E-02	1.03E-02	1.03E-02	1.03E-02	1.03E-02	1.03E-02	1.03E-02
H	1.10E-05	1.10E-05	1.10E-05	1.10E-05	1.10E-05	1.08E-05	1.04E-05	9.30E-06	7.43E-06
Pb	6.53E-13	6.59E-13	6.81E-13	7.49E-13	1.02E-12	2.16E-12	1.05E-11	7.33E-11	3.44E-10
Bi	8.18E-16	8.40E-16	8.49E-16	9.26E-16	1.16E-15	1.71E-15	3.46E-15	8.50E-15	1.61E-14
Rn	9.15E-18	9.21E-18	9.45E-18	1.02E-17	1.28E-17	2.12E-17	5.12E-17	1.47E-16	3.37E-16
Total	5.13E+02	5.13E+02	5.13E+02	5.13E+02	5.13E+02	5.13E+02	5.13E+02	5.13E+02	5.13E+02

Table A-14: CANDU J49093C outer (burnup=308 MWh/kgU, linear power=50 kW/m). Decay. Masses of isotopes (g).

Time (y)	1.00E-03	3.00E-03	1.00E-02	3.00E-02	1.00E-01	3.00E-01	1.00E+00	3.00E+00	7.00E+00
Cs137	2.57E-01	2.57E-01	2.57E-01	2.57E-01	2.56E-01	2.55E-01	2.51E-01	2.40E-01	2.18E-01
Tc99	1.66E-01	1.66E-01	1.67E-01	1.68E-01	1.68E-01	1.68E-01	1.68E-01	1.68E-01	1.68E-01
Sr90	9.39E-02	9.39E-02	9.38E-02	9.38E-02	9.36E-02	9.32E-02	9.16E-02	8.72E-02	7.90E-02
I129	3.90E-02	3.90E-02	3.91E-02	3.93E-02	3.98E-02	4.04E-02	4.05E-02	4.05E-02	4.05E-02
C14	5.26E-09	5.26E-09	5.26E-09	5.26E-09	5.26E-09	5.26E-09	5.26E-09	5.26E-09	5.26E-09

Table A-15: CANDU J49093C inner (burnup=225 MWh/kgU, linear power=37 kW/m). Decay. Masses of chemical elements (g).

Time (y)	1.00E-03	3.00E-03	1.00E-02	3.00E-02	1.00E-01	3.00E-01	1.00E+00	3.00E+00	7.00E+00
U	5.06E+02	5.06E+02	5.06E+02	5.06E+02	5.06E+02	5.06E+02	5.06E+02	5.06E+02	5.06E+02
Xe	8.26E-01	8.26E-01	8.26E-01	8.26E-01	8.26E-01	8.27E-01	8.27E-01	8.27E-01	8.27E-01
Mo	4.32E-01	4.32E-01	4.32E-01	4.34E-01	4.43E-01	4.63E-01	4.82E-01	4.84E-01	4.84E-01
Cs	3.84E-01	3.85E-01	3.86E-01	3.88E-01	3.89E-01	3.88E-01	3.83E-01	3.72E-01	3.55E-01
Ru	3.91E-01	3.91E-01	3.89E-01	3.86E-01	3.76E-01	3.61E-01	3.44E-01	3.27E-01	3.22E-01
Ba	2.00E-01	2.00E-01	1.99E-01	1.96E-01	1.91E-01	1.91E-01	1.96E-01	2.07E-01	2.24E-01
Pd	1.69E-01	1.69E-01	1.69E-01	1.70E-01	1.72E-01	1.77E-01	1.91E-01	2.08E-01	2.13E-01
Tc	1.23E-01	1.24E-01	1.24E-01	1.25E-01	1.25E-01	1.25E-01	1.25E-01	1.25E-01	1.25E-01
Sr	1.35E-01	1.35E-01	1.34E-01	1.33E-01	1.29E-01	1.24E-01	1.20E-01	1.16E-01	1.09E-01
Rh	6.99E-02	7.01E-02	7.08E-02	7.36E-02	8.12E-02	9.08E-02	9.44E-02	9.45E-02	9.45E-02
Te	7.36E-02	7.32E-02	7.23E-02	7.13E-02	7.06E-02	7.01E-02	6.99E-02	7.04E-02	7.08E-02
Kr	4.96E-02	4.96E-02	4.96E-02	4.96E-02	4.96E-02	4.96E-02	4.94E-02	4.90E-02	4.84E-02
Rb	4.50E-02	4.50E-02	4.50E-02	4.50E-02	4.50E-02	4.51E-02	4.52E-02	4.56E-02	4.62E-02
I	3.93E-02	3.88E-02	3.78E-02	3.66E-02	3.56E-02	3.61E-02	3.65E-02	3.65E-02	3.65E-02
Se	7.77E-03	7.77E-03	7.77E-03	7.77E-03	7.77E-03	7.77E-03	7.77E-03	7.77E-03	7.77E-03
H	7.89E-06	7.89E-06	7.89E-06	7.88E-06	7.85E-06	7.76E-06	7.46E-06	6.67E-06	5.32E-06
Pb	4.57E-13	4.62E-13	4.77E-13	5.24E-13	7.14E-13	1.49E-12	6.99E-12	4.61E-11	2.06E-10
Bi	5.09E-16	5.24E-16	5.28E-16	5.74E-16	7.16E-16	1.07E-15	2.16E-15	5.13E-15	9.49E-15
Rn	6.76E-18	6.81E-18	6.97E-18	7.47E-18	9.30E-18	1.52E-17	3.56E-17	1.02E-16	2.53E-16
Total	5.13E+02	5.13E+02	5.13E+02	5.13E+02	5.13E+02	5.13E+02	5.13E+02	5.13E+02	5.13E+02

Table A-16: CANDU J49093C inner (burnup=225 MWh/kgU, linear power=37 kW/m). Decay. Masses of isotopes (g).

Time (y)	1.00E-03	3.00E-03	1.00E-02	3.00E-02	1.00E-01	3.00E-01	1.00E+00	3.00E+00	7.00E+00
Cs137	1.87E-01	1.87E-01	1.87E-01	1.87E-01	1.86E-01	1.86E-01	1.83E-01	1.74E-01	1.59E-01
Tc99	1.23E-01	1.24E-01	1.24E-01	1.25E-01	1.25E-01	1.25E-01	1.25E-01	1.25E-01	1.25E-01
Sr90	7.48E-02	7.48E-02	7.48E-02	7.48E-02	7.46E-02	7.43E-02	7.30E-02	6.95E-02	6.30E-02
I129	2.77E-02	2.78E-02	2.78E-02	2.80E-02	2.83E-02	2.87E-02	2.89E-02	2.89E-02	2.89E-02
C14	3.86E-09	3.86E-09	3.86E-09	3.86E-09	3.86E-09	3.86E-09	3.85E-09	3.85E-09	3.85E-09

Table A-17: CANDU G13374S outer (burnup=300 MWh/kgU, linear power=50 kW/m). Decay. Masses of chemical elements (g).

Time (y)	1.00E-03	3.00E-03	1.00E-02	3.00E-02	1.00E-01	3.00E-01	1.00E+00	3.00E+00	7.00E+00
U	5.04E+02	5.04E+02	5.04E+02	5.04E+02	5.04E+02	5.04E+02	5.04E+02	5.04E+02	5.04E+02
Xe	1.11E+00	1.11E+00	1.11E+00	1.11E+00	1.11E+00	1.11E+00	1.11E+00	1.11E+00	1.11E+00
Mo	5.72E-01	5.72E-01	5.73E-01	5.75E-01	5.87E-01	6.12E-01	6.38E-01	6.39E-01	6.39E-01
Cs	5.08E-01	5.08E-01	5.10E-01	5.13E-01	5.14E-01	5.12E-01	5.06E-01	4.90E-01	4.66E-01
Ru	5.48E-01	5.48E-01	5.46E-01	5.41E-01	5.27E-01	5.05E-01	4.80E-01	4.55E-01	4.46E-01
Pd	2.59E-01	2.59E-01	2.60E-01	2.61E-01	2.64E-01	2.72E-01	2.93E-01	3.18E-01	3.26E-01
Ba	2.66E-01	2.65E-01	2.63E-01	2.59E-01	2.54E-01	2.54E-01	2.60E-01	2.76E-01	3.00E-01
Tc	1.62E-01	1.62E-01	1.63E-01	1.64E-01	1.64E-01	1.64E-01	1.64E-01	1.64E-01	1.64E-01
Sr	1.66E-01	1.66E-01	1.65E-01	1.64E-01	1.59E-01	1.53E-01	1.48E-01	1.43E-01	1.35E-01
Rh	9.16E-02	9.19E-02	9.30E-02	9.69E-02	1.08E-01	1.21E-01	1.26E-01	1.27E-01	1.27E-01
Te	9.99E-02	9.94E-02	9.82E-02	9.68E-02	9.59E-02	9.52E-02	9.49E-02	9.55E-02	9.62E-02
Kr	6.21E-02	6.20E-02	6.20E-02	6.20E-02	6.20E-02	6.20E-02	6.18E-02	6.13E-02	6.05E-02
Rb	5.59E-02	5.59E-02	5.59E-02	5.59E-02	5.60E-02	5.60E-02	5.62E-02	5.67E-02	5.75E-02
I	5.40E-02	5.33E-02	5.21E-02	5.04E-02	4.91E-02	4.97E-02	5.02E-02	5.03E-02	5.03E-02
Se	1.00E-02	1.00E-02	1.00E-02	1.00E-02	1.00E-02	1.00E-02	1.00E-02	1.00E-02	1.00E-02
H	1.07E-05	1.07E-05	1.07E-05	1.07E-05	1.07E-05	1.05E-05	1.01E-05	9.05E-06	7.23E-06
Pb	5.96E-13	6.02E-13	6.22E-13	6.85E-13	9.42E-13	2.01E-12	9.94E-12	6.95E-11	3.26E-10
Bi	7.52E-16	7.73E-16	7.82E-16	8.54E-16	1.08E-15	1.60E-15	3.26E-15	8.05E-15	1.53E-14
Rn	8.56E-18	8.62E-18	8.84E-18	9.52E-18	1.20E-17	2.01E-17	4.88E-17	1.41E-16	3.26E-16
Total	5.13E+02	5.13E+02	5.13E+02	5.13E+02	5.13E+02	5.13E+02	5.13E+02	5.13E+02	5.13E+02

Table A-18: CANDU G13374S outer (burnup=300 MWh/kgU, linear power=50 kW/m). Decay. Masses of isotopes (g).

Time (y)	1.00E-03	3.00E-03	1.00E-02	3.00E-02	1.00E-01	3.00E-01	1.00E+00	3.00E+00	7.00E+00
Cs137	2.50E-01	2.50E-01	2.50E-01	2.50E-01	2.49E-01	2.48E-01	2.44E-01	2.33E-01	2.13E-01
Tc99	1.62E-01	1.62E-01	1.63E-01	1.64E-01	1.64E-01	1.64E-01	1.64E-01	1.64E-01	1.64E-01
Sr90	9.22E-02	9.22E-02	9.22E-02	9.21E-02	9.19E-02	9.15E-02	8.99E-02	8.56E-02	7.76E-02
I129	3.79E-02	3.79E-02	3.80E-02	3.82E-02	3.87E-02	3.93E-02	3.94E-02	3.94E-02	3.94E-02
C14	5.13E-09	5.13E-09	5.13E-09	5.13E-09	5.13E-09	5.13E-09	5.13E-09	5.13E-09	5.13E-09

Table A-19: CANDU G13374S intermediate (burnup=244 MWh/kgU, linear power=42 kW/m). Decay. Masses of chemical elements (g).

Time (y)	1.00E-03	3.00E-03	1.00E-02	3.00E-02	1.00E-01	3.00E-01	1.00E+00	3.00E+00	7.00E+00
U	5.05E+02	5.05E+02	5.05E+02	5.05E+02	5.05E+02	5.05E+02	5.05E+02	5.05E+02	5.05E+02
Xe	8.99E-01	8.99E-01	8.99E-01	8.99E-01	9.00E-01	9.00E-01	9.00E-01	9.00E-01	9.00E-01
Mo	4.66E-01	4.66E-01	4.66E-01	4.68E-01	4.78E-01	5.00E-01	5.22E-01	5.23E-01	5.23E-01
Cs	4.15E-01	4.15E-01	4.17E-01	4.19E-01	4.20E-01	4.19E-01	4.14E-01	4.02E-01	3.83E-01
Ru	4.32E-01	4.31E-01	4.30E-01	4.26E-01	4.15E-01	3.98E-01	3.78E-01	3.59E-01	3.53E-01
Pd	1.90E-01	1.90E-01	1.91E-01	1.91E-01	1.94E-01	2.00E-01	2.15E-01	2.34E-01	2.40E-01
Ba	2.17E-01	2.17E-01	2.15E-01	2.12E-01	2.07E-01	2.07E-01	2.12E-01	2.24E-01	2.43E-01
Tc	1.33E-01	1.34E-01	1.34E-01	1.35E-01	1.35E-01	1.35E-01	1.35E-01	1.35E-01	1.35E-01
Sr	1.44E-01	1.44E-01	1.43E-01	1.42E-01	1.38E-01	1.32E-01	1.27E-01	1.23E-01	1.16E-01
Rh	7.48E-02	7.50E-02	7.59E-02	7.90E-02	8.77E-02	9.88E-02	1.03E-01	1.03E-01	1.03E-01
Te	8.04E-02	8.00E-02	7.90E-02	7.78E-02	7.70E-02	7.64E-02	7.62E-02	7.67E-02	7.73E-02
Kr	5.29E-02	5.29E-02	5.29E-02	5.29E-02	5.29E-02	5.28E-02	5.27E-02	5.23E-02	5.16E-02
Rb	4.79E-02	4.79E-02	4.79E-02	4.79E-02	4.79E-02	4.80E-02	4.81E-02	4.85E-02	4.92E-02
I	4.32E-02	4.26E-02	4.15E-02	4.01E-02	3.90E-02	3.95E-02	3.99E-02	4.00E-02	4.00E-02
Se	8.35E-03	8.35E-03	8.35E-03	8.35E-03	8.35E-03	8.35E-03	8.35E-03	8.35E-03	8.35E-03
H	8.61E-06	8.61E-06	8.60E-06	8.59E-06	8.56E-06	8.47E-06	8.14E-06	7.27E-06	5.81E-06
Pb	4.45E-13	4.50E-13	4.65E-13	5.14E-13	7.09E-13	1.52E-12	7.42E-12	5.05E-11	2.31E-10
Bi	5.29E-16	5.45E-16	5.50E-16	6.01E-16	7.58E-16	1.14E-15	2.34E-15	5.70E-15	1.07E-14
Rn	6.75E-18	6.79E-18	6.97E-18	7.50E-18	9.45E-18	1.57E-17	3.77E-17	1.09E-16	2.67E-16
Total	5.13E+02	5.13E+02	5.13E+02	5.13E+02	5.13E+02	5.13E+02	5.13E+02	5.13E+02	5.13E+02

Table A-20: CANDU G13374S intermediate (burnup=244 MWh/kgU, linear power=42 kW/m). Decay. Masses of isotopes (g).

Time (y)	1.00E-03	3.00E-03	1.00E-02	3.00E-02	1.00E-01	3.00E-01	1.00E+00	3.00E+00	7.00E+00
Cs137	2.03E-01	2.03E-01	2.03E-01	2.03E-01	2.02E-01	2.02E-01	1.98E-01	1.89E-01	1.73E-01
Tc99	1.33E-01	1.33E-01	1.34E-01	1.35E-01	1.35E-01	1.35E-01	1.35E-01	1.35E-01	1.35E-01
Sr90	7.95E-02	7.95E-02	7.95E-02	7.94E-02	7.93E-02	7.89E-02	7.75E-02	7.38E-02	6.69E-02
I129	3.03E-02	3.03E-02	3.04E-02	3.05E-02	3.09E-02	3.14E-02	3.15E-02	3.15E-02	3.15E-02
C14	4.18E-09	4.18E-09	4.18E-09	4.18E-09	4.18E-09	4.18E-09	4.18E-09	4.18E-09	4.18E-09
Total	5.13E+02	5.13E+02	5.13E+02	5.13E+02	5.13E+02	5.13E+02	5.13E+02	5.13E+02	5.13E+02

A.2 CALCULATION OF AVERAGE AND PESSIMISTIC INSTANT RELEASE FRACTIONS

Table A-21: Average Bundle Case with 455 kW and 220 MWh/kgU and 30 Years of Decay (masses in grams)

Time (y)	1.00E-02	3.00E-02	1.00E-01	3.00E-01	1.00E+00	3.00E+00	1.00E+01	3.00E+01
U	1.89E+04	1.89E+04	1.89E+04	1.89E+04	1.89E+04	1.89E+04	1.89E+04	1.89E+04
Xe	3.00E+01	3.00E+01	3.00E+01	3.00E+01	3.00E+01	3.00E+01	3.00E+01	3.00E+01
Mo	1.63E+01	1.64E+01	1.66E+01	1.71E+01	1.76E+01	1.77E+01	1.77E+01	1.77E+01
Cs	1.43E+01	1.44E+01	1.44E+01	1.43E+01	1.42E+01	1.38E+01	1.27E+01	1.07E+01
Ru	1.38E+01	1.37E+01	1.34E+01	1.30E+01	1.25E+01	1.19E+01	1.17E+01	1.17E+01
Ba	7.19E+00	7.12E+00	7.01E+00	7.02E+00	7.18E+00	7.58E+00	8.62E+00	1.06E+01
Pd	6.30E+00	6.32E+00	6.39E+00	6.56E+00	7.02E+00	7.57E+00	7.76E+00	7.76E+00
Tc	4.54E+00	4.55E+00	4.56E+00	4.56E+00	4.56E+00	4.56E+00	4.56E+00	4.56E+00
Sr	4.77E+00	4.74E+00	4.64E+00	4.50E+00	4.38E+00	4.25E+00	3.85E+00	3.01E+00
Rh	2.78E+00	2.85E+00	3.04E+00	3.29E+00	3.39E+00	3.39E+00	3.39E+00	3.39E+00
Te	2.61E+00	2.59E+00	2.57E+00	2.56E+00	2.55E+00	2.57E+00	2.59E+00	2.59E+00
Kr	1.82E+00	1.82E+00	1.82E+00	1.82E+00	1.81E+00	1.80E+00	1.76E+00	1.72E+00
Rb	1.65E+00	1.66E+00	1.66E+00	1.66E+00	1.66E+00	1.68E+00	1.71E+00	1.76E+00
I	1.36E+00	1.33E+00	1.30E+00	1.32E+00	1.33E+00	1.33E+00	1.33E+00	1.33E+00
Ag	6.97E-01	6.95E-01	6.93E-01	6.92E-01	6.91E-01	6.91E-01	6.90E-01	6.90E-01
Cd	3.97E-01	3.99E-01	4.01E-01	4.01E-01	4.02E-01	4.03E-01	4.03E-01	4.03E-01
Sn	3.12E-01	3.12E-01	3.12E-01	3.12E-01	3.11E-01	3.11E-01	3.11E-01	3.11E-01
Se	2.85E-01	2.85E-01	2.85E-01	2.85E-01	2.85E-01	2.85E-01	2.85E-01	2.85E-01
Br	1.09E-01	1.09E-01	1.09E-01	1.09E-01	1.09E-01	1.09E-01	1.09E-01	1.09E-01
Sb	1.09E-01	1.07E-01	1.06E-01	1.03E-01	9.52E-02	7.78E-02	5.59E-02	5.15E-02
In	1.51E-02	1.52E-02	1.53E-02	1.53E-02	1.54E-02	1.55E-02	1.56E-02	1.59E-02
Ge	2.03E-03	2.03E-03	2.03E-03	2.03E-03	2.03E-03	2.03E-03	2.03E-03	2.03E-03
As	6.52E-04	6.46E-04	6.46E-04	6.46E-04	6.46E-04	6.46E-04	6.46E-04	6.46E-04
H	2.85E-04	2.85E-04	2.84E-04	2.81E-04	2.70E-04	2.41E-04	1.63E-04	5.28E-05
C	1.41E-07	1.41E-07	1.41E-07	1.41E-07	1.41E-07	1.41E-07	1.41E-07	1.40E-07
Zn	1.36E-07	6.85E-08	6.31E-08	6.31E-08	6.31E-08	6.31E-08	6.31E-08	6.31E-08
Pb	4.21E-11	4.51E-11	5.65E-11	9.95E-11	3.73E-10	2.12E-09	1.54E-08	6.33E-08
Pb	4.21E-11	4.51E-11	5.65E-11	9.95E-11	3.73E-10	2.12E-09	1.54E-08	6.33E-08
Ra	1.65E-11	1.71E-11	1.93E-11	2.63E-11	5.79E-11	2.10E-10	1.47E-09	1.14E-08
Bi	3.53E-14	3.70E-14	4.34E-14	5.94E-14	1.07E-13	2.29E-13	4.77E-13	1.09E-12
Po	2.41E-17	2.57E-17	3.20E-17	5.24E-17	1.59E-16	1.23E-15	3.31E-14	6.41E-13
Rn	4.68E-16	4.85E-16	5.67E-16	8.35E-16	1.73E-15	4.45E-15	1.54E-14	7.91E-14
Tl	4.23E-16	4.40E-16	5.20E-16	7.76E-16	1.59E-15	3.62E-15	7.03E-15	6.86E-15
Total	1.92E+04	1.92E+04	1.92E+04	1.92E+04	1.92E+04	1.92E+04	1.92E+04	1.92E+04

Table A-22: Average Bundle Case with 455 kW and 320 MWh/kgU and 30 Years of Decay (masses in grams)

Time (y)	1.00E-02	3.00E-02	1.00E-01	3.00E-01	1.00E+00	3.00E+00	1.00E+01	3.00E+01
U	1.88E+04	1.88E+04	1.88E+04	1.88E+04	1.88E+04	1.88E+04	1.88E+04	1.88E+04
Xe	4.38E+01	4.38E+01	4.38E+01	4.38E+01	4.38E+01	4.38E+01	4.38E+01	4.38E+01
Mo	2.40E+01	2.41E+01	2.43E+01	2.48E+01	2.53E+01	2.53E+01	2.53E+01	2.53E+01
Ru	2.07E+01	2.06E+01	2.03E+01	1.98E+01	1.90E+01	1.81E+01	1.79E+01	1.78E+01
Cs	2.09E+01	2.09E+01	2.09E+01	2.08E+01	2.06E+01	2.00E+01	1.84E+01	1.55E+01
Pd	1.14E+01	1.14E+01	1.15E+01	1.18E+01	1.24E+01	1.33E+01	1.36E+01	1.36E+01
Ba	1.03E+01	1.03E+01	1.02E+01	1.02E+01	1.05E+01	1.11E+01	1.27E+01	1.56E+01
Tc	6.46E+00	6.48E+00	6.48E+00	6.48E+00	6.48E+00	6.48E+00	6.48E+00	6.48E+00
Rh	4.12E+00	4.20E+00	4.41E+00	4.68E+00	4.78E+00	4.78E+00	4.78E+00	4.78E+00
Sr	6.07E+00	6.04E+00	5.96E+00	5.84E+00	5.71E+00	5.55E+00	5.02E+00	3.94E+00
Te	3.85E+00	3.82E+00	3.80E+00	3.79E+00	3.79E+00	3.81E+00	3.85E+00	3.85E+00
Kr	2.42E+00	2.42E+00	2.42E+00	2.42E+00	2.41E+00	2.40E+00	2.35E+00	2.29E+00
Rb	2.19E+00	2.19E+00	2.19E+00	2.19E+00	2.20E+00	2.22E+00	2.27E+00	2.33E+00
I	2.04E+00	2.01E+00	1.98E+00	2.00E+00	2.01E+00	2.01E+00	2.01E+00	2.01E+00
Ag	1.15E+00	1.15E+00	1.15E+00	1.15E+00	1.14E+00	1.14E+00	1.14E+00	1.14E+00
Cd	7.58E-01	7.60E-01	7.63E-01	7.64E-01	7.67E-01	7.68E-01	7.68E-01	7.68E-01
Sn	4.99E-01	4.99E-01	4.99E-01	4.98E-01	4.98E-01	4.98E-01	4.98E-01	4.97E-01
Se	3.95E-01	3.95E-01	3.95E-01	3.95E-01	3.95E-01	3.95E-01	3.95E-01	3.95E-01
Br	1.53E-01	1.53E-01	1.53E-01	1.53E-01	1.53E-01	1.53E-01	1.53E-01	1.53E-01
Sb	1.66E-01	1.63E-01	1.62E-01	1.58E-01	1.45E-01	1.19E-01	8.62E-02	7.96E-02
In	2.11E-02	2.12E-02	2.13E-02	2.14E-02	2.15E-02	2.16E-02	2.19E-02	2.23E-02
Ge	2.82E-03	2.82E-03	2.82E-03	2.82E-03	2.82E-03	2.82E-03	2.82E-03	2.82E-03
As	9.19E-04	9.14E-04	9.14E-04	9.14E-04	9.14E-04	9.14E-04	9.14E-04	9.14E-04
H	4.18E-04	4.17E-04	4.16E-04	4.11E-04	3.95E-04	3.53E-04	2.38E-04	7.74E-05
C	2.04E-07	2.04E-07	2.04E-07	2.04E-07	2.04E-07	2.04E-07	2.03E-07	2.03E-07
Zn	1.80E-07	1.09E-07	1.04E-07	1.04E-07	1.04E-07	1.04E-07	1.04E-07	1.04E-07
Pb	1.65E-10	1.73E-10	2.05E-10	3.16E-10	9.69E-10	4.89E-09	3.37E-08	1.37E-07
Pb	1.65E-10	1.73E-10	2.05E-10	3.16E-10	9.69E-10	4.89E-09	3.37E-08	1.37E-07
Ra	3.37E-11	3.45E-11	3.76E-11	4.73E-11	8.67E-11	2.52E-10	1.45E-09	1.05E-08
Bi	1.20E-13	1.24E-13	1.40E-13	1.76E-13	2.80E-13	5.46E-13	1.06E-12	1.98E-12
Po	9.37E-17	9.81E-17	1.14E-16	1.62E-16	3.52E-16	1.67E-15	3.31E-14	5.94E-13
Rn	1.25E-15	1.28E-15	1.45E-15	1.98E-15	3.72E-15	8.47E-15	2.23E-14	8.00E-14
Tl	1.20E-15	1.24E-15	1.41E-15	1.96E-15	3.68E-15	7.99E-15	1.51E-14	1.46E-14
Total	1.92E+04	1.92E+04	1.92E+04	1.92E+04	1.92E+04	1.92E+04	1.92E+04	1.92E+04

Table A-23: Average Bundle Case with 900 kW and 220 MWh/kgU and 30 Years of Decay (masses in grams)

Time (y)	1.00E-02	3.00E-02	1.00E-01	3.00E-01	1.00E+00	3.00E+00	1.00E+01	3.00E+01
U	1.89E+04	1.89E+04	1.89E+04	1.89E+04	1.89E+04	1.89E+04	1.89E+04	1.89E+04
Xe	3.01E+01	3.01E+01	3.01E+01	3.01E+01	3.01E+01	3.01E+01	3.01E+01	3.01E+01
Mo	1.52E+01	1.53E+01	1.57E+01	1.66E+01	1.75E+01	1.76E+01	1.76E+01	1.76E+01
Cs	1.38E+01	1.40E+01	1.40E+01	1.40E+01	1.38E+01	1.34E+01	1.24E+01	1.04E+01
Ru	1.44E+01	1.42E+01	1.38E+01	1.31E+01	1.25E+01	1.18E+01	1.16E+01	1.16E+01
Ba	7.31E+00	7.16E+00	6.94E+00	6.91E+00	7.07E+00	7.47E+00	8.51E+00	1.05E+01
Pd	5.89E+00	5.92E+00	6.00E+00	6.19E+00	6.71E+00	7.33E+00	7.54E+00	7.54E+00
Tc	4.52E+00	4.55E+00	4.56E+00	4.56E+00	4.56E+00	4.56E+00	4.56E+00	4.56E+00
Sr	5.10E+00	5.04E+00	4.86E+00	4.58E+00	4.38E+00	4.25E+00	3.85E+00	3.01E+00
Rh	2.35E+00	2.48E+00	2.84E+00	3.30E+00	3.48E+00	3.48E+00	3.48E+00	3.48E+00
Te	2.65E+00	2.60E+00	2.56E+00	2.54E+00	2.53E+00	2.54E+00	2.57E+00	2.57E+00
Kr	1.82E+00	1.82E+00	1.81E+00	1.81E+00	1.81E+00	1.79E+00	1.76E+00	1.71E+00
Rb	1.65E+00	1.65E+00	1.65E+00	1.65E+00	1.65E+00	1.67E+00	1.70E+00	1.75E+00
I	1.39E+00	1.33E+00	1.28E+00	1.30E+00	1.32E+00	1.32E+00	1.32E+00	1.32E+00
Ag	6.94E-01	6.90E-01	6.86E-01	6.86E-01	6.84E-01	6.83E-01	6.83E-01	6.83E-01
Cd	3.87E-01	3.90E-01	3.94E-01	3.95E-01	3.96E-01	3.97E-01	3.97E-01	3.97E-01
Sn	3.09E-01	3.09E-01	3.08E-01	3.08E-01	3.07E-01	3.07E-01	3.07E-01	3.07E-01
Se	2.83E-01	2.83E-01	2.83E-01	2.83E-01	2.83E-01	2.83E-01	2.83E-01	2.83E-01
Br	1.08E-01	1.08E-01	1.08E-01	1.08E-01	1.08E-01	1.08E-01	1.08E-01	1.08E-01
Sb	1.13E-01	1.10E-01	1.08E-01	1.05E-01	9.68E-02	7.86E-02	5.56E-02	5.10E-02
In	1.50E-02	1.51E-02	1.52E-02	1.54E-02	1.54E-02	1.55E-02	1.57E-02	1.59E-02
Ge	2.02E-03	2.02E-03	2.02E-03	2.02E-03	2.02E-03	2.02E-03	2.02E-03	2.02E-03
As	6.52E-04	6.42E-04	6.41E-04	6.41E-04	6.41E-04	6.41E-04	6.41E-04	6.41E-04
H	2.87E-04	2.87E-04	2.85E-04	2.82E-04	2.71E-04	2.43E-04	1.64E-04	5.31E-05
C	1.40E-07	1.40E-07	1.40E-07	1.40E-07	1.40E-07	1.40E-07	1.40E-07	1.39E-07
Zn	2.06E-07	7.26E-08	6.21E-08	6.21E-08	6.21E-08	6.21E-08	6.21E-08	6.21E-08
Pb	8.14E-12	9.22E-12	1.37E-11	3.38E-11	1.90E-10	1.38E-09	1.18E-08	5.16E-08
Pb	8.14E-12	9.22E-12	1.37E-11	3.38E-11	1.90E-10	1.38E-09	1.18E-08	5.16E-08
Ra	4.47E-12	4.80E-12	6.03E-12	1.03E-11	3.24E-11	1.59E-10	1.33E-09	1.10E-08
Bi	1.14E-14	1.27E-14	1.69E-14	2.74E-14	6.09E-14	1.57E-13	3.77E-13	9.67E-13
Po	5.08E-18	5.79E-18	8.66E-18	1.80E-17	6.63E-17	7.74E-16	2.88E-14	6.12E-13
Rn	1.54E-16	1.69E-16	2.23E-16	3.99E-16	1.04E-15	3.25E-15	1.34E-14	7.56E-14
Tl	1.46E-16	1.62E-16	2.16E-16	3.88E-16	9.68E-16	2.60E-15	5.71E-15	5.73E-15
Total	1.92E+04	1.92E+04	1.92E+04	1.92E+04	1.92E+04	1.92E+04	1.92E+04	1.92E+04

Table A-24: Average Bundle Case with 900 kW and 320 MWh/kgU and 30 Years of Decay (masses in grams)

Time (y)	1.00E-02	3.00E-02	1.00E-01	3.00E-01	1.00E+00	3.00E+00	1.00E+01	3.00E+01
U	1.88E+04	1.88E+04	1.88E+04	1.88E+04	1.88E+04	1.88E+04	1.88E+04	1.88E+04
Xe	4.45E+01	4.45E+01	4.45E+01	4.45E+01	4.45E+01	4.45E+01	4.45E+01	4.45E+01
Mo	2.30E+01	2.31E+01	2.35E+01	2.45E+01	2.54E+01	2.55E+01	2.55E+01	2.55E+01
Ru	2.19E+01	2.17E+01	2.12E+01	2.04E+01	1.93E+01	1.83E+01	1.80E+01	1.80E+01
Cs	2.04E+01	2.05E+01	2.05E+01	2.04E+01	2.02E+01	1.95E+01	1.80E+01	1.50E+01
Pd	1.08E+01	1.08E+01	1.09E+01	1.12E+01	1.21E+01	1.31E+01	1.34E+01	1.34E+01
Ba	1.05E+01	1.03E+01	1.01E+01	1.01E+01	1.04E+01	1.10E+01	1.26E+01	1.56E+01
Tc	6.51E+00	6.54E+00	6.55E+00	6.55E+00	6.55E+00	6.55E+00	6.55E+00	6.55E+00
Rh	3.74E+00	3.89E+00	4.30E+00	4.82E+00	5.01E+00	5.02E+00	5.02E+00	5.02E+00
Sr	6.43E+00	6.37E+00	6.21E+00	5.97E+00	5.78E+00	5.60E+00	5.07E+00	3.98E+00
Te	3.93E+00	3.87E+00	3.84E+00	3.81E+00	3.80E+00	3.83E+00	3.86E+00	3.87E+00
Kr	2.44E+00	2.44E+00	2.44E+00	2.44E+00	2.43E+00	2.41E+00	2.36E+00	2.30E+00
Rb	2.20E+00	2.20E+00	2.20E+00	2.20E+00	2.21E+00	2.22E+00	2.27E+00	2.34E+00
I	2.08E+00	2.02E+00	1.97E+00	2.00E+00	2.02E+00	2.02E+00	2.02E+00	2.02E+00
Ag	1.17E+00	1.16E+00	1.16E+00	1.16E+00	1.15E+00	1.15E+00	1.15E+00	1.15E+00
Cd	7.60E-01	7.64E-01	7.69E-01	7.71E-01	7.74E-01	7.76E-01	7.76E-01	7.75E-01
Sn	5.03E-01	5.02E-01	5.01E-01	5.01E-01	5.00E-01	5.00E-01	5.00E-01	5.00E-01
Se	3.96E-01	3.97E-01	3.97E-01	3.97E-01	3.97E-01	3.97E-01	3.96E-01	3.96E-01
Br	1.53E-01	1.53E-01	1.53E-01	1.53E-01	1.53E-01	1.53E-01	1.53E-01	1.53E-01
Sb	1.75E-01	1.72E-01	1.69E-01	1.65E-01	1.52E-01	1.23E-01	8.74E-02	8.02E-02
In	2.13E-02	2.14E-02	2.16E-02	2.17E-02	2.18E-02	2.20E-02	2.23E-02	2.27E-02
Ge	2.83E-03	2.83E-03	2.83E-03	2.83E-03	2.83E-03	2.83E-03	2.83E-03	2.83E-03
As	9.28E-04	9.18E-04	9.17E-04	9.17E-04	9.17E-04	9.17E-04	9.17E-04	9.17E-04
H	4.28E-04	4.28E-04	4.26E-04	4.22E-04	4.05E-04	3.62E-04	2.44E-04	7.94E-05
C	2.05E-07	2.05E-07	2.05E-07	2.05E-07	2.05E-07	2.05E-07	2.04E-07	2.04E-07
Zn	2.55E-07	1.15E-07	1.04E-07	1.04E-07	1.04E-07	1.04E-07	1.04E-07	1.04E-07
Pb	2.92E-11	3.20E-11	4.33E-11	9.00E-11	4.30E-10	2.97E-09	2.53E-08	1.11E-07
Pb	2.92E-11	3.20E-11	4.33E-11	9.00E-11	4.30E-10	2.97E-09	2.53E-08	1.11E-07
Ra	9.09E-12	9.56E-12	1.13E-11	1.70E-11	4.32E-11	1.74E-10	1.26E-09	9.98E-09
Bi	3.59E-14	3.92E-14	4.88E-14	7.12E-14	1.42E-13	3.45E-13	7.92E-13	1.60E-12
Po	2.01E-17	2.21E-17	2.98E-17	5.25E-17	1.35E-16	9.01E-16	2.70E-14	5.54E-13
Rn	3.91E-16	4.19E-16	5.25E-16	8.64E-16	2.06E-15	5.86E-15	1.86E-14	7.45E-14
Tl	3.86E-16	4.19E-16	5.29E-16	8.79E-16	2.08E-15	5.52E-15	1.22E-14	1.22E-14
Total	1.92E+04	1.92E+04	1.92E+04	1.92E+04	1.92E+04	1.92E+04	1.92E+04	1.92E+04

APPENDIX B: POWER-BURNUP REDUCED HISTORIES AND COMPARISON TO PROVIDED HISTORIES

CONTENTS

Page

B.1 EVALUATION OF EXPERIMENTAL INSTANT RELEASE FRACTIONS

Table B-1: Intermediate and Outer Element Power Histories for F12059C

F12059C			
Intermediate		Outer	
Burnup (MWd/tU)	Linear element power (W/cm)	Burnup (MWd/tU)	Linear element power (W/cm)
42.4	106.5	51.3	129.9
185	107	224	130.5
346.9	101.3	420	123.5
508.8	103.3	616	126
651.4	92.3	788.7	112.6
794	95	961.3	115.8
959.7	101.8	1162	124.1
1121.6	105	1358	128
1283.4	118.6	1554	144.6
1796	395.7	2174.7	482.5
2385.7	399.8	2888.7	487.6
2894.5	403	3504.7	491.5
3464.9	383.1	4195.3	467.2
4016	368.9	4862.7	449.9
4524.8	374.2	5478.7	456.3
5118.3	374.2	6197.3	456.3
5669.5	337.4	6864.7	411.5
6178.2	352.6	7480.7	430
6667.7	363.7	8073.3	443.5
7095.5	339.5	8591.3	414
7523.3	233	9109.3	284.1
7808.5	229.3	9454.7	279.6
8155.4	194.2	9874.7	236
8502.3	214.1	10294.7	261.1
9215.3	228.8	11158	279

Table B-2: Intermediate and Outer Element Power Histories for F21271C

F21271C			
Intermediate		Outer	
Burnup (MWd/tU)	Linear element power (W/cm)	Burnup (MWd/tU)	Linear element power (W/cm)
111.8	290.1	135.3	353.8
520.3	278.2	630	339.3
963.5	279.5	1166.7	340.8
1473.6	279.3	1740.7	340.6
1892.4	267.8	2291.3	326.6
2181.5	272.4	2641.3	332.2
2744.2	282.1	3322.7	344.1
3048.6	272.4	3691.3	332.2
3584.4	265.8	4340	324.2
4289.7	384.8	5194	469.3
5037.4	382.5	6099.3	466.4
5769.7	368.7	6986	449.6
6463.4	355.5	7826	433.6
7060.8	351.8	8549.3	429
7662.1	349.5	9277.3	426.2
8201.7	313.1	9930.7	381.8
8783.6	314.8	10635.3	383.9
9304	286.5	11265.3	349.4
9820.4	303.3	11890.7	369.9
10205.8	82.9	12357.3	101.1
10352.3	82.8	12534.7	100.9
10498.8	81.3	12712	99.1
10645.2	83.1	12889.3	101.4
10749.3	79.9	13015.3	97.4
9215.3	228.8	11158	279

Table B-3: Intermediate and Outer Element Power Histories for G00815W

G00815W			
Intermediate		Outer	
Burnup (MWd/tU)	Linear element power (W/cm)	Burnup (MWd/tU)	Linear element power (W/cm)
123.3	360.5	149.3	439.6
389.3	359.5	471.3	438.4
674.5	365.7	816.7	446
959.7	373.1	1162	455
1244.9	361.4	1507.3	440.9
1507	340.6	1824.7	415.3
1734.4	372	2100	453.7
1996.5	343.7	2417.3	419.2
2243.1	362.1	2716	441.6
2466.7	354.2	2986.7	432
2671	344.2	3234	419.8
2894.5	329.6	3504.7	401.9
3160.4	342.7	3826.7	417.9
3384	326.4	4097.3	398
3588.2	345.8	4344.7	421.7
3792.5	333.7	4592	407
4035.3	310.1	4886	378.2
4301.3	281.8	5208	343.6
4547.9	288.1	5506.7	351.3
4771.5	295.9	5777.3	360.9
5056.7	326.9	6122.7	398.7
5322.6	306.4	6444.7	373.7
5607.8	341.1	6790	416

Table B-4: Intermediate and Outer Element Power Histories for G13374S

G13374S			
Intermediate		Outer	
Burnup (MWd/tU)	Linear element power (W/cm)	Burnup (MWd/tU)	Linear element power (W/cm)
88.6	173.6	107.3	211.7
416.3	211.7	504	258.1
801.7	203.6	970.7	248.3
1129.3	212.5	1367.3	259.2
1534.0	232.5	1857.3	283.5
1861.6	204.8	2254	249.7
2154.5	206.6	2608.7	252
2439.7	203.8	2954	248.6
2705.6	206.9	3276	252.3
3241.4	440.1	3924.7	536.7
3723.1	430.1	4508	524.5
4224.2	430.8	5114.7	525.4
4894.8	410.8	5926.7	501
5395.8	411.3	6533.3	501.6
5746.6	393.6	6958	480.1
6224.5	397.6	7536.7	484.9
6690.8	382.8	8101.3	466.9
7095.5	389.8	8591.3	475.3
7534.9	381.3	9123.3	465
7835.5	195.0	9487.3	237.8
8043.6	200.1	9739.3	244
8290.3	202.6	10038	247.1
8567.8	201.8	10374	246.1
8729.7	200.9	10570	245.1
8968.6	196.0	10859.3	239
9145.9	194.2	11074	236.8
9373.3	192.3	11349.3	234.5
9600.7	187.9	11624.7	229.1
9789.6	188.5	11853.3	229.9
9993.9	176.1	12100.7	214.8
10240.5	177.4	12399.3	216.4

Table B-5: Intermediate and Outer Element Power Histories for J49093C

J49093C			
Inner		Outer	
Burnup (MWd/tU)	Linear element power (W/cm)	Burnup (MWd/tU)	Linear element power (W/cm)
75.2	190.4	102.7	260.8
396.3	185.6	541.3	254.3
727.8	181.3	994	248.3
1021.6	180.7	1395.3	247.5
1322.3	177.6	1806	243.3
1701.5	182.9	2324	250.5
2036.3	191.5	2781.3	262.3
2275.5	179.2	3108	245.5
2914.4	400.0	3980.7	547.9
3560.2	371.7	4862.7	509.2
4267.4	370.6	5828.7	507.7
4879.0	361.3	6664	494.9
5299.3	362.4	7238	496.4
5709.3	345.9	7798	473.9
6129.5	365.6	8372	500.8
6488.3	355.2	8862	486.6
7007.6	340.5	9571.3	466.5
7209.2	165.6	9846.7	226.8
7362.9	173.0	10056.7	237
7561.1	164.7	10327.3	225.6
7755.8	157.1	10593.3	215.2
7926.7	159.6	10826.7	218.7
8118.0	159.9	11088	219
8271.8	156.4	11298	214.3
8442.6	158.2	11531.3	216.7
8644.2	155.3	11806.7	212.7
8859.4	161.9	12100.7	221.7
9037.1	162.9	12343.3	223.1
9214.8	164.7	12586	225.6
9368.5	161.5	12796	221.2

B.2 CALCULATION OF AVERAGE AND PESSIMISTIC INSTANT RELEASE FRACTIONS

Table B-6: Power Histories for Task 2

Bundle Power (kW)	Linear Element Power (W/cm)			
	Outer	Intermediate	Inner	Centre
450.0	273.8	224.9	201.8	199.5
900.0	547.6	449.9	403.5	399.0

Burnup History 220 MWh/kgU		Burnup History 320 MWh/kgU	
(MWh/kgU)	(MWd/tU)	(MWh/kgU)	(MWd/tU)
0.0	0.0	0.0	0.0
22.0	916.7	32.0	1333.3
44.0	1833.3	64.0	2666.7
66.0	2750.0	96.0	4000.0
88.0	3666.7	128.0	5333.3
110.0	4583.3	160.0	6666.7
132.0	5500.0	192.0	8000.0
154.0	6416.7	224.0	9333.3
176.0	7333.3	256.0	10666.7
198.0	8250.0	288.0	12000.0
220.0	9166.7	320.0	13333.3

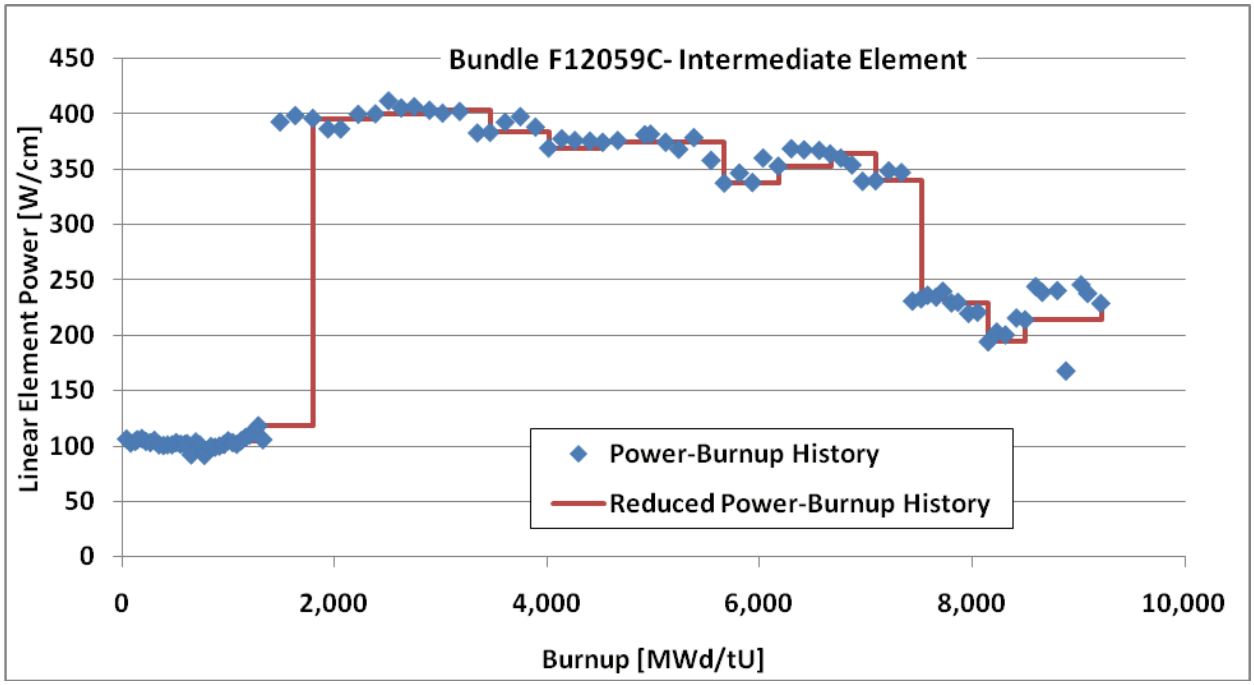

Figure B-1: Reference and Reduced Power-Burnup History for F12059C Intermediate Element

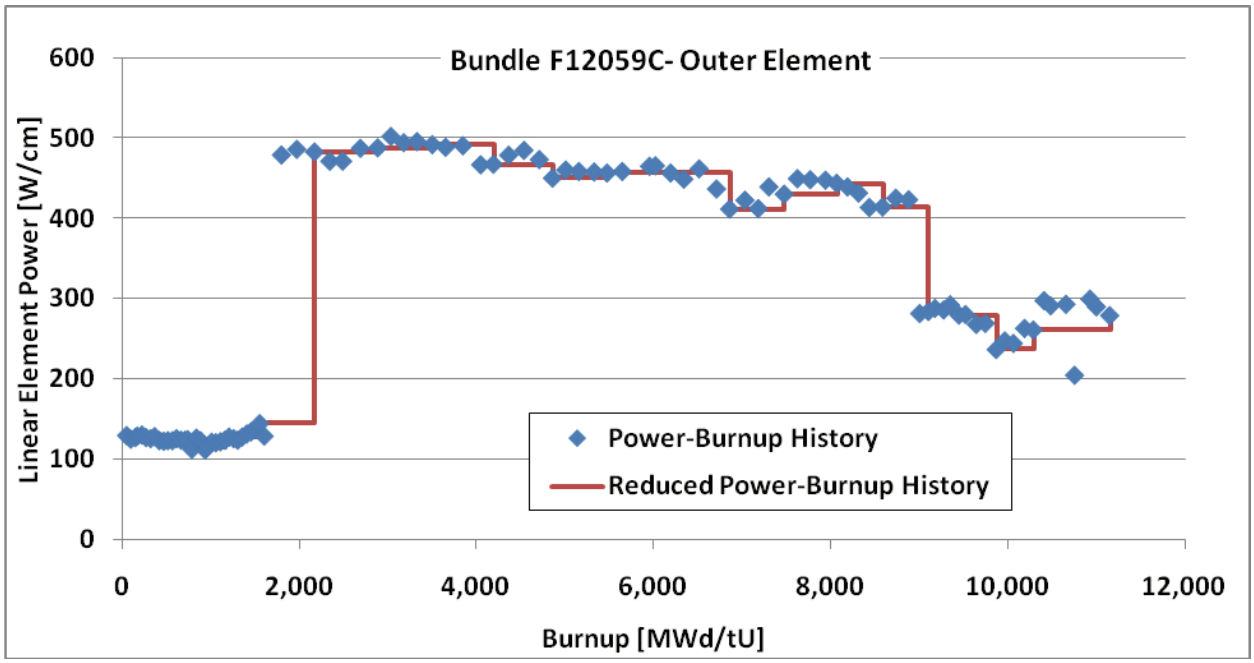

Figure B-2: Reference and Reduced Power-Burnup History for F12059C Outer Element

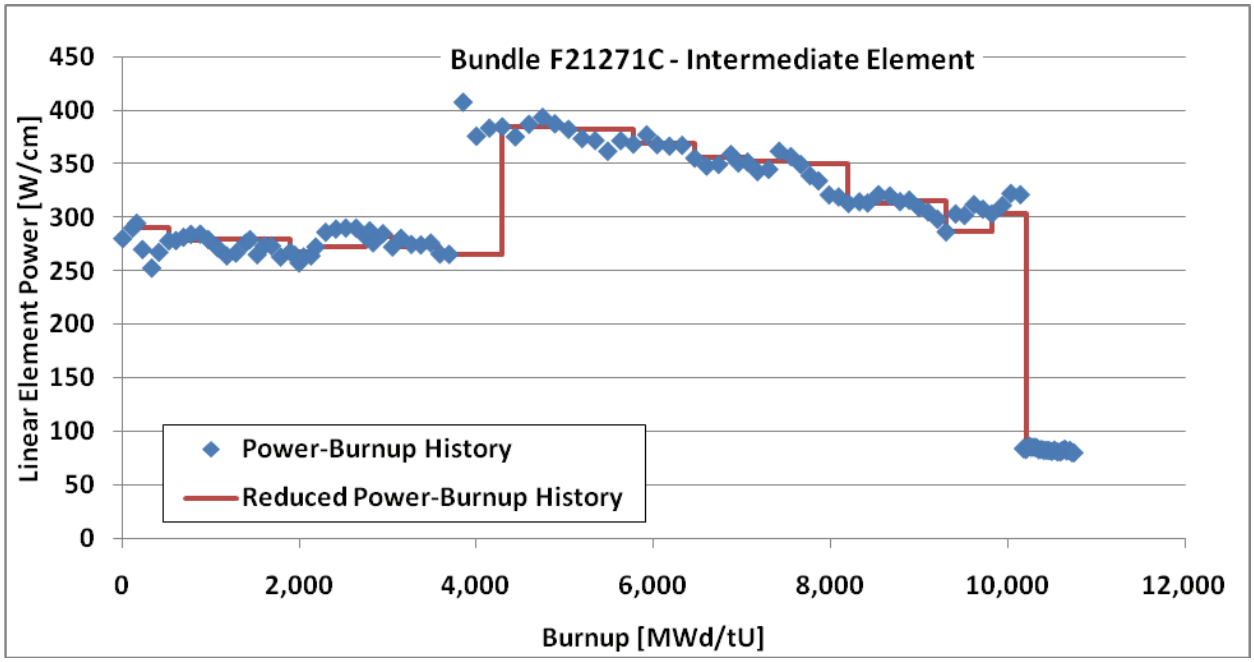

Figure B-3: Reference and Reduced Power-Burnup History for F21271C Intermediate Element

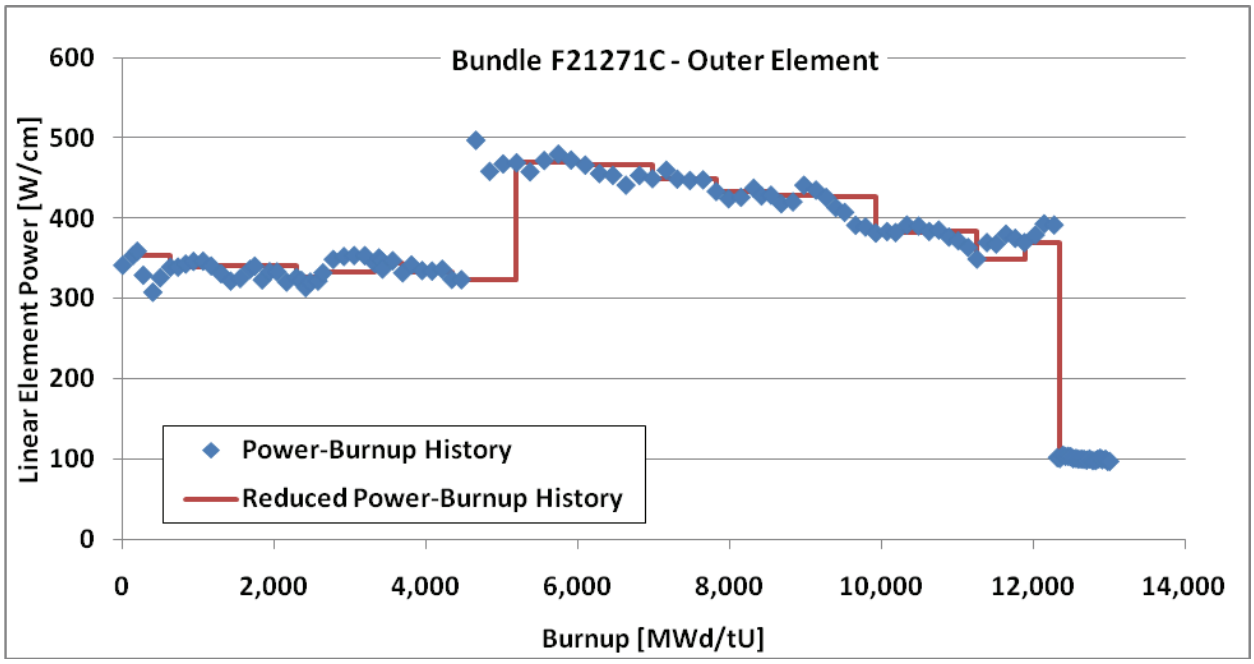

Figure B-4: Reference and Reduced Power-Burnup History for F21271C Outer Element

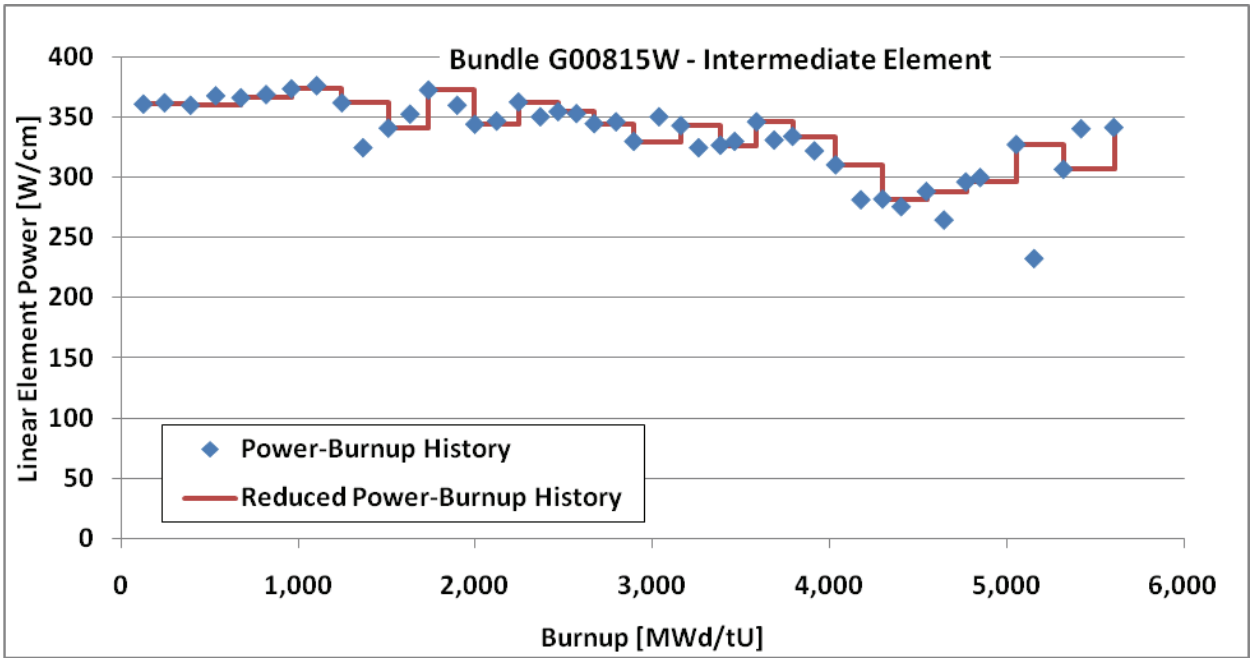

Figure B-5: Reference and Reduced Power-Burnup History for G00815W Intermediate Element

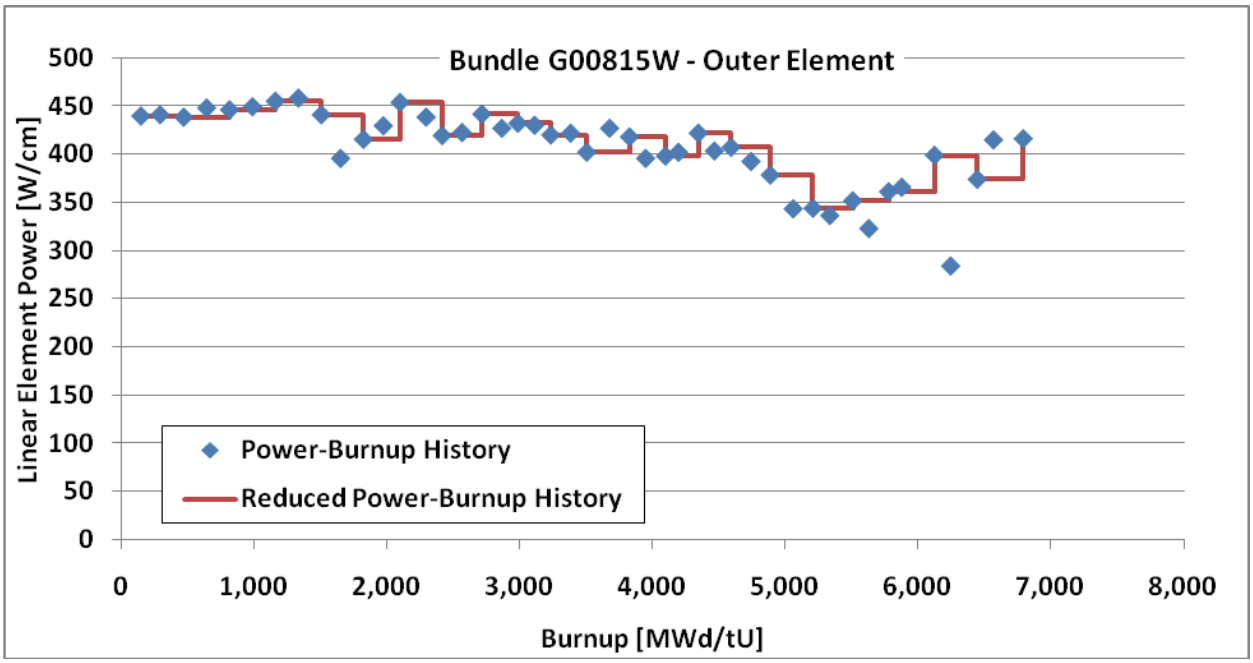

Figure B-6: Reference and Reduced Power-Burnup History for G00815W Outer Element

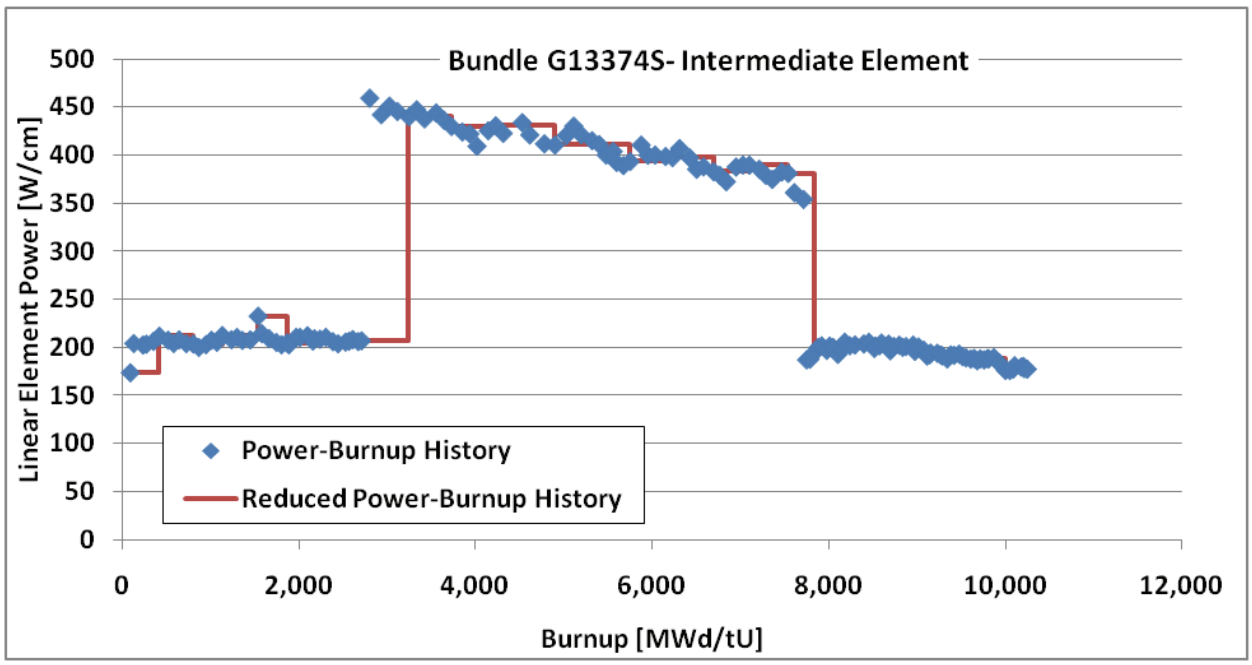

Figure B-7: Reference and Reduced Power-Burnup History for G13374S Intermediate Element

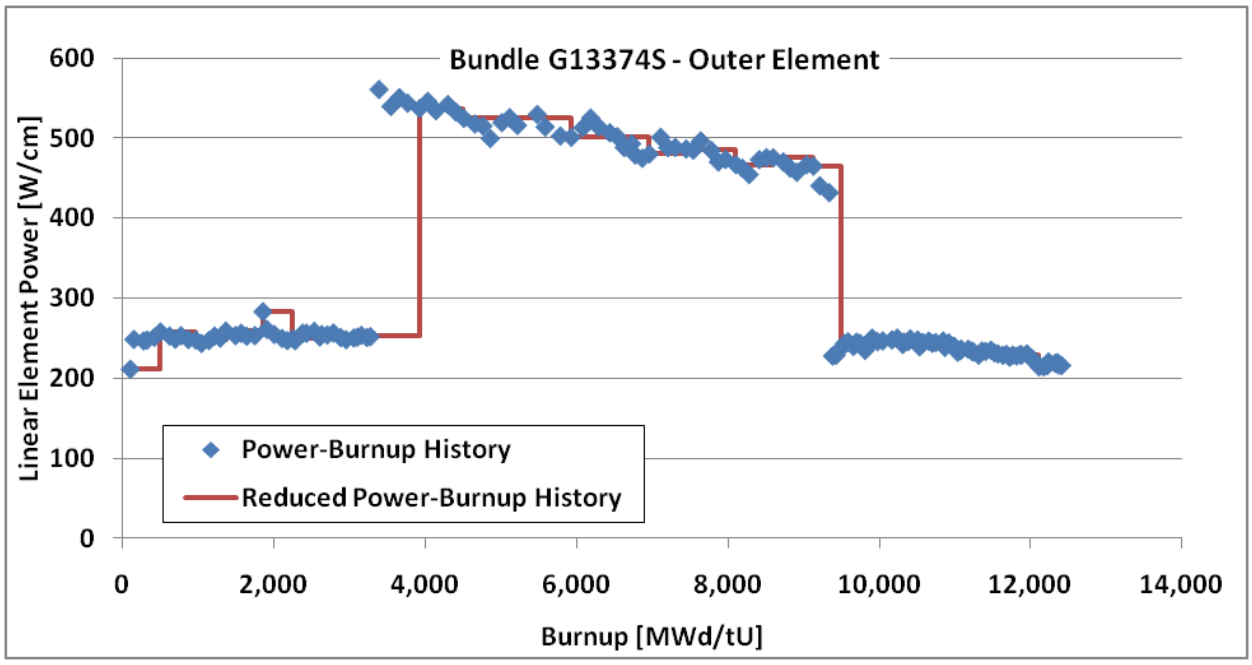

Figure B-8: Reference and Reduced Power-Burnup History for G13374S Outer Element

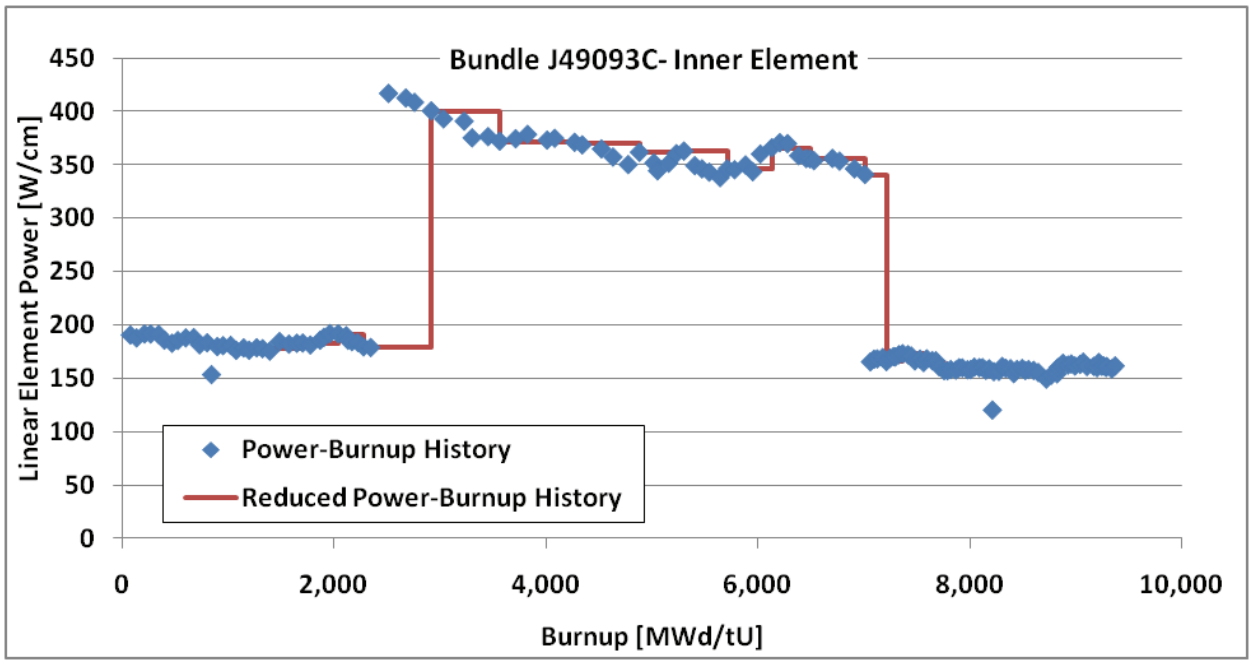

Figure B-9: Reference and Reduced Power-Burnup History for J49093C Inner Element

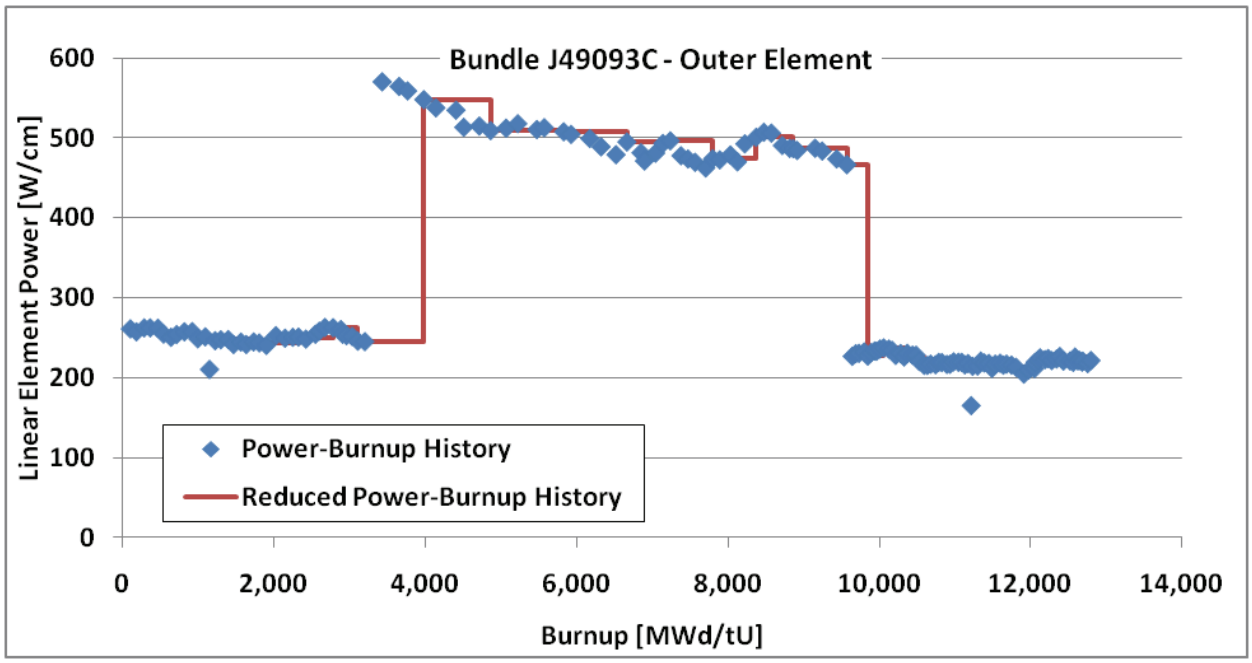

Figure B-10: Reference and Reduced Power-Burnup History for J49093C Outer Element

APPENDIX C: CHEMICAL SPECIATION

CONTENTS

Page

C.1 EVALUATION OF EXPERIMENTAL INSTANT RELEASE FRACTIONS

Table C-1: CANDU F12059C outer (Masses of chemical elements (g)).

F12059C OUTER		Units (Grams)	
		Grain-Boundary	Gap Release
Time (y)	**7.00E+00**	**Case 2 B**	**Case 2 R**
U	5.05E+02		
Xe	9.77E-01	2.53E-02	2.69E-02
Mo	5.65E-01	1.46E-02	1.56E-02
Cs	4.12E-01	1.07E-02	1.14E-02
Ru	3.86E-01	9.99E-03	1.06E-02
Pd	2.70E-01	6.99E-03	7.44E-03
Ba	2.64E-01	6.84E-03	7.28E-03
Tc	1.46E-01	3.78E-03	4.02E-03
Sr	1.23E-01	3.18E-03	3.39E-03
Rh	1.12E-01	2.90E-03	3.09E-03
Te	8.40E-02	2.17E-03	2.32E-03
Kr	5.49E-02	1.42E-03	1.51E-03
Rb	5.22E-02	1.35E-03	1.44E-03
I	4.37E-02	1.13E-03	1.20E-03
Se	8.96E-03	2.32E-04	2.47E-04
H	6.32E-06	1.64E-07	1.74E-07
Pb	2.61E-10	6.76E-12	7.20E-12
Bi	1.22E-14	3.16E-16	3.36E-16
Rn	2.86E-16	7.41E-18	7.88E-18
Temperature (°C)		992.4	343.6

Case 2 B: **Input is gram (note for the calculation Xe and Kr were combined)**

2.672E-2 Xe + 1.46E-2 Mo + 1.07E-2 Cs + 9.99E-3 Ru + 6.99E-3 Pd + 6.84E-3 Ba + 3.78E-3 Tc + 3.18E-3 Sr + 2.90E-3 Rh + 2.17E-3 Te + 1.35E-3 Rb + 1.13E-3 I + 2.32E-4 Se + 1.64E-7 H + 6.76E-12 Pb + 3.16E-16 Bi + 7.41E-18 Rn + 637 UO2

Output

2.1840E-04 mol (2.1679E-04 litre) of gas_ideal at (992.40 °C, 1.0600E-02 GPa, a=1.0000)
(0.93187 Xe
+ 4.8837E-02 Cs
+ 1.0393E-02 Rb
+ 4.8278E-03 Cs2
+ 1.9057E-03 CsRb
+ 8.2749E-04 Cs2I2
+ 5.6671E-04 CsI
+ 2.8700E-04 H2
+ 2.0714E-04 Rb2
+ 1.7095E-04 CsH
+ 1.0714E-04 IRb
+ 2.6988E-06 I2Rb2
+ 2.8138E-08 CsOH
+ 1.3415E-08 RbOH
+ 9.1421E-09 Ba
+ 1.0368E-09 H cut off at 10^{-10}

+ 637.00 gram Fluorite (UO_2) at 992.40 °C, 1.0600E-02 GPa, a=1.0000
(99.997 wt.% UO2
+ 2.4392E-10 wt.% UO3
+ 2.3645E-04 wt.% UO
+ 5.3946E-04 wt.% Cs2O
+ 5.9037E-04 wt.% SrO
+ 1.1282E-03 wt.% BaO
+ 7.4010E-23 wt.% MoO2
+ 1.7251E-15 wt.% TeO2
+ 1.9067E-04 wt.% Rb2O)

+ 2.6362E-02 gram $U(Pd\_Rh\_Ru)_3$ at 992.40 °C, 1.0600E-02 GPa, a=1.0000
(46.281 wt.% UPd3
+ 19.286 wt.% URh3
+ 34.433 wt.% URu3)

+ 1.8106E-02 gram BCC Noble Metal Phase at 992.40 °C, 1.0600E-02 GPa, a=1.0000
(71.982 wt.% Mo
+ 3.1805E-03 wt.% Pd
+ 18.831 wt.% Tc
+ 9.1575 wt.% Ru
+ 2.6738E-02 wt.% Rh)

+ 5.2085E-03 gram HCP Noble Metal Phase at 992.40 °C, 1.0600E-02 GPa, a=1.0000
(30.082 wt.% Mo

+ 8.8475E-05 wt.% Pd
+ 7.1118 wt.% Tc
+ 62.336 wt.% Ru
+ 0.47022 wt.% Rh)

+ 6.6905E-03 gram Cs_2Te_solid(s)
+ 2.1810E-03 gram CsI_liquid(liq)
+ 6.3549E-04 gram BaSe_solid
+ 0.00000 gram Mo_solid(s) a=0.79213

Case 2 R: Input is gram (note for the calculation Xe and Kr were combined)

2.841E-2 Xe + 1.56E-2 Mo + 1.14E-2 Cs + 1.06E-2 Ru + 7.44E-3 Pd + 7.28E-3 Ba + 4.02E-3 Tc + 3.39E-3 Sr + 3.09E-3 Rh + 2.32E-3 Te + 1.44E-3 Rb + 1.20E-3 I + 2.47E-4 Se + 1.74E-7 H + 7.20E-12 Pb + 3.36E-16 Bi + 7.88E-18 Rn + 637 UO2

Output

2.1651E-04 mol (1.0474E-04 litre) gas_ideal at (343.60 °C, 1.0600E-02 GPa, a=1.0000)
(0.99946 Xe
+ 3.9865E-04 H2
+ 8.2327E-05 Cs
+ 4.9747E-05 Rb
+ 1.8565E-06 CsRb
+ 1.6379E-06 Cs2
+ 7.5965E-07 Rb2
+ 2.9747E-08 CsH cut off at 10^{-10}

+ 636.99 gram Fluorite (UO_2) at 343.60 °C, 1.0600E-02 GPa, a=1.0000
(99.999 wt.% UO2
+ 3.5663E-20 wt.% UO3
+ 9.2577E-11 wt.% UO
+ 4.4649E-07 wt.% Cs2O
+ 6.2937E-04 wt.% SrO
+ 3.4607E-07 wt.% BaO
+ 1.1973E-63 wt.% MoO2
+ 3.7520E-37 wt.% TeO2
+ 1.2745E-06 wt.% Rb2O)

+ 2.4413E-02 gram $U(Pd\_Rh\_Ru)_3$ at 343.60 °C, 1.0600E-02 GPa, a=1.0000
(53.196 wt.% UPd3
+ 22.412 wt.% URh3
+ 24.391 wt.% URu3)

+ 1.0722E-02 gram BCC Noble Metal Phase at 343.60 °C, 1.0600E-02 GPa, a=1.0000
(95.834 wt.% Mo
+ 6.0363E-10 wt.% Pd
+ 4.1123 wt.% Tc
+ 5.3342E-02 wt.% Ru
+ 3.6567E-06 wt.% Rh)

+ 9.7554E-03 gram HCP Noble Metal Phase at 343.60 °C, 1.0600E-02 GPa, a=1.0000
(25.356 wt.% Mo
+ 8.5061E-11 wt.% Pd
+ 0.23594 wt.% Tc
+ 74.404 wt.% Ru
+ 4.7654E-03 wt.% Rh)

+ 7.6463E-03 gram BaO_solid(s)
+ 7.1529E-03 gram Cs_2Te_solid(s)
+ 6.4071E-03 gram $Tc_{11}Mo_9$_solid(s)

+ 5.3051E-03 gram Cs_liquid(liq)
+ 2.4567E-03 gram CsI_solid(s)
+ 1.4316E-03 gram Rb_liquid(liq)
+ 6.7658E-04 gram BaSe_solid
+ 1.6744E-11 gram Ba_2Pb_solid
+ 0.00000 gram Mo_solid(s) a=0.96465

Table C-2: CANDU F21271C outer (Masses of chemical elements (g)).

F21271C OUTER	Units (Grams)	
		Gap Release
Time (y)	**7.00E+00**	**Case 4 R**
U	5.03E+02	
Xe	1.22E+00	4.85E-02
Mo	6.96E-01	2.77E-02
Cs	5.08E-01	2.02E-02
Ru	4.94E-01	1.97E-02
Ba	3.72E-01	1.48E-02
Pd	3.29E-01	1.31E-02
Tc	1.79E-01	7.12E-03
Sr	1.44E-01	5.73E-03
Rh	1.36E-01	5.41E-03
Te	1.06E-01	4.22E-03
Kr	6.47E-02	2.57E-03
Rb	6.13E-02	2.44E-03
I	5.54E-02	2.20E-03
Se	1.08E-02	4.30E-04
H	7.91E-06	3.15E-07
Pb	3.99E-10	1.59E-11
Bi	1.87E-14	7.44E-16
Rn	3.72E-16	1.48E-17
Temperature (°C)		355.4

Case 4 R: Input is gram (note for the calculation Xe and Kr were combined)

5.107E-2 Xe + 2.77E-2 Mo + 2.02E-2 Cs + 1.97E-2 Ru + 1.31E-2 Pd + 1.48E-2 Ba + 7.12E-3 Tc + 5.73E-3 Sr + 5.41E-3 Rh + 4.22E-3 Te + 2.44E-3 Rb + 2.20E-3 I + 4.30E-4 Se + 3.15E-7 H + 1.59E-11 Pb + 7.44E-16 Bi + 1.48E-17 Rn + 637 UO2

Output

3.8921E-04 mol (1.9189E-04 litre) gas_ideal at (355.40 °C, 1.0600E-02 GPa, a=1.0000)
(0.99942 Xe
+ 4.0146E-04 H2
+ 1.0675E-04 Cs
+ 6.5529E-05 Rb
+ 2.6704E-06 CsRb
+ 2.3224E-06 Cs2
+ 1.0995E-06 Rb2
+ 4.2146E-08 CsH cut off at 10^{-10}

+ 636.98 gram Fluorite (UO_2) at 355.40 °C, 1.0600E-02 GPa, a=1.0000
(99.999 wt.% UO2
+ 1.6085E-19 wt.% UO3
+ 2.0143E-10 wt.% UO
+ 5.1331E-07 wt.% Cs2O
+ 1.0638E-03 wt.% SrO
+ 4.9362E-07 wt.% BaO
+ 2.1855E-62 wt.% MoO2
+ 1.3145E-36 wt.% TeO2
+ 1.4314E-06 wt.% Rb2O)

+ 4.6160E-02 gram $U(Pd\_Rh\_Ru)_3$ at 355.40 °C, 1.0600E-02 GPa, a=1.0000
(49.538 wt.% UPd3
+ 20.754 wt.% URh3
+ 29.708 wt.% URu3)

+ 1.9444E-02 gram BCC Noble Metal Phase at 355.40 °C, 1.0600E-02 GPa, a=1.0000
(95.593 wt.% Mo
+ 8.7152E-10 wt.% Pd
+ 4.3424 wt.% Tc
+ 6.4531E-02 wt.% Ru
+ 3.8600E-06 wt.% Rh)

+ 1.6164E-02 gram HCP Noble Metal Phase at 355.40 °C, 1.0600E-02 GPa, a=1.0000
(25.461 wt.% Mo
+ 1.0940E-10 wt.% Pd
+ 0.26647 wt.% Tc
+ 74.268 wt.% Ru
+ 4.3106E-03 wt.% Rh)

+ 1.5686E-02 gram BaO_solid(s)
+ 1.3011E-02 gram Cs_2Te_solid(s)
+ 1.1229E-02 gram $Tc_{11}Mo_9$_solid(s)

+ 9.0961E-03 gram Cs_liquid(liq)
+ 4.5040E-03 gram CsI_solid(s)
+ 2.4293E-03 gram Rb_liquid(liq)
+ 1.1779E-03 gram BaSe_solid
+ 3.6976E-11 gram Ba_2Pb_solid
+ 0.00000 gram Mo_solid(s) a=0.96275

Table C-3: CANDU G00815W outer (Masses of chemical elements (g)).

G00815W OUTER	Units (Grams)	
		Grain-Boundary
Time (y)	**7.00E+00**	**Case 6 B**
U	5.08E+02	
Xe	5.93E-01	2.43E-02
Mo	3.51E-01	1.44E-02
Cs	2.56E-01	1.05E-02
Ru	2.22E-01	9.11E-03
Ba	1.60E-01	6.56E-03
Pd	1.29E-01	5.29E-03
Tc	9.17E-02	3.76E-03
Sr	8.53E-02	3.50E-03
Rh	6.78E-02	2.78E-03
Te	4.98E-02	2.04E-03
Kr	3.72E-02	1.53E-03
Rb	3.57E-02	1.46E-03
I	2.52E-02	1.03E-03
Se	5.78E-03	2.37E-04
H	3.78E-06	1.55E-07
Pb	1.03E-10	4.23E-12
Bi	4.82E-15	1.98E-16
Rn	1.88E-16	7.71E-18
Temperature (°C)		915.85

Case 6 B: Input is gram (note for the calculation Xe and Kr were combined)

(2.583E-2 Xe + 1.44E-2 Mo + 1.05E-2 Cs + 9.11E-3 Ru + 5.29E-3 Pd + 6.56E-3 Ba + 3.76E-3 Tc + 3.50E-3 Sr + 2.78E-3 Rh + 2.04E-3 Te + 1.46E-3 Rb + 1.03E-3 I + 2.37E-4 Se + 1.55E-7 H + 4.23E-12 Pb + 1.98E-16 Bi + 7.71E-18 Rn + 637 UO2

Output

2.1349E-04 mol (1.9910E-04 litre) gas_ideal at (915.85 °C, 1.0600E-02 GPa, a=1.0000)
(0.92155 Xe
+ 5.2231E-02 Cs
+ 1.3514E-02 Rb
+ 7.5304E-03 Cs2
+ 3.6008E-03 CsRb
+ 4.8572E-04 Rb2
+ 3.9675E-04 Cs2I2
+ 2.8274E-04 H2
+ 1.9962E-04 CsI
+ 1.5483E-04 CsH
+ 5.3261E-05 IRb
+ 1.6665E-06 I2Rb2
+ 8.4152E-09 CsOH
+ 5.5992E-09 Ba
+ 3.2841E-09 RbOH
+ 2.6217E-10 H) cut off at 10^{-10}

+ 637.00 gram Fluorite (UO_2) at 915.85 °C, 1.0600E-02 GPa, a=1.0000
(99.998 wt.% UO2
+ 2.3617E-11 wt.% UO3
+ 1.4112E-04 wt.% UO
+ 4.2490E-04 wt.% Cs2O
+ 6.4978E-04 wt.% SrO
+ 1.0776E-03 wt.% BaO
+ 9.2743E-26 wt.% MoO2
+ 1.3542E-17 wt.% TeO2
+ 1.9382E-04 wt.% Rb2O)

+ 2.6669E-02 gram $U(Pd\_Rh\_Ru)_3$ at 915.85 °C, 1.0600E-02 GPa, a=1.0000
(34.623 wt.% UPd3
+ 18.429 wt.% URh3
+ 46.948 wt.% URu3)

+ 1.9125E-02 gram BCC Noble Metal Phase at 915.85 °C, 1.0600E-02 GPa, a=1.0000
(73.547 wt.% Mo
+ 7.0410E-04 wt.% Pd
+ 19.296 wt.% Tc
+ 7.1461 wt.% Ru
+ 1.0720E-02 wt.% Rh)

+ 1.1353E-03 gram HCP Noble Metal Phase at 915.85 °C, 1.0600E-02 GPa, a=1.0000
(29.403 wt.% Mo

+ 1.9793E-05 wt.% Pd
+ 6.1331 wt.% Tc
+ 64.215 wt.% Ru
+ 0.24854 wt.% Rh)

+ 2.0505E-03 gram CsI_liquid(liq)
+ 6.4919E-04 gram BaSe_solid
+ 6.0441E-04 gram Cs_liquid(liq)
+ 0.00000 gram Mo_solid(s) a=0.80706

Table C-4: CANDU G13374S outer (Masses of chemical elements (g)).

G13374S OUTER	Units (Grams)	
		Gap Release
Time (y)	7.00E+00	Case 8 R
U	5.04E+02	
Xe	1.11E+00	8.52E-02
Mo	6.39E-01	4.90E-02
Cs	4.66E-01	3.58E-02
Ru	4.46E-01	3.42E-02
Ba	3.26E-01	2.50E-02
Pd	3.00E-01	2.30E-02
Tc	1.64E-01	1.26E-02
Sr	1.35E-01	1.04E-02
Rh	1.27E-01	9.75E-03
Te	9.62E-02	7.38E-03
Kr	6.05E-02	4.64E-03
Rb	5.75E-02	4.41E-03
I	5.03E-02	3.86E-03
Se	1.00E-02	7.68E-04
H	7.23E-06	5.55E-07
Pb	3.26E-10	2.50E-11
Bi	1.53E-14	1.17E-15
Rn	3.26E-16	2.50E-17
Temperature (°C)		368

Case 8 R: Input is gram (note for the calculation Xe and Kr were combined)

8.984E-2 Xe + 4.90E-2 Mo + 3.58E-2 Cs + 3.42E-2 Ru + 2.30E-2 Pd + 2.50E-2 Ba + 1.26E-2 Tc + 1.04E-2 Sr + 9.75E-3 Rh + 7.38E-3 Te + 4.41E-3 Rb + 3.86E-3 I + 7.68E-4 Se + 5.55E-7 H + 2.50E-11 Pb + 1.17E-15 Bi + 2.50E-17 Rn + 637 UO2

Output

6.8472E-04 mol (3.4435E-04 litre) gas_ideal at (368.00 °C, 1.0600E-02 GPa, a=1.0000)
(0.99936 Xe
+ 4.0205E-04 H2
+ 1.3934E-04 Cs
+ 8.6926E-05 Rb
+ 3.8752E-06 CsRb
+ 3.3208E-06 Cs2
+ 1.6057E-06 Rb2
+ 6.0093E-08 CsH
+ 1.1954E-10 Cs2I2 cut off at 10^{-10}

+ 636.97 gram Fluorite (UO_2) at 368.00 °C, 1.0600E-02 GPa, a=1.0000
(99.998 wt.% UO2
+ 1.0122E-18 wt.% UO3
+ 3.0893E-10 wt.% UO
+ 7.1374E-07 wt.% Cs2O
+ 1.9309E-03 wt.% SrO
+ 7.1090E-07 wt.% BaO
+ 9.0939E-61 wt.% MoO2
+ 1.0041E-35 wt.% TeO2
+ 1.9431E-06 wt.% Rb2O)

+ 8.0107E-02 gram $U(Pd\_Rh\_Ru)_3$ at 368.00 °C, 1.0600E-02 GPa, a=1.0000
(50.118 wt.% UPd3
+ 21.552 wt.% URh3
+ 28.330 wt.% URu3)

+ 3.4442E-02 gram BCC Noble Metal Phase at 368.00 °C, 1.0600E-02 GPa, a=1.0000
(95.327 wt.% Mo
+ 1.7745E-09 wt.% Pd
+ 4.5942 wt.% Tc
+ 7.8485E-02 wt.% Ru
+ 5.8917E-06 wt.% Rh)

+ 2.8952E-02 gram HCP Noble Metal Phase at 368.00 °C, 1.0600E-02 GPa, a=1.0000
(25.573 wt.% Mo
+ 1.9813E-10 wt.% Pd
+ 0.30211 wt.% Tc
+ 74.120 wt.% Ru
+ 5.6130E-03 wt.% Rh)

+ 2.6417E-02 gram BaO_solid(s)
+ 2.2754E-02 gram Cs_2Te_solid(s)

+ 1.9693E-02	gram	$Tc_{11}Mo_9$_solid(s)	
+ 1.6366E-02	gram	Cs_liquid(liq)	
+ 7.9025E-03	gram	CsI_solid(s)	
+ 4.3932E-03	gram	Rb_liquid(liq)	
+ 2.1037E-03	gram	BaSe_solid	
+ 5.8139E-11	gram	Ba_2Pb_solid	
+ 0.00000	gram	Mo_solid(s)	a=0.96067

Table C-5: CANDU J49093C inner (Masses of chemical elements (g)).

J49093C INNER	Units (Grams)	
		Grain-Boundary
Time (y)	**7.00E+00**	**Case 9 B**
U	5.06E+02	
Xe	8.27E-01	1.92E-02
Mo	4.84E-01	1.12E-02
Cs	3.55E-01	8.24E-03
Ru	3.22E-01	7.48E-03
Ba	2.24E-01	5.20E-03
Pd	2.13E-01	4.95E-03
Tc	1.25E-01	2.90E-03
Sr	1.09E-01	2.53E-03
Rh	9.45E-02	2.19E-03
Te	7.08E-02	1.64E-03
Kr	4.84E-02	1.12E-03
Rb	4.62E-02	1.07E-03
I	3.65E-02	8.48E-04
Se	7.77E-03	1.80E-04
H	5.32E-06	1.24E-07
Pb	2.06E-10	4.78E-12
Bi	9.49E-15	2.20E-16
Rn	2.53E-16	5.87E-18
Temperature (°C)		803.35

Case 9 B: Input is gram (note for the calculation Xe and Kr were combined)

2.032E-2 Xe + 1.12E-2 Mo + 8.24E-3 Cs + 7.48E-3 Ru + 4.95E-3 Pd + 5.20E-3 Ba + 2.90E-3 Tc + 2.53E-3 Sr + 2.19E-3 Rh + 1.64E-3 Te + 1.07E-3 Rb + 8.48E-3 I + 1.80E-4 Se + 1.24E-7 H + 4.78E-12 Pb + 2.20E-16 Bi + 5.87E-18 Rn + 637 UO2

Output

1.5488E-04 mol (1.3078E-04 litre) gas_ideal at (803.35 °C, 1.0600E-02 GPa, a=1.0000)
(0.99929 Xe
+ 3.9713E-04 H2
+ 1.0249E-04 Cs2I2
+ 9.1088E-05 IRb
+ 4.3191E-05 Rb
+ 3.1474E-05 CsI
+ 2.3859E-05 I2Rb2
+ 1.9908E-05 Cs
+ 5.3383E-08 CsH
+ 1.0849E-08 BaI2
+ 8.6464E-09 Rb2
+ 7.3911E-09 CsRb
+ 1.8500E-09 Cs2
+ 1.4380E-09 BaI
+ 1.7448E-10 Ba
+ 1.4892E-10 Pb

+ 637.00 gram Fluorite (UO_2) at 803.35 °C, 1.0600E-02 GPa, a=1.0000
(99.999 wt.% UO2
+ 3.7713E-12 wt.% UO3
+ 6.8796E-06 wt.% UO
+ 2.8559E-07 wt.% Cs2O
+ 4.6970E-04 wt.% SrO
+ 6.3856E-04 wt.% BaO
+ 6.8989E-29 wt.% MoO2
+ 2.0046E-12 wt.% TeO2
+ 1.2140E-06 wt.% Rb2O)

+ 1.5247E-02 gram $U(Pd\_Rh\_Ru)_3$ at 803.35 °C, 1.0600E-02 GPa, a=1.0000
(56.671 wt.% UPd3
+ 24.960 wt.% URh3
+ 18.369 wt.% URu3)

+ 1.0855E-02 gram BCC Noble Metal Phase at 803.35 °C, 1.0600E-02 GPa, a=1.0000
(77.563 wt.% Mo
+ 6.3957E-04 wt.% Pd
+ 18.059 wt.% Tc
+ 4.3633 wt.% Ru
+ 1.3402E-02 wt.% Rh)

+ 8.1921E-03 gram HCP Noble Metal Phase at 803.35 °C, 1.0600E-02 GPa, a=1.0000
(28.482 wt.% Mo

+ 1.8161E-05	wt.% Pd	
+ 4.6592	wt.% Tc	
+ 66.374	wt.% Ru	
+ 0.48477	wt.% Rh)	
+ 9.4158E-03 gram	CsI_liquid(liq)	
+ 5.0564E-03 gram	Cs_2Te_solid(s)	
+ 3.5426E-03 gram	BaI_2_liquid(liq)	
+ 2.6352E-03 gram	IRb_liquid(liq)	
+ 1.0054E-03 gram	$Tc_{11}Mo_9$_solid(s)	
+ 4.9306E-04 gram	BaSe_solid	
+ 0.00000 gram	Mo_solid(s)	a=0.83733

C.2 BASIS OF SOLUBILITY ASSESSMENT

Consider the reaction: 0.1 mol HCl + 55.5 mol H_2O + species → Products
(note that 1 L H_2O = 1000 g = 55.5 mol H_2O)

Reaction 1:
0.1 mol HCl + 55.5 mol H_2O + CsI

57.700 mol aqueous at 298.15 K, 1 atm
(55.508 H2O_liquid
+ 1.0002 Cs[+]
+ 1.0002 I[-]
+ 0.10002 Cl[-]
+ 0.10002 H[+]

Reaction 2:
0.1 mol HCl + 55.5 mol H_2O + Cs_2Te

1.0291 mol (25.239 litre) gas_ideal at 298.15 K, 1 atm
(0.97090 H2
+ 2.9096E-02 H2O

+ 57.571 mol aqueous at 298.15 K, 1 atm
(55.508 H2O_liquid
+ 2.0724 Cs[+]
+ 1.9687 OH[-]
+ 0.10362 Cl[-]
+ 8.2403E-04 H2
(Eh=-0.848 V, pH=14.332)

+ 1.0000 mol Te solid

Reaction 3:
0.1 mol HCl + 55.5 mol H_2O + BaI_2

58.700 mol aqueous at 298.15 K, 1 atm
(55.508 H2O_liquid
+ 2.0003 I[-]
+ 1.0002 Ba[2+]
+ 0.10002 Cl[-]
+ 0.10002 H[+]

Reaction 4:
0.1 mol HCl + 55.5 mol H_2O + RbI

57.700 mol aqueous at 298.15 K, 1 atm
(55.508 H2O_liquid
+ 1.0002 Rb[+]
+ 1.0002 I[-]

+ 0.10002 Cl[-]
+ 0.10002 H[+]

Reaction 5:
0.1 mol HCl + 55.5 mol H_2O + $Tc_{11}Mo_9$

18.579 mol (455.72 litre) gas_ideal at 298.15 K, 1 atm
(0.96882 H2
+ 3.1182E-02 OH2
+ 1.1443E-08 HCl

+ 37.121 mol aqueous at 298.15 K, 1 atm
(55.508 H2O_liquid
+ 0.15034 H[+]
+ 0.15034 Cl[-]
+ 8.2226E-04 H2
(Eh=-0.048 V, pH= 0.823)

+ 11.000 mol Tc_solid(s)
+ 9.0000 mol MoO_2_solid(s)

Reaction 6:
0.1 mol HCl + 55.5 mol H_2O + BaSe

52.739 mol aqueous at 298.15 K, 1 atm
(55.508 H2O_liquid
+ 1.0870 HSe[-]
+ 0.60664 Ba[2+]
+ 0.10870 Cl[-]
+ 1.7546E-02 OH[-]

Reaction 7:
0.1 mol HCl + 55.5 mol H_2O + BaO

47.351 mol aqueous at 298.15 K, 1 atm
(55.508 H2O_liquid
+ 0.11774 Cl[-]
+ 8.0378E-02 Ba[2+]
+ 4.3019E-02 OH[-]

Reaction 8:
0.1 mol HCl + 55.5 mol H_2O + Ba_2Pb

2.0638 mol (50.624 litre) gas_ideal at 298.15 K, 1 atm
(0.96881 H2
+ 3.1188E-02 OH2

+ 36.227 mol aqueous at 298.15 K, 1 atm
(55.508 H2O_liquid

+ 0.15403 Cl[-]
+ 9.6695E-02 Ba[2+]
+ 3.9363E-02 OH[-]
+ 8.2225E-04 H2
(Eh=-0.745 V, pH=12.602)

+ 1.9372 mol BaO10H18_solid
+ 1.0000 mol Pb_solid

Reaction 9:
0.1 mol HCl + 55.5 mol H_2O + Rb

56.585 mol aqueous at 298.15 K, 1 atm
(55.508 H2O_liquid
+ 1.0169 Rb[+]
+ 0.91523 OH[-]
+ 0.10169 Cl[-]

Reaction 10:
0.1 mol HCl + 55.5 mol H_2O + Cs

56.585 mol aqueous at 298.15 K, 1 atm
(55.508 H2O_liquid
+ 1.0169 Cs[+]
+ 0.91523 OH[-]
+ 0.10169 Cl[-]

C.3 CALCULATION FO AVERAGE AND PESSIMISTIC INSTANT RELEASE FRACTIONS

Table C-6: CANDU-Pessimistic-900 kW-320 MWh/kgU Case: Outer Elements Grain Boundaries (Masses of chemical elements (g))

Element	Outer (g)	Element	Outer (g)
U	9.15E+03	I	8.88E-02
Xe	1.96E+00	Ag	5.05E-02
Mo	1.12E+00	Cd	3.41E-02
Ru	7.91E-01	Sn	2.20E-02
Cs	6.59E-01	Se	1.74E-02
Pd	5.89E-01	Br	6.72E-03
Ba	6.85E-01	Sb	3.52E-03
Tc	2.88E-01	In	9.97E-04
Rh	2.21E-01	Ge	1.24E-04
Sr	1.75E-01	As	4.03E-05
Te	1.70E-01	H	3.49E-06
Kr	1.01E-01	Pb	4.88E-09
Rb	1.03E-01	Bi	7.03E-14

Temperature (°C)	1412.4
Pressure (MPa)	3.53

Estimated Speciation- CANDU-Pessimistic-900 kW-320 MWh/kgU Case: Outer Elements Grain Boundaries

Input:

2.061 Xe + 1.12 Mo + 0.791 Ru + 0.659 Cs + 0.589 Pd + 0.685 Ba + 0.288 Tc + 0.221 Rh + 0.175 Sr + 0.17 Te + 0.103 Rb + 8.88E-2 I + 5.05E-2 Ag + 3.41E-2 Cd + 2.20E-2 Sn + 1.74E-2 Se + 6.72E-3 Br + 3.52E-3 Sb + 3.49E-6 H + 4.88E-9 Pb + 7.03E-14 Bi + 9150 U + 1230.1 O_2

Output:

1.7943E-02 mol (7.1235E-02 litre) gas_ideal (1412.40 ^{o}C, 3.5300E-03 GPa)

(0.87488	Xe
+ 4.5687E-02	Cs
+ 2.6408E-02	CsI
+ 2.0303E-02	Rb
+ 1.6906E-02	Cd
+ 5.8494E-03	IRb
+ 4.3237E-03	CsBr
+ 3.2904E-03	Cs_2I_2
+ 6.7990E-04	Sb_2
+ 3.9532E-04	Cs_2
+ 3.6333E-04	RbBr
+ 3.3572E-04	CsRb
+ 1.0336E-04	Ag
+ 9.2725E-05	Sb
+ 7.9731E-05	I_2Rb_2
+ 7.1156E-05	CsH
+ 6.9503E-05	Rb_2
+ 4.7997E-05	H_2
+ 3.9651E-05	Sb_4
+ 3.7295E-05	SnSe
+ 2.2879E-05	RbOH
+ 4.8175E-06	SnTe
+ 4.4249E-06	Sn
+ 2.7771E-06	CsOH
+ 4.1839E-07	Ag_2
+ 2.6412E-07	BaI
+ 2.6077E-07	Ba
+ 1.5001E-07	H
+ 1.4395E-07	SbTe
+ 8.5019E-08	BaBr
+ 6.7709E-08	AgI
+ 5.8285E-08	BaI_2
+ 4.2410E-08	Te
+ 2.1925E-08	Sn_2
+ 1.8066E-08	I
+ 1.7746E-08	SnO
+ 1.7224E-08	SbSe
+ 1.3153E-08	BaO
+ 7.6858E-09	$BaBr_2$

+ 6.0389E-09 OH_2
+ 2.8901E-09 BaOH
+ 1.9162E-09 Se
+ 1.2948E-09 Pb
+ 1.1679E-09 IH
+ 8.3118E-10 AgBr
+ 5.9850E-10 Rb_2O
+ 5.2689E-10 Sr
+ 4.8814E-10 Cs_2O
+ 4.1325E-10 Ba_2O
+ 2.6227E-10 HBr
+ 1.7242E-10 (CdI)
+ 1.3413E-10 CdSe
+ 1.3186E-10 Pd

+ 10381. gram Fluorite
(99.989 wt.% UO_2
+ 7.5284E-06 wt.% UO_3
+ 6.1295E-04 wt.% UO
+ 1.0896E-03 wt.% Cs_2O
+ 1.9937E-03 wt.% SrO
+ 7.0432E-03 wt.% BaO
+ 1.5132E-10 wt.% MoO_2
+ 1.5005E-05 wt.% TeO_2
+ 6.4610E-04 wt.% Rb_2O

+ 1.2723 gram $U(Pd\_Rh\_Ru)_3$
(79.791 wt.% UPd_3
+ 16.304 wt.% URh_3
+ 3.9053 wt.% URu_3

+ 1.2697 gram HCP Noble Metal Phase
(34.356 wt.% Mo
+ 4.7669E-02 wt.% Pd
+ 12.356 wt.% Tc
+ 46.100 wt.% Ru
+ 7.1402 wt.% Rh

+ 1.0128 gram BCC Noble Metal Phase
(67.516 wt.% Mo
+ 0.67455 wt.% Pd
+ 12.947 wt.% Tc
+ 17.558 wt.% Ru
+ 1.3047 wt.% Rh

+ 0.52026 gram $Cs_2Te\_solid(s)$
+ 5.0298E-02 gram Ag_liquid
+ 4.7517E-02 gram BaSe_solid
+ 2.1901E-02 gram Sn_liquid

+ 0.00000 gram Ag_solid a=0.73847

Table C-7: CANDU-Pessimistic-900 kW-320 MWh/kgU Case: Intermediate Elements Grain Boundaries (Masses of chemical elements (g))

Element	Inter (g)	Element	Inter (g)
U	6.10E+03	I	4.68E-02
Xe	1.03E+00	Ag	2.66E-02
Mo	5.91E-01	Cd	1.80E-02
Ru	4.17E-01	Sn	1.16E-02
Cs	3.48E-01	Se	9.18E-03
Pd	3.11E-01	Br	3.55E-03
Ba	3.61E-01	Sb	1.86E-03
Tc	1.52E-01	In	5.26E-04
Rh	1.16E-01	Ge	6.56E-05
Sr	9.22E-02	As	2.12E-05
Te	8.97E-02	H	1.84E-06
Kr	5.33E-02	Pb	2.57E-09
Rb	5.42E-02	Bi	3.71E-14

Temperature (°C) 1170.9

Pressure (MPa) 2.41

Estimated Speciation – CANDU-Pessimistic-900 kW-320 MWh/kgU Case: Intermediate Elements Grain Boundaries

Input:

1.0833 Xe + 0.591 Mo + 0.417 Ru + 0.348 Cs + 0.311 Pd + 0.361 Ba + 0.152 Tc + 0.116 Rh + 9.22E-2 Sr + 8.97E-2 Te + 5.42E-2 Rb + 4.68E-2 I + 2.66E-2 Ag + 1.80E-2 Cd + 1.16E-2 Sn + 9.18E-3 Se + 3.55E-3 Br + 1.86E-3 Sb + 1.84E-6 H + 2.57E-9 Pb + 3.71E-14 Bi + 6100 U + 820.04 O_2

Output:

9.8158E-03 mol (4.8902E-02 litre) gas_ideal (1170.90 ^{o}C, 2.4100E-03 GPa)

(0.84060	Xe
+ 6.8883E-02	Cs
+ 3.8117E-02	Rb
+ 1.6313E-02	Cd
+ 1.4163E-02	CsI
+ 8.8361E-03	Cs_2I_2
+ 5.2267E-03	IRb
+ 4.1896E-03	CsBr
+ 1.2276E-03	CsRb
+ 1.1830E-03	Cs_2
+ 3.3651E-04	RbBr
+ 3.3246E-04	Rb_2
+ 2.5378E-04	I_2Rb_2
+ 1.5824E-04	Sb_2
+ 7.0291E-05	CsH
+ 5.7663E-05	H_2
+ 2.9908E-05	Sb_4
+ 9.1041E-06	Sb
+ 6.6615E-06	Ag
+ 5.0862E-07	Ba
+ 2.6069E-07	RbOH
+ 2.5408E-07	BaI
+ 1.1283E-07	BaBr
+ 9.9736E-08	Sn
+ 8.4955E-08	CsOH
+ 4.1871E-08	BaI_2
+ 1.3560E-08	H
+ 8.8195E-09	$BaBr_2$
+ 8.7976E-09	SnSe
+ 8.4063E-09	Ag_2
+ 2.4261E-09	SnTe
+ 1.2577E-09	Pb
+ 9.8747E-10	AgI
+ 5.3123E-10	Ba_2O
+ 4.0572E-10	BaO
+ 3.3123E-10	Sr
+ 2.6659E-10	BaOH
+ 2.4451E-10	I

+ 6920.1 gram Fluorite
(99.992 wt.% UO_2
+ 1.9775E-08 wt.% UO_3
+ 7.5549E-04 wt.% UO
+ 2.9876E-04 wt.% Cs_2O
+ 1.5756E-03 wt.% SrO
+ 5.4947E-03 wt.% BaO
+ 2.1755E-17 wt.% MoO_2
+ 1.0792E-10 wt.% TeO_2
+ 2.4561E-04 wt.% Rb_2O

+ 0.92391 gram $U(Pd\_Rh\_Ru)_3$
(58.711 wt.% UPd_3
+ 21.036 wt.% URh_3
+ 20.253 wt.% URu_3

+ 0.68499 gram BCC Noble Metal Phase
(68.752 wt.% Mo
+ 3.5739E-02 wt.% Pd
+ 17.087 wt.% Tc
+ 13.986 wt.% Ru
+ 0.13934 wt.% Rh

+ 0.37669 gram HCP Noble Metal Phase
(31.872 wt.% Mo
+ 1.0917E-03 wt.% Pd
+ 9.2795 wt.% Tc
+ 57.439 wt.% Ru
+ 1.4083 wt.% Rh

+ 0.27656 gram $Cs_2Te\_solid(s)$
+ 2.5146E-02 gram BaSe_solid
+ 2.3063E-02 gram Ag_liquid
+ 1.6073E-02 gram $BaSn_3$_solid
+ 4.8575E-03 gram Ag_3Sb_solid

+ 0.00000 gram Ag_solid a=0.85011)

Table C-8: CANDU-Pessimistic-900 kW-320 MWh/kgU Case: Inner Elements Grain Boundaries (Masses of chemical elements (g))

Element	Inner (g)	Element	Inter (g)
U	3.05E+03	I	1.75E-02
Xe	3.85E-01	Ag	9.96E-03
Mo	2.21E-01	Cd	6.71E-03
Ru	1.56E-01	Sn	4.33E-03
Cs	1.30E-01	Se	3.43E-03
Pd	1.16E-01	Br	1.33E-03
Ba	1.35E-01	Sb	6.95E-04
Tc	5.67E-02	In	1.97E-04
Rh	4.35E-02	Ge	2.45E-05
Sr	3.45E-02	As	7.94E-06
Te	3.35E-02	H	6.88E-07
Kr	1.99E-02	Pb	9.61E-10
Rb	2.03E-02	Bi	1.39E-14

Temperature (°C)	1022.7
Pressure (MPa)	1.45

Estimated Speciation – CANDU-Pessimistic-900 kW-320 MWh/kgU Case: Inner Elements Grain Boundaries

Input:

0.4049 Xe + 0.221 Mo + 0.156 Ru + 0.130 Cs + 0.116 Pd + 0.135 Ba + 5.67E-2 Tc + 4.35E-2 Rh + 3.45E-2 Sr + 3.35E-2 Te + 2.03E-2 Rb + 1.75E-2 I + 9.96E-3 Ag + 6.71E-3 Cd + 4.33E-3 Sn + 3.43E-3 Se + 1.33E-3 Br + 6.95E-4 Sb + 6.88E-7 H + 9.61E-10 Pb + 1.39E-14 Bi + 3050 U + 410.03 O_2

Output:

3.3755E-03 mol (2.5084E-02 litre) gas_ideal (1022.70 °C, 1.4500E-03 GPa)

(0.91365 Xe
+ 3.3819E-02 Cs
+ 1.7684E-02 Cd
+ 1.3338E-02 Rb
+ 7.8102E-03 Cs_2I_2
+ 6.0152E-03 CsI
+ 4.7126E-03 CsBr
+ 1.9963E-03 IRb
+ 2.8257E-04 Cs_2
+ 2.1850E-04 RbBr
+ 2.0704E-04 CsRb
+ 9.1968E-05 I_2Rb_2
+ 8.7154E-05 H_2
+ 4.1385E-05 Rb_2
+ 2.5572E-05 CsH
+ 1.3632E-05 Sb_2
+ 1.5045E-06 Sb_4
+ 1.1843E-06 RbOH
+ 1.1477E-06 CsOH
+ 8.9409E-07 Ag
+ 8.3388E-07 Sb
+ 2.6582E-08 SnSe
+ 1.7760E-08 Sn
+ 2.5399E-09 H
+ 1.5853E-09 Ba
+ 1.3722E-09 Pb
+ 1.1685E-09 OH_2
+ 8.8599E-10 BaI
+ 8.4036E-10 BaBr
+ 4.3121E-10 Ag_2
+ 2.3004E-10 SnTe
+ 2.2906E-10 BaI_2
+ 1.9145E-10 $BaBr_2$

+ 3460.1 gram Fluorite
(99.993 wt.% UO_2
+ 1.0424E-07 wt.% UO_3
+ 1.5688E-06 wt.% UO
+ 7.7281E-04 wt.% Cs_2O

+ 1.1791E-03 wt.% SrO
+ 4.1636E-03 wt.% BaO
+ 2.9209E-17 wt.% MoO_2
+ 3.5367E-08 wt.% TeO_2
+ 4.9545E-04 wt.% Rb_2O

+ 0.27304 gram HCP Noble Metal Phase
(27.163 wt.% Mo
+ 1.0976E-02 wt.% Pd
+ 11.299 wt.% Tc
+ 51.344 wt.% Ru
+ 10.183 wt.% Rh

+ 0.22904 gram $U(Pd\_Rh\_Ru)_3$
(87.962 wt.% UPd_3
+ 11.236 wt.% URh_3
+ 0.80193 wt.% URu_3

+ 0.18918 gram BCC Noble Metal Phase
(77.616 wt.% Mo
+ 0.29145 wt.% Pd
+ 13.664 wt.% Tc
+ 7.8131 wt.% Ru
+ 0.61626 wt.% Rh

+ 0.10328 gram $Cs_2Te\_solid(s)$
+ 1.4941E-02 gram CsI_liquid(liq)
+ 9.3954E-03 gram BaSe_solid
+ 8.1497E-03 gram Ag_liquid
+ 4.3300E-03 gram Sn_liquid
+ 2.4910E-03 gram Ag_3Sb_solid

+ 0.00000 gram Ag_solid a=0.94855

Table C-9: CANDU-Pessimistic-900 kW-320 MWh/kgU Case: Center Element Grain Boundaries (Masses of chemical elements (g))

Element	Center (g)	Element	Center (g)
U	5.08E+02	I	2.84E-03
Xe	6.25E-02	Ag	1.62E-03
Mo	3.58E-02	Cd	1.09E-03
Ru	2.53E-02	Sn	7.03E-04
Cs	2.11E-02	Se	5.56E-04
Pd	1.88E-02	Br	2.15E-04
Ba	2.19E-02	Sb	1.13E-04
Tc	9.20E-03	In	3.19E-05
Rh	7.05E-03	Ge	3.98E-06
Sr	5.59E-03	As	1.29E-06
Te	5.44E-03	H	1.12E-07
Kr	3.23E-03	Pb	1.56E-10
Rb	3.29E-03	Bi	2.25E-15

Temperature (°C)	1004.1
Pressure (MPa)	1.13

Estimated Speciation – CANDU-Pessimistic-900 kW-320 MWh/kgU Case: Center Element Grain Boundaries

Input:

0.06573 Xe + 3.58E-2 Mo + 2.53E-2 Ru + 2.11E-2 Cs + 1.88E-2 Pd + 2.19E-2 Ba + 9.20E-3 Tc + 7.05E-3 Rh + 5.59E-3 Sr + 5.44E-3 Te + 3.29E-3 Rb + 2.84E-3 I + 1.62E-3 Ag + 1.09E-3 Cd + 7.03E-4 Sn + 5.56E-4 Se + 2.15E-4 Br + 1.13E-4 Sb + 1.12E-7 H + 1.56E-10 Pb + 2.25E-15 Bi + 508 U + 68.294 O_2

Output:

5.3135E-04 mol (4.9941E-03 litre) gas_ideal (1004.10 C, 1.1300E-03 GPa)

(0.94221 Xe
+ 1.8249E-02 Cd
+ 1.3819E-02 Cs
+ 8.5864E-03 Cs_2I_2
+ 6.1549E-03 CsI
+ 4.8987E-03 CsBr
+ 4.0836E-03 Rb
+ 1.5818E-03 IRb
+ 1.6517E-04 RbBr
+ 9.2730E-05 H_2
+ 5.5062E-05 I_2Rb_2
+ 3.9411E-05 Cs_2
+ 2.1615E-05 CsRb
+ 1.1470E-05 Sb_2
+ 9.1841E-06 CsH
+ 8.4749E-06 CsOH
+ 5.9575E-06 RbOH
+ 3.2525E-06 Rb_2
+ 1.1714E-06 Sb_4
+ 8.0167E-07 Ag
+ 7.0865E-07 Sb
+ 4.1357E-07 SnSe
+ 2.1993E-08 OH_2
+ 1.5213E-08 Sn
+ 2.1931E-09 H
+ 1.4147E-09 Pb
+ 1.2511E-09 SnTe
+ 3.3668E-10 Ag_2
+ 3.2933E-10 SnO
+ 3.2483E-10 Cs_2MoO_4
+ 2.4395E-10 $MoRb_2O_4$
+ 1.7077E-10 AgI

+ 576.32 gram Fluorite
(99.993 wt.% UO_2
+ 1.6291E-06 wt.% UO_3
+ 5.3190E-08 wt.% UO
+ 1.1770E-03 wt.% Cs_2O

+ 1.1471E-03 wt.% SrO
+ 4.0554E-03 wt.% BaO
+ 4.6035E-15 wt.% MoO_2
+ 8.4986E-05 wt.% TeO_2
+ 5.7281E-04 wt.% Rb_2O

+ 4.8225E-02 gram HCP Noble Metal Phase
(26.011 wt.% Mo
+ 8.9221E-02 wt.% Pd
+ 11.983 wt.% Tc
+ 48.484 wt.% Ru
+ 13.433 wt.% Rh

+ 3.2958E-02 gram $U(Pd\_Rh\_Ru)_3$
(97.962 wt.% UPd_3
+ 1.9459 wt.% URh_3
+ 9.2053E-02 wt.% URu_3

+ 2.9050E-02 gram BCC Noble Metal Phase
(80.057 wt.% Mo
+ 0.89797 wt.% Pd
+ 11.778 wt.% Tc
+ 6.5459 wt.% Ru
+ 0.72179 wt.% Rh

+ 1.5565E-02 gram $Cs_2Te\_solid(s)$
+ 2.3603E-03 gram CsI_liquid(liq)
+ 1.5229E-03 gram BaSe_solid
+ 1.3245E-03 gram Ag_liquid
+ 7.0297E-04 gram Sn_liquid
+ 4.0664E-04 gram Ag_3Sb_solid

+ 0.00000 gram Ag_solid a=0.96325

Table C-10: CANDU-Pessimistic-900 kW-320 MWh/kgU Case: Outer Elements Gap (Masses of chemical elements (g))

Element	Outer (g)	Element	Outer (g)
U	9.15E+03	I	2.58E-01
Xe	5.69E+00	Ag	1.47E-01
Mo	3.26E+00	Cd	9.91E-02
Ru	2.30E+00	Sn	6.39E-02
Cs	1.92E+00	Se	5.06E-02
Pd	1.71E+00	Br	1.96E-02
Ba	1.99E+00	Sb	1.03E-02
Tc	8.37E-01	In	2.90E-03
Rh	6.42E-01	Ge	3.62E-04
Sr	5.09E-01	As	1.17E-04
Te	4.95E-01	H	1.02E-05
Kr	2.94E-01	Pb	1.42E-08
Rb	2.99E-01	Bi	2.05E-13

Temperature (°C)	455
Pressure (MPa)	3.53

Estimated Speciation – CANDU-Pessimistic-900 kW-320 MWh/kgU Case: Outer Elements Gap

Input:

5.984 Xe + 3.26 Mo + 2.3 Ru + 1.92 Cs + 1.71 Pd + 1.99 Ba + 0.837 Tc + 0.642 Rh + 0.509 Sr + 0.495 Te + 0.299 Rb + 0.258 I + 0.147 Ag + 0.0991 Cd + 0.0639 Sn + 0.0506 Se + 0.0196 Br + 0.0103 Sb + 1.02E-5 H + 1.42E-8 Pb + 2.05E-13 Bi+ 9150 U + 1230.1 O_2

Output:

4.5578E-02 mol (7.4950E-08 litre) gas_ideal (455.00 C, 3530.0 GPa)
- (1.0000 Xe
- + 6.2316E-08 H_2
- + 1.2318E-09 Cs
- + 8.2077E-10 Rb
- + 9.2983E-11 Cd
- + 5.2384E-11 CsRb
- + 4.2261E-11 Cs_2
- + 2.2274E-11 Rb_2
- + 5.4667E-12 CsH
- + 2.5429E-14 CsBr

+ 10378. gram Fluorite
- (99.994 wt.% UO_2
- + 2.6242E-15 wt.% UO_3
- + 5.9561E-10 wt.% UO
- + 4.7538E-06 wt.% Cs_2O
- + 5.8000E-03 wt.% SrO
- + 3.1407E-06 wt.% BaO
- + 3.2530E-53 wt.% MoO_2
- + 3.6179E-31 wt.% TeO_2
- + 1.1738E-05 wt.% Rb_2O

+ 4.6359 gram $U(Pd\_Rh\_Ru)_3$
- (64.388 wt.% UPd_3
- + 24.491 wt.% URh_3
- + 11.122 wt.% URu_3

+ 2.7353 gram HCP Noble Metal Phase
- (26.068 wt.% Mo
- + 5.7566E-09 wt.% Pd
- + 0.50721 wt.% Tc
- + 73.391 wt.% Ru
- + 3.3810E-02 wt.% Rh

+ 2.1118 gram BCC Noble Metal Phase
- (94.016 wt.% Mo
- + 8.1363E-08 wt.% Pd
- + 5.8097 wt.% Tc
- + 0.17450 wt.% Ru

+ 6.7905E-05 wt.% Rh

+ 2.0950 gram BaO_solid(s)
+ 1.5262 gram Cs_2Te_solid(s)
+ 1.2620 gram $Tc_{11}Mo_9$_solid(s)
+ 0.58557 gram Cs_liquid(liq)
+ 0.52820 gram CsI_solid(s)
+ 0.29789 gram Rb_liquid(liq)
+ 0.13860 gram BaSe_solid
+ 0.11962 gram Ag_solid
+ 9.9100E-02 gram Cd_liquid
+ 8.8540E-02 gram $BaSn_3$_solid
+ 5.2201E-02 gram CsBr_solid
+ 3.7677E-02 gram Ag_3Sb_solid
+ 7.0465E-04 gram BaH_2_solid(s)
+ 3.3023E-08 gram Ba_2Pb_solid
+ 2.0500E-13 gram Bi_liquid

Table C-11: CANDU-Pessimistic-900 kW-320 MWh/kgU Case: Intermediate Elements Gap (Masses of chemical elements (g))

Element	Inter (g)	Element	Inter (g)
U	6.10E+03	I	9.59E-02
Xe	2.11E+00	Ag	5.46E-02
Mo	1.21E+00	Cd	3.68E-02
Ru	8.55E-01	Sn	2.37E-02
Cs	7.12E-01	Se	1.88E-02
Pd	6.36E-01	Br	7.27E-03
Ba	7.41E-01	Sb	3.81E-03
Tc	3.11E-01	In	1.08E-03
Rh	2.38E-01	Ge	1.34E-04
Sr	1.89E-01	As	4.35E-05
Te	1.84E-01	H	3.77E-06
Kr	1.09E-01	Pb	5.27E-09
Rb	1.11E-01	Bi	7.60E-14

Temperature (°C)	417
Pressure (MPa)	2.41

Estimated Speciation – CANDU-Pessimistic-900 kW-320 MWh/kgU Case: Intermediate Elements Gap

Input:

2.219 Xe + 1.21 Mo + 0.855 Ru + 0.712 Cs + 0.636 Pd + 0.741 Ba + 0.311 Tc + 0.238 Rh + 0.189 Sr + 0.184 Te + 0.111 Rb + 0.0959 I + 0.0546 Ag + 0.0368 Cd + 0.0237 Sn + 0.0188 Se + 0.00727 Br + 0.00381 Sb + 3.77E-6 H + 5.27E-9 Pb + 7.6E-14 Bi + 6100 U + 820.04 O_2 =

Output:

1.6952E-02 mol (4.0399E-02 litre) gas_ideal (417.60 C, 2.4100E-03 GPa)
(0.99700 Xe
+ 1.5849E-03 Cs
+ 1.0477E-03 Rb
+ 1.1269E-04 Cd
+ 1.1020E-04 H_2
+ 6.4076E-05 CsRb
+ 5.2073E-05 Cs_2
+ 2.7161E-05 Rb_2
+ 2.3399E-07 CsH
+ 2.6772E-08 CsBr
+ 7.7508E-09 Cs_2I_2
+ 2.1859E-09 IRb
+ 5.4829E-10 CsI
+ 3.4542E-10 RbBr

+ 6919.3 gram Fluorite
(99.997 wt.% UO_2
+ 4.6442E-16 wt.% UO_3
+ 1.2748E-09 wt.% UO
+ 2.4828E-06 wt.% Cs_2O
+ 3.2303E-03 wt.% SrO
+ 2.6258E-06 wt.% BaO
+ 7.4287E-55 wt.% MoO_2
+ 1.8971E-32 wt.% TeO_2
+ 6.2029E-06 wt.% Rb_2O

+ 1.9602 gram $U(Pd\_Rh\_Ru)_3$
(56.636 wt.% UPd_3
+ 21.493 wt.% URh_3
+ 21.872 wt.% URu_3

+ 0.83466 gram HCP Noble Metal Phase
(26.009 wt.% Mo
+ 1.9760E-09 wt.% Pd
+ 0.47489 wt.% Tc
+ 73.503 wt.% Ru
+ 1.3837E-02 wt.% Rh

+ 0.83277 gram BCC Noble Metal Phase

(94.197 wt.% Mo
+ 2.6521E-08 wt.% Pd
+ 5.6449 wt.% Tc
+ 0.15848 wt.% Ru
+ 2.5642E-05 wt.% Rh

+ 0.78044 gram BaO_solid(s)
+ 0.56730 gram Cs_2Te_solid(s)
+ 0.46850 gram $Tc_{11}Mo_9$_solid(s)
+ 0.21206 gram Cs_liquid(liq)
+ 0.19633 gram CsI_solid(s)
+ 0.10892 gram Rb_liquid(liq)
+ 5.1497E-02 gram BaSe_solid
+ 4.4473E-02 gram Ag_solid
+ 3.6585E-02 gram Cd_liquid
+ 3.2839E-02 gram $BaSn_3$_solid
+ 1.9362E-02 gram CsBr_solid
+ 1.3937E-02 gram Ag_3Sb_solid
+ 1.2256E-08 gram Ba_2Pb_solid

Table C-12: CANDU-Pessimistic-900 kW-320 MWh/kgU Case: Inner Elements Gap (Masses of chemical elements (g))

Element	Inner (g)	Element	Inter (g)
U	3.05E+03	I	2.43E-02
Xe	5.35E-01	Ag	1.38E-02
Mo	3.06E-01	Cd	9.31E-03
Ru	2.16E-01	Sn	6.01E-03
Cs	1.80E-01	Se	4.76E-03
Pd	1.61E-01	Br	1.84E-03
Ba	1.87E-01	Sb	9.64E-04
Tc	7.87E-02	In	2.73E-04
Rh	6.03E-02	Ge	3.40E-05
Sr	4.78E-02	As	1.10E-05
Te	4.65E-02	H	9.54E-07
Kr	2.76E-02	Pb	1.33E-09
Rb	2.81E-02	Bi	1.92E-14

Temperature (°C)	389
Pressure (MPa)	1.45

Estimated Speciation – CANDU-Pessimistic-900 kW-320 MWh/kgU Case: Inner Elements Gap

Input:

0.5626 Xe + 0.306 Mo + 0.216 Ru + 0.18 Cs + 0.161 Pd + 0.187 Ba + 0.0787 Tc + 0.0603 Rh + 0.0478 Sr + 0.0465 Te + 0.0281 Rb + 0.0243 I + 0.0138 Ag + 9.31E-3 Cd + 6.01E-3 Sn + 4.76E-3 Se +1.84E-3 Br + 9.64E-4 Sb + 9.54E-7 H + 1.33E-9 Pb + 1.92E-14 Bi + 3050 U + 410.03 O_2 =

Output:

4.2920E-03 mol (1.5582E-02 litre) gas_ideal (389.00 C, 1.4500E-03 GPa)
(0.99841 Xe
+ 8.6122E-04 Cs
+ 5.3182E-04 Rb
+ 1.1023E-04 H2
+ 3.6667E-05 Cd
+ 2.2406E-05 CsRb
+ 1.9380E-05 Cs2
+ 9.2467E-06 Rb2
+ 6.8062E-08 CsH
+ 2.5914E-09 CsBr
+ 5.4298E-10 Cs2I2
+ 1.7308E-10 IRb

+ 3459.9 gram Fluorite
(99.998 wt.% UO_2
+ 3.8561E-15 wt.% UO_3
+ 1.9596E-14 wt.% UO
+ 6.3617E-05 wt.% Cs_2O
+ 1.6338E-03 wt.% SrO
+ 5.6488E-07 wt.% BaO
+ 1.2568E-53 wt.% MoO_2
+ 4.0391E-28 wt.% TeO_2
+ 1.7583E-04 wt.% Rb_2O

+ 0.36749 gram $U(Pd\_Rh\_Ru)_3$
(76.475 wt.% UPd_3
+ 23.473 wt.% URh_3
+ 5.2783E-02 wt.% URu_3

+ 0.30276 gram HCP Noble Metal Phase
(24.535 wt.% Mo
+ 1.5585E-07 wt.% Pd
+ 0.36994 wt.% Tc
+ 71.267 wt.% Ru
+ 3.8280 wt.% Rh

+ 0.18438 gram BCC Noble Metal Phase
(95.497 wt.% Mo
+ 9.2297E-07 wt.% Pd

+ 4.4334 wt.% Tc
+ 6.6434E-02 wt.% Ru
+ 2.6656E-03 wt.% Rh

+ 0.19694 gram BaO_solid(s)
+ 0.14337 gram Cs_2Te_solid(s)
+ 0.12505 gram $Tc_{11}Mo_9$_solid(s)
+ 5.6058E-02 gram $U_2Cs_4O_7$_solid(s)
+ 4.9749E-02 gram CsI_solid(s)
+ 2.5405E-02 gram Cs_liquid(liq)
+ 2.2327E-02 gram Rb_liquid(liq)
+ 1.3039E-02 gram BaSe_solid
+ 1.1238E-02 gram Ag_solid
+ 9.2923E-03 gram Cd_liquid
+ 8.3275E-03 gram $BaSn_3$_solid
+ 4.9005E-03 gram CsBr_solid
+ 3.5263E-03 gram Ag_3Sb_solid
+ 3.0923E-09 gram Ba_2Pb_solid

Table C-13: CANDU-Pessimistic-900 kW-320 MWh/kgU Case: Center Element Gap (Masses of chemical elements (g))

Element	Center (g)	Element	Center (g)
U	5.08E+02	I	3.54E-03
Xe	7.80E-02	Ag	2.01E-03
Mo	4.47E-02	Cd	1.36E-03
Ru	3.15E-02	Sn	8.76E-04
Cs	2.63E-02	Se	6.94E-04
Pd	2.35E-02	Br	2.68E-04
Ba	2.73E-02	Sb	1.40E-04
Tc	1.15E-02	In	3.98E-05
Rh	8.79E-03	Ge	4.96E-06
Sr	6.97E-03	As	1.61E-06
Te	6.78E-03	H	1.39E-07
Kr	4.03E-03	Pb	1.94E-10
Rb	4.10E-03	Bi	2.80E-15

Temperature (°C)	385.3
Pressure (MPa)	1.31

Estimated Speciation – CANDU-Pessimistic-900 kW-320 MWh/kgU Case: Center Element Gap

Input:

0.08203 Xe + 4.47E-2 Mo + 3.15E-2 Ru + 2.63E-2 Cs + 2.35E-2 Pd + 2.73E-2 Ba + 1.15E-2 Tc + 8.79E-3 Rh + 6.97E-3 Sr + 6.78E-3 Te + 4.1E-3 Rb + 3.54E-3 I + 2.01E-3 Ag + 1.36E-3 Cd + 8.76E-4 Sn + 6.94E-4 Se + 2.68E-4 Br + 1.4E-4 Sb + 1.39E-7 H + 1.94E-10 Pb + 2.80E-15 Bi + 508 U + 68.294 O_2 =

Output:

6.2537E-04 mol (2.4734E-03 litre) gas_ideal (385.00 C, 1.3100E-03 GPa)
(0.99909 Xe
+ 4.6805E-04 Rb
+ 2.8293E-04 Cs
+ 1.1025E-04 H_2
+ 2.9627E-05 Cd
+ 7.5257E-06 Rb_2
+ 6.7533E-06 CsRb
+ 2.1779E-06 Cs_2
+ 1.9800E-08 CsH
+ 1.1006E-09 CsBr
+ 3.2558E-10 Cs_2I_2
+ 2.8884E-10 IRb

+ 576.27 gram Fluorite
(99.998 wt.% UO_2
+ 3.7613E-15 wt.% UO_3
+ 3.0896E-15 wt.% UO
+ 3.8011E-05 wt.% Cs_2O
+ 1.4304E-03 wt.% SrO
+ 4.2028E-07 wt.% BaO
+ 1.2323E-53 wt.% MoO_2
+ 1.1531E-26 wt.% TeO_2
+ 2.9076E-04 wt.% Rb_2O

+ 4.9954E-02 gram $U(Pd\_Rh\_Ru)_3$
(82.118 wt.% UPd_3
+ 17.863 wt.% URh_3
+ 1.9255E-02 wt.% URu_3

+ 4.6259E-02 gram HCP Noble Metal Phase
(23.431 wt.% Mo
+ 3.9839E-07 wt.% Pd
+ 0.40955 wt.% Tc
+ 68.052 wt.% Ru
+ 8.1075 wt.% Rh

+ 2.6859E-02 gram BCC Noble Metal Phase

(95.706 wt.% Mo
+ 1.5312E-06 wt.% Pd
+ 4.2360 wt.% Tc
+ 5.4215E-02 wt.% Ru
+ 4.0456E-03 wt.% Rh

+ 2.8753E-02 gram BaO_solid(s)
+ 2.0904E-02 gram Cs_2Te_solid(s)
+ 1.8329E-02 gram $Tc_{11}Mo_9$_solid(s)
+ 1.7350E-02 gram $U_2Cs_4O_7$_solid(s)
+ 7.2474E-03 gram CsI_solid(s)
+ 2.0514E-03 gram Rb_liquid(liq)
+ 1.9010E-03 gram BaSe_solid
+ 1.6379E-03 gram Ag_solid
+ 1.3579E-03 gram Cd_liquid
+ 1.2138E-03 gram $BaSn_3$_solid
+ 8.8492E-04 gram $URbO_3$_solid
+ 5.5466E-04 gram RbBr_solid
+ 5.1211E-04 gram Ag_3Sb_solid
+ 2.3680E-10 gram $BaPb_3$_solid